



Steel Fiber Reinforced Concrete Ground Slabs

A Comparative Evaluation of Plain and Steel Fiber Reinforced Concrete Ground Slabs

W.A. Elsaigh

A dissertation submitted in partial fulfillment of the requirements for the degree of

Master of Engineering (Transportation Engineering)

In the
Faculty of Engineering
University of Pretoria

20/2/2001





ABSTRACT

Steel Fiber Reinforced Concrete Ground Slabs

**A Comparative Evaluation of Plain and Steel fiber Reinforced Concrete
Ground Slabs**

By: W.A. Elsaigh

Supervisor: Prof. E.P. Kearsley
Department: Civil Engineering
University: University of Pretoria
Degree: Master Engineering (Transportation Engineering)

Steel Fiber Reinforced Concrete (SFRC) is defined as concrete containing randomly oriented discontinuous discrete steel fibers. The literature on SFRC revealed that addition of steel fiber to concrete improves its engineering characteristics and impart a significant after cracking toughness, which make the material superior for ground slab applications.

In this study the effect of steel fiber content on properties of concrete was investigated by using beam and cube specimens, SFRC was compared with plain concrete. A comparative study was conducted by applying a static load on two full-scale slabs having different depths. The first slab is SFRC and the second is plain concrete having identical mix to the first slab but containing no steel fibers. The measured loads and deflections were compared to theoretical calculated values using models given by Westergaard, Meyerhof, Falkner et al and Shentu et al.

It was found that the steel fiber content has an influence ranging between little and significant on the tested properties. The load capacity and deflection value for the SFRC slab was approximately equal to that of plain concrete bearing in mind that the SFRC slab had 16.6% less depth. The theoretical loads and deflections did not correlate with the measured values.





BLOKEER

Staalveselversterkte Beton Grondvloer Blaaië

‘n Vergelykende studie van gewone en staalveselversterkte beton
grondvloerblaaië

W.A. Elsaigh

Promotor: Prof. E.P. Kearsley
Department: Siviele Ingenieurswese
Universiteit: Universiteit van Pretoria
Graad: Magister in Ingenieurswese (Vervoeringenieurswese)

Staalveselversterkte beton word gedefinieer as beton wat willekeurig georiënteerde, diskontinue, diskrete staal vesels bevat. Literatuur dui daarop dat die gebruik van staalvesels in beton die ingenieurseienskappe sowel as die na-gekraakte taatheid van die beton kan verbeter en dus die material meer geskik maak vir gebruik in grondvloerblaaië.

Tydens hierdie projek is die effek van die toevoeging van staalvesels op die eienskappe van beton ondersoek deur die gedrag van balke en kubusse wat staalvesels bevat te vergelyk met soortgelyke monsters wat nie vesels bevat nie. ‘n Vergelykende studie is uitgevoer deur twee volskaalse grondvloerblaaië, met verskillende diktes, staties te belas. Die eerste blad het staalvesels bevat terwyl die tweede blad gegiet is met ‘n identiese betonmengsel wat nie vesels bevat het nie. Die gemete belastings en defleksies is vergelyk met teoretiese waardes soos bereken met die modelle voorgestel deur Westergaard, Meyerhof, Falkner et al en Shentu et al.

Daar is bevind dat die staalveselinhoud van beton die gemete materiaaleienskappe tot ‘n mate beïnvloed wat wissel tussen gering en betekenisvol. Alhoewel die staalveselversterkte blad 16.6% dunner was as die ander blad was die laskapasiteit en defleksiewaardes van die staalveselversterkte blad vergelykbaar met die gewone betonblad (sonder vesels). Daar was geen korrelasie tussen die teoretiese belastings en defleksies en die gemete waardes nie.





ACKNOWLEDGEMENTS

The author wishes to express his sincere gratitude and appreciation towards **Prof. E.P. Kearsley** for her valuable comments, criticism, encouragement, and guidance. The advice and knowledge provided by **Prof. A. Visser** is also gratefully acknowledged.

A special word of gratitude is extended to:

- The staff at the Civil Engineering Laboratory of the University of Pretoria for practical and administrative assistance.
- The library personnel at the Cement and Concrete Institute and at the University of Pretoria for providing and facilitating access to literature.
- My family for their encouragement, moral support and all sacrifices they made.
- To my creator.





Table of Contents

	Page
<u>Chapter 1: Introduction</u>	
1.1 Background	1-1
1.2 Objectives of Study	1-2
1.3 Scope and Limitations of Study	1-2
1.4 Study Metodology	1-3
1.5 Need for Research in this Field	1-4
1.6 Organization od Dissertation	1-4
<u>Chapter 2: Steel Fiber Reinforced Concrete</u>	
2.1 Synopsis	2-1
2.2 Steel Fibers	2-1
2.3 Mix Design	2-3
2.4 Advantages and Disadvantages	2-4
2.5 Practical Aspects	2-5
2.6 Mechanical Properties	2-6
2.6.1 Toughness	2-6
2.6.2 Flexural Strength	2-9
2.6.3 Fatigue Endurance	2-11
2.6.4 Impact Strength	2-13
2.6.5 Compressive Strength	2-14
2.6.6 Shear Strength	2-16
2.6.7 Modulus of Elasticity	2-17
2.6.8 Poisson's Ratio	2-18
2.7 Physical Properties	2-18
2.7.1 Shrinkage	2-18
2.7.2 Creep	2-20
2.7.3 Durability	2-21
2.7.4 Abrasion and Skid Resistance	2-22
2.7.5 Thermal Properties	2-23
2.7.6 Electrical Conductivity	2-24
2.8 Conclusions	2-24





Chapter 3: Steel Fiber Reinforced Concrete Ground Slabs

3.1 Synopsis	3-1
3.2 Design Methods	3-1
3.3 Ground Slabs Distresses	3-3
3.4 Insight Through Previous Projects	3-4
3.5 Economic Evaluation	3-10
3.6 Conclusions	3-11

Chapter 4: Basic Analytical Theories and

Similar Studies Conducted by other Agencies

4.1 Background	4-1
4.2 Theoretical Analysis Approaches	4-1
4.2.1 Westergaard	4-1
4.2.2 Meyerhof	4-2
4.2.3 Falkner et al	4-4
4.2.4 Shentu et al	4-4
4.3 Similar Studies Conducted by other Agencies	4-5
4.3.1 Kaushik et al (1989)	4-5
4.3.2 Beckett (1990)	4-6
4.3.3 Falkner et al (1995)	4-7
4.3.4 Beckett (1999)	4-8
4.4 Conclusions	4-10

Chapter 5: Experimental Procedure

5.1 Introduction	5-1
5.2 Mix Composition	5-1
5.3 Effect of Steel Fiber Content on Properties of Concrete	5-2
5.3.1 Standard Slump Test	5-2
5.3.2 Standard Compressive Strength Test	5-2
5.3.3 Standard Flexural Strength Test	5-3
5.3.4 Standard Modulus of Elasticity Test	5-3
5.3.5 Third-Point Loading Test on Standard Beams	5-3
5.4 Slab Test	5-5
5.4.1 Full-scale Test	5-6





5.4.1.1 Interior Load	5-7
5.4.1.2 Edge Load	5-8
5.4.1.3 Corner Load	5-8
5.4.1.4 Comments on the Slab Setup	5-11
5.4.2 Plate-Bearing Test	5-12
5.4.3 Core Test	5-13
5.4.4 Third-Point Loading test on Sawn Beams	5-14
5.5 Theoretical Analysis	5-14

Chapter 6: Effect of Steel Fiber Content on Properties of Concrete

6.1 Background	6-1
6.2 Results	6-1
6.3 Discussion	6-1
6.3.1 Workability	6-1
6.3.2. Compressive Strength	6-2
6.3.3 Modulus of Rupture	6-3
6.3.4 Modulus of Elasticity	6-3
6.3.5 Toughness	6-4
6.4 Conclusion	6-5

Chapter 7: Results of Slab test

7.1 Background	7-1
7.2 Full-scale Slab Test	7-1
7.2.1 Results	7-1
7.2.2 Comparison between the Slabs	7-2
7.2.2.1 Load Capacity	7-5
7.2.2.2 Deflection Characteristics	7-6
7.2.2.3 Failure Characteristics	7-10
7.3 Compressive Strength Test on Cores	7-11
7.3.1 Results	7-12
7.3.2 Strength variation	7-12
7.3.3 Mode of Failure	7-12
7.3.4 Strength gain	7-13
7.3.5 Conversion Formula	7-14





7.4 Third-Point Loading Test on Sawn Beams	7-14
7.4.1 Results	7-14
7.4.2 Capacity	7-15
7.4.3 Toughness Characteristics	7-16
7.4.4 Modulus of Elasticity	7-18
7.4.5 Mode of Failure	7-18
7.4.6 Empirical Formula for Flexural Strength	7-18
7.5 Conclusion	7-19
7.5.1 Full-scale Slabs	7-19
7.5.2 Cores	7-19
7.5.3 Sawn Beams	7-20

Chapter 8: Comparison Between Practice and Theory

8.1 Background	8-1
8.2 Results	8-1
8.2.1 Westergaard K-value	8-1
8.2.2 Characters Used for Analysis	8-2
8.2.3 Interior Load Capacity	8-2
8.2.4 Edge and Corner Load Capacity	8-3
8.2.5 Deflection	8-3
8.3 Comparison Between Theory and Practice	8-4
8.3.1 Westergaard	8-4
8.3.1.1 Load Capacity	8-4
8.3.1.2 Deflection	8-6
8.3.1.3 Failure Characteristics	8-8
8.3.2 Meyerhof	8-9
8.3.2.1 Load Capacity	8-9
8.3.2.2 Deflection	8-11
8.3.2.3 Failure Characteristics	8-11
8.3.3 Falkner et al	8-13
8.3.3.1 Load Capacity	8-13
8.3.3.2 Failure Characteristics	8-14
8.3.4 Shentu et al	8-15
8.4 Conclusions	8-16





Chapter 9: Conclusions and Recommendations

9.1 Background	9-1
9.2 Conclusions	9-1
9.2.1 Literature Reviwed	9-1
9.2.2 Fffect of Steel Fiber Content on Properties of Concrete	9-2
9.2.3 Slab Test	9-2
9.2.4 Comparison Between Theory and Practice	9-3
9.3 Recommendation	9-4

Chapter 10: List of References

Chapter 11: Appendices

Appendix A Systematic Approach for SFRC Mixes Proportioing	11-1
Appendix B Flexural Strength Ratio	11-3
Appendix C First Crack Determination Technique	11-5
Appendix D Example of Modulus of Elasticity calculation	11-8
Appendix E Example of Theoretical Analysis Calculation	11-10
Appendix F Properties of Concrete Used for the Slabs	11-14



List of Figures

	Page
Figure 2-1: Types and Notations of Steel Fibers.	2-2
Figure 2-2: Mixing Sequences for SFRC.	2-5
Figure 2-3: Schematic Diagram Showing the (ASTM C1018) Toughness Parameters (Chen et al).	2-7
Figure 2-4: Schematic Diagram Showing the (JSCE-SF4) Toughness Parameters (Chen et al).	2-8
Figure 2-5: Schematic Load-Deflection Diagram.	2-10
Figure 2-6: S-N Relationship Based on First Crack Strength (Johnston et al).	2-12
Figure 2-7: Effect of Strain-Rate and Fiber Content on Flexural Strength (Gopalaratnam et al).	2-14
Figure 2-8: Shows the Influence of the Steel Fibers on Shear Capacity of Edges (Grondziel).	2-17
Figure 5-1: Test Set-up: Third-Point Loading Test.	5-5
Figure 5-2: Photo Shows the General Test Setting: Full-scale Test (Interior Load).	5-8
Figure 5-3: Photo Shows the General Tests Setting: Full-scale Test (Corner Load).	5-9
Figure 5-4: Loading and Measuring Points: Full-scale Test.	5-10
Figure 5-5: Diagram of Stratton to Correct for Bearing-Plate Size.	5-12
Figure 6-1: Effect of Steel Fibers Dosage on Workability.	6-2
Figure 6-2: Effect of Steel Fibers Dosage on Compressive Strength at 7 Days.	6-2
Figure 6-3: Effect of Steel Fibers Dosage on Compressive Strength at 28 Days.	6-3
Figure 6-4: Effect of Steel Fibers Dosage on Modulus of Rupture.	6-3
Figure 6-5: Effect of Steel Fibers Dosage on Modulus of Elasticity.	6-4
Figure 6-6: Effect of Steel Fiber Dosage on First Crack Strength.	6-4
Figure 6-7: Effect of Steel Fiber Dosage on Toughness.	6-5
Figure 7-1: Relationship Between Depth of SFRC and Plain Concrete Slabs.	7-2
Figure 7-2: Full-scale test: Load-Deflection Diagram	

	(Interior Loading-Test 1).	7-3
Figure 7-3:	Full-scale Test: Load-Deflection Diagram	
	(Edge Loading-Test 2).	7-3
Figure 7-4:	Full-scale test: Load-Deflection Diagram	
	(Load @ 150mm from corner angle bisector-Test 3).	7-4
Figure 7-5:	Full-scale Test: Load-Deflection Diagram	
	(Load@ 300 mm from corner angle bisector-Test 4).	7-4
Figure 7-6:	Load capacity of the Slabs at First Crack.	7-5
Figure 7-7:	Load Capacity of the Slabs at Max. Load.	7-6
Figure 7-8:	Deflection at Loading Point (at First Crack).	7-6
Figure 7-9:	Deflection at Loading Point (at maximum load).	7-7
Figure 7-10:	Deflection Profile at First Crack (Interior Loading-Test 1).	7-8
Figure 7-11:	Deflection Profile at Maximum Load	
	(Interior Loading –Test 1).	7-8
Figure 7-12:	Deflection Profile at First crack (Edge Loading-Test 2).	7-8
Figure 7-13:	Deflection Profile at maximum Load	
	(Edge Loading –Test 2).	7-9
Figure 7-14:	Deflection Profile at First Crack (Corner at 150 mm-Test 3).	7-9
Figure 7-15:	Deflection Profile at Maximum Load	
	(Corner at 150 mm-Test 3).	7-9
Figure 7-16:	Deflection Profile at First Crack (Corner at 300 mm-Test 4).	7-10
Figure 7-17:	Deflection profile at Maximum load	
	(Cornet at 300 mm-Test 4).	7-10
Figure 7-18:	Strength gain for SFRC and Plain Concrete.	7-13
Figure 7-19:	Stress-Deflection Diagram: Third-Point Loading test	
	(IS&IP-Inner Beams).	7-17
Figure 7-20:	Stress-Deflection Diagram: Third-point Loading Test	
	(OS&OP-Outer Beams).	7-17
Figure 8-1:	Stress-Deflection diagram: Plate-Bearing Test	
	on Foamed Concrete Sub base.	8-1
Figure 8-2:	Measured Load and Westergaard Load For SFRC Slab.	8-4
Figure 8-3:	Measured Load and Westergaard Load for Plain Concrete Slab.	8-5
Figure 8-4:	Sub grade Reaction- Load Capacity Relationship (Westergaard).	8-5

Figure 8-5:	Calculated and Measured Deflections at Westergaard Load for SFRC slab.	8-7
Figure 8-6:	Calculated and Measured Deflections at Westergaard Load for Plain Concrete Slab.	8-7
Figure 8-7:	Measured Load and Meyerhof Load for SFRC Slab.	8-9
Figure 8-8:	Measured Load and Meyerhof Load for Plain Concrete Slab.	8-10
Figure 8-9:	Failure Mechanism for Meyerhof Model.	8-12
Figure 8-10:	Measured Load and Falkner et al Load for SFRC and Plain Concrete Slabs.	8-13
Figure 8-11:	Principle Load-Deflection Behaviour and Failure Mechanism (Falkner et al).	8-14
Figure 8-12:	Measured Load and Shentu et al Load for SFRC and Plain Concrete Slabs.	8-15
Figure 8-13:	Sub grade Reaction-Load Capacity Relationship (Shentu et al).	8-16
Figure C-1:	Load-Deflection Diagram for the Plain Concrete Slab Corner.	11-6
Figure C-2:	Load-Deflection Diagram for the Normalized Data.	11-6
Figure C-3:	Load- R^2 Diagram.	11-7
Figure D-1:	Load-Deflection Diagram for the Sawn SFRC Beam (IS).	11-9
Figure D-2:	Slope Determination for the Elastic Zone of Sawn SFRC Beam (IS).	11-9
Figure F-1:	Third-Point Loading Test: Load-Deflection Diagram (SF.1).	11-15
Figure F-2:	Third-Point Loading Test: Load-Deflection Diagram (SF.2).	11-15
Figure F-3:	Third-Point Loading Test: Load-Deflection Diagram (SF.3).	11-16
Figure F-4:	Third-Point Loading Test: Load-Deflection Diagram (SF.4).	11-16
Figure F-5:	Third-Point Loading Test: Load-Deflection Diagram (SF.5).	11-16
Figure F-6:	Third-Point Loading Test: Load-Deflection Diagram (SF.6).	11-17
Figure F-7:	Third-Point Loading Test: Load-Deflection Diagram (P.C.1).	11-18
Figure F-8:	Third-Point Loading Test: Load-Deflection Diagram (P.C.2).	11-18
Figure F-9:	Third-Point Loading Test: Load-Deflection Diagram (P.C.3).	11-18
Figure F-10:	Third-Point Loading Test: Load-Deflection Diagram (P.C.4).	11-19
Figure F-11:	Third-Point Loading Test: Load-Deflection Diagram (P.C.5).	11-19
Figure F-12:	Third-Point Loading Test: Load-Deflection Diagram (P.C.6).	11-19



List of Tables

	Page
Table 4-1: Results from Similar Previous Tests (Kaushik 1989)._____	4-6
Table 4-2: Results from Similar Previous Tests (Beckett 1990)._____	4-6
Table 4-3: Results from Similar Previous Tests (Falkner et al 1995)._____	4-7
Table 4-4: Results from Similar Previous Tests (Beckett 1999)._____	4-9
Table 5-1: Constituents of the Used Mix._____	5-2
Table 6-1: Effect of Steel Fiber Dosage on Properties of Concrete._____	6-1
Table 7-1: Strength Properties of Slabs Mix._____	7-1
Table 7-2: Full-scale Test Results._____	7-1
Table 7-3: Compressive Strength Test on Cores Taken from the Slabs._____	7-12
Table 7-4: The JSCE-SF4 Characteristics for Beams Sawn from the Slabs._____	7-15
Table 8-1: Properties of the Slabs Mix._____	8-2
Table 8-2: Calculated Interior Load Capacity for Various K-values._____	8-2
Table 8-3: Calculated Edge and Corner Load for Various K-values._____	8-3
Table 8-4: Deflection for Various K-values (Using Westergaard)._____	8-3
Table B-1: Equivalent Strength Ratios for Various Steel Fiber Dosages (Hook-ended Steel Fibers)._____	11-3
Table B-2: Equivalent Flexural Strength Characteristic (Hook-ended Steel Fibers)._____	11-4
Table F-1: Cube Compressive Strength for SFRC and Plain Concrete._____	11-14
Table F-2: Results from Third-Point Loading Test (SFRC Beams)._____	11-14
Table F-3: Results from Third-Point Loading Test (Plain Concrete Beams)._____	11-17





List of Equations

	Page
Equation 2-1: Design Flexural Strength for SFRC.	2-11
Equation 2-2: Equivalent Flexural Strength for SFRC.	2-11
Equation 2-3: Equivalent Flexural Strength Ratio for SFRC.	2-11
Equation 2-4: Compressive Strength of SFRC as Function of Steel Fiber Dosage and Compressive Strength of Parent Plain Concrete.	2-15
Equation 2-5: Modulus of Elasticity Calculated from Third-Point Loading Test.	2-18
Equation 2-6: Efficiency Factor for the SFRC.	2-19
Equation 4-1: Westergaard Maximum Interior Strength.	4-2
Equation 4-2: Westergaard Maximum Elastic Deflection (Interior load).	4-2
Equation 4-3: Westergaard Maximum Edge Strength.	4-2
Equation 4-4: Westergaard maximum Elastic deflection (Edge Load).	4-2
Equation 4-5: Westergaard Maximum Corner Strength.	4-2
Equation (4-6): Westergaard Maximum Elastic Deflection (Corner Load).	4-2
Equation 4-7: Radius of Relative Stiffness as Given by Westergaard.	4-2
Equation 4-8: Meyerhof Maximum Interior Load.	4-3
Equation 4-9: Meyerhof Maximum Edge Load.	4-3
Equation 4-10: Meyerhof Maximum Corner Load.	4-3
Equation 4-11: Limit Moment of Resistance for Plain Concrete Slab.	4-3
Equation 4-12: Limit Moment of Resistance for SFRC Slab.	4-3
Equation 4-13: Falkner et al Equation for Slab's Ultimate Load Capacity.	4-4
Equation 4-14: Shentu et al Equation for Slab's ultimate Load capacity.	4-5
Equation 5-1: Modulus of Rupture.	5-3
Equation 5-2: Flexural Strength as function of the Moment and the Modulus of Section.	5-6
Equation 5-3: Flexural Strength of SFRC as a Function of the Moment and Depth.	5-6
Equation 5-4: Flexural Strength of Plain Concrete as Function of the Moment and Depth.	5-6



Equation 5-5:	Relationship Between the Depth of the SFRC and Plain Concrete Slab.	5-7
Equation 5-6:	Modulus of Sub grade Reaction Derived from Bearing-Plate of 250 mm Diameter.	5-13
Equation 5-7:	Modulus of Sub grade Reaction Corrected to Bearing-Plate of 750 mm Diameter.	5-13
Equation 5-8:	Actual Cube Strength Derived from Vertical Cores.	5-13
Equation 5-9:	Potential Cube Strength Derived from Vertical Cores.	5-13
Equation 7-1:	Flexural Strength as Function of Cube Strength.	7-18
Equation 8-1:	Radius of Circumferential Crack for Interior Load (As Given by Westergaard).	8-9
Equation 8-2:	Moment of Resistance for SFRC Corner as Suggested by British Concrete Society Technical Report No. 34.	8-10
Equation 8-3:	Radius of Circumferential Crack for Interior Load (As Given by Meyerhof).	8-12
Equation 9-1:	Ground Slab's Joint Efficiency.	9-4
Equation A-1:	Relationship between Steel Fiber Dosage and the Required Coating Paste.	11-2
Equation A-2:	Cement Content in the SFRC Mixture.	11-2
Equation A-3:	Aggregate Content in the SFRC Mixture.	11-2
Equation A-4:	Water Content for the SFRC Mixture.	11-2
Equation B-1:	Empirical Formula to calculate the Equivalent Flexural Strength Ratio For SFRC.	11-4
Equation D-1:	Modulus of Elasticity Calculated from Third-Point Loading Test.	11-8

Chapter 1

Introduction

1.1 Background

Steel Fiber Reinforced Concrete (SFRC) is defined as concrete containing randomly oriented discontinuous discrete steel fibers.

Historically, many types of fibers have been used to reinforce brittle materials. Straw was used to reinforce sun-baked bricks; horse-hair was used to reinforce plaster and more recently, asbestos fibers are being used to reinforce Portland cement ^[1]. At various intervals since the turn of the 20th century short pieces of steel have been included within concrete in an attempt to increase the tensile strength and ductility ^[2]. Studies to determine strength properties of SFRC and mortar began in the laboratories of the Portland Cement Association in the late 1950's ^[3]. During the late 1960's and early 70's, fiber reinforced concrete was studied and tested extensively, and subsequently was used in a variety of demonstration projects in the USA ^[4].

Although the technology has been broadly accepted and the advantages of the SFRC are well recognized, the actual practical usage in South Africa is still in its young stages. The real usage of SFRC started in 1992, when a hundred segmented SFRC rings (with fiber dosage of 50 kg/m³) were used in the Delivery Tunnel North (D.T.N.) section of Lesotho High Water Project (L.H.W.P.). This tunnel was designed to secure future water supplies to the area of Pretoria and Johannesburg. It is stated that the inclusion of the steel fiber has reduced shrinkage cracks and the incidents of corner break-offs compared to the very first segments at the beginning of the project where rings contained no steel fibers ^[5].

This research contains a discussion of the behavioral properties of the SFRC and the possible effects of these properties on the performance of ground slabs constructed with the material.

The cost is always the major issue controlling designs and development of infrastructure. A reduction of design thickness and increasing the maintenance intervals are normally associated with SFRC. Optimizing the strength and fatigue characteristics, which is possible by using various steel fiber dosages, can minimize

the cost.

The focus of this research is to evaluate the capacity and behaviour of SFRC used for ground slabs. The evaluation was conducted using a comparative approach, on which two full-scale slabs were theoretically and physically analyzed.

1.2 Objectives of Study

The general objective of this research is to evaluate the usage of SFRC for ground slabs and to give broader ideas about its behaviour in comparison to that of normal conventional concrete. The core objectives are to:

- Determine the influence of the steel fiber dosage on the properties of concrete. The properties measured include workability, compressive strength, modulus of rupture, modulus of elasticity and toughness characteristics.
- Compare the bearing capacity, deformation characteristics and mode of failure of slabs with and without steel fibers. The comparison is also aimed to evaluate the influence of low dosages SF (as low as 15 kg/m^3).
- Compare the strength development, mode of failure of the concrete used in the slabs and compare the measured values to theoretical values.
- Compare the calculated results using theoretical models of Westergaard, Meyerhof, Falkner et al and Shentu et al to the measured results from the full-scale test and to assess the capability for each model when applied to the SFRC.

1.3 Scope and Limitations of Study

The scope of this research covers plain concrete and SFRC mixtures fabricated using Portland cement, pozzolan, fine and coarse aggregates and water. Hook-ended steel fibers with various contents (ranging between 0 and 30 kg/m^3) are added to manufacture the SFRC mixture.

The effect of steel fiber dosage on workability, compressive strength, modulus of rupture, modulus of elasticity and toughness characteristics is studied using mixtures containing steel fiber dosage between 0 and 30 kg/m^3 .

Two slabs, the first slab containing 15 kg/m^3 of steel fiber and second slab containing no fiber is loaded at four points on each slab. Slabs are subjected to a curing condition similar to those found in normal construction sites. Specimens are either cast or taken from the slabs. The cast samples had standard curing conditions while the sawn or cored ones had curing conditions similar to the slabs.

Only a semi static loading scenario is investigated, with the load applied gradually at a low rate. In the case of full-scale testing, only single loading plate configuration is considered.

The two slabs are not completely simulating the field situation because of the limited dimensions, unconstrained edges and corners. Moreover, the subgrade reaction of the underlying layers is greater than the usual values found in the field. The stiff foundation consists of solid floor and foam concrete subbase layers.

The literature is also reviewed from a ground slabs perspectives. Many aspects concerning SFRC not relevant to ground slabs are not discussed or included. Several theoretical methods are found, but only four theoretical methods are included and used in the comparative study. These models are Westergaard, Meyerhof, Falkner et al, and Shentu et al.

1.4 Study Methodology

Steel fibers with dosages ranging between 0 and 30 kg/m^3 are added to a 30 MPa mix. Standard beams and cubes are cast for each fiber dosage and tested for tensile strength at 28 days and compressive strength at 7 and 28 days respectively.

For the slab test, two approaches were followed by this research to compare the SFRC and the plain concrete:

- (a) Experimental approach
- (b) Analytical approach

In the experimental approach, full-scale slab tests are conducted on two slabs having identical mix (30 MPa). The first is a plain concrete slab 150mm thick and the second is a SFRC slab 125mm thick containing 15 kg/m^3 hook-ended steel fibers. Both slabs are subjected to interior edge and corner load. The interior of the slabs is loaded after 28 days while the edges and corners are tested after 90 days. Cores are drilled from the slabs and tested for compressive strength. Beams are sawn from the

edge, interior and tested for tensile strength. The cores and beams are tested after 90 days at the time of testing the edges and corners.

The analytical approach utilized either measured or fairly estimated data to serve as inputs to theoretical models of Westergaard, Meyerhof, Falkner et al and Shentu et al. Theoretical analysis is performed using these four models to compare the measured load capacities and deflection with the calculated ones.

1.5 Need for research in this field

The rapid increase in traffic and load on pavements in the recent years, necessitate some sort of modifications to pavement materials to cope with these new issues. SFRC could improve engineering properties, resulting in better performance under traffic and load.

Despite of the wide range of lab information available, the information is fragmented and research concentrate on SFRC as material rather than its applications.

Full-scale tests are more realistic and give a broader idea about the tested element. They are also more relevant to the field of pavements. Few tests are conducted to clarify and address issues such as load capacity and deformation characteristics for the SFRC.

This research is essential; as similar tests and investigations using the South African material are rare or/and not exists.

1.6 Organization of Dissertation

The dissertation has been divided into ten chapters as follows:

Chapter 1: serves as an introduction to the dissertation.

Chapter 2: consists of an introduction to the steel fibers and SFRC. The engineering properties of the SFRC are also discussed.

Chapter 3: the SFRC pavement design methods, distresses, review for previous projects and economical implications are included.

Chapter 4: includes the basic theoretical analysis methods used in the comparison between SFRC and plain concrete.

It also contains the similar previous full-scale tests conducted by other researchers.



Chapter 5: contains the experimental procedure and tests setting.

Chapter 6: contains the study of the influence of steel fiber dosage on
mechanical properties of concrete

Chapter 7: contains the results and discussion of the full-scale slab tests.

Chapter 8: contains the result and discussion of the comparison between
practice and theory.

Chapter 9: contains the ultimate conclusion of the study and the
recommendations.

Chapter 10: comprises the list of references.

Chapter 11: appendices contain various calculations, tables and design
formulas are provided in this chapter and referred to the main
body and after body of the dissertation.



Chapter 2

Steel Fiber Reinforced Concrete

2.1 Synopsis

Different types of steel fibers can be used to reinforce concrete. Steel fibers are generally classified depending on their manufacturing method. Hooked-end stainless steel has proven to give the best performance. The addition of steel fibers to concrete necessitate an alteration to the mix design to compensate for the loss of workability due to the extra paste required for coating the surface of the added steel fibers. While many technical and economical advantages are benefited from using SFRC, drawbacks can also be found. They are however not likely to cause major problems. It was thought that steel fibers will have negative implications in concrete practice (i.e. transporting, surfacing, finishing etc), but experience has shown that the influence of steel fibers on these practical aspects is negligible.

Dispersion of steel fibers in concrete alter its engineering characteristics. The after-crack mechanism associated with the SFRC positively influences its mechanical and physical properties. The improvement differs depending upon the dosage and the steel fiber parameters considering the other strength-determining factors to be constant.

2.2 Steel Fibers

There are a number of different types of steel fibers with different commercial names. Basically, steel fibers can be categorized into four groups depending on the manufacturing process viz: cut wire (cold drawn), slit sheet, melt extract and mill cut. It can also be classified according to its shape and/or section. Various notations were previously used to nominate the specific type of the steel fibers but in this dissertation the following notations are used:

- (h x w x l) to nominate the straight rectangular section steel fibers. The letters h, w and l stand for section depth, width and the fiber length respectively.
- (d x l) was used to name circular or semi-circular section straight or deformed steel fibers, d and l stand for diameter and length respectively.
- Hook-ended steel fiber (i.e. 80/60 H means aspect ratio/Length of steel fiber).

The popular shapes, sections used and the recent standard notations are compiled in figure 2-1.


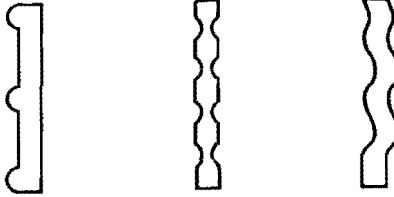
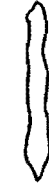
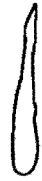
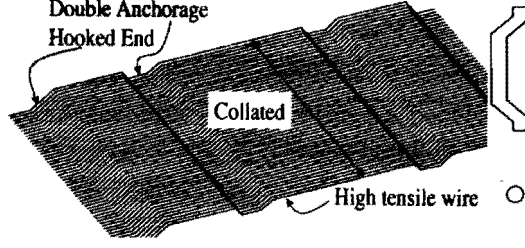




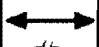






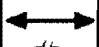






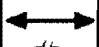



Straight slit sheet or wire	Deformed slit sheet or wire	Machined chips													
 □ or ○	 □ ○ ○ or ◡	 ◡													
Melt extract	Hooked-end wire (Crimped)	Enlarged-end													
 ◡															
Steel Fiber Manufacturers Notations															
<table border="1" style="width: 100%; border-collapse: collapse;"> <tr> <td style="text-align: center;">C Collated </td> <td style="text-align: center;">H Hooked End </td> <td style="text-align: center;">D Double Anchorage </td> <td style="text-align: center;">8060 Aspect Ratio l/d</td> <td style="text-align: center;">N Length </td> <td style="text-align: center;">B Normal Low Carbon</td> <td style="text-align: center;">B Bright Steel</td> </tr> </table> <table border="1" style="width: 100%; border-collapse: collapse;"> <tr> <td style="text-align: center;">R </td> <td style="text-align: center;">C </td> <td style="text-align: center;">-65/35- 45 65 80 l/d</td> <td style="text-align: center;">B </td> <td style="text-align: center;">N Bright</td> <td style="text-align: center;">Low Carbon</td> </tr> </table>			C Collated 	H Hooked End 	D Double Anchorage 	8060 Aspect Ratio l/d	N Length 	B Normal Low Carbon	B Bright Steel	R 	C 	-65/35- 45 65 80 l/d	B 	N Bright	Low Carbon
C Collated 	H Hooked End 	D Double Anchorage 	8060 Aspect Ratio l/d	N Length 	B Normal Low Carbon	B Bright Steel									
R 	C 	-65/35- 45 65 80 l/d	B 	N Bright	Low Carbon										

Figure 2-1: Types and Notations of Steel Fibers

Major efforts have been made in recent years to optimize the shape and size of the steel fibers to achieve improved fiber-matrix bond characteristics and to enhance fiber dispersability ^[6]. It was found that SFRC containing hook-ended stainless steel wires has better physical properties than that containing straight fibers. This is attributed to the better anchorage provided and higher effective aspect ratio than that for the equivalent length of straight fiber ^[7]. In addition, the high tensile stresses localized at cracks necessitate that steel fibers have high tensile strength. Typical steel fiber tensile strengths are ranged between 1100 and 1700MPa.

Apart from other mix constituents, there are four important parameters found to affect the properties of, namely, type and shape of fibers, dosage, aspect ratio, and orientation of fibers in the matrix. The effect of each shall be clarified when discussing the physical and mechanical properties of SFRC.

2.3 Mix Design

The main objective in designing a structural fiber concrete mix is to produce adequate workability, ease of placing and efficient use of fibers as crack arrestors, besides the other objectives desired in any normal concrete.

Preliminary trial mixes indicated that the addition of steel fibers to a properly designed concrete mix reduced the slump. To maintain the level of workability and to ensure adequate bond of the fibers to the concrete matrix, it was concluded that the addition of steel fiber to the concrete mix should be accompanied by the addition of cement paste. The amount of added cement paste depends on three principal factors as follows ^[3]:

- Amount of fibers.
- Shape and surface characteristics of the fibers.
- Flow characteristics of the cement paste.

The concept of coupling is used to design mixes having steel fibers. In other words, normal concrete mix proportioning criteria's can be used for the designing of trail mix; thereafter the workability can be adjusted when adding steel fibers.

The mechanistic mix proportioning design method, introduced by the Portland Cement Association in 1977 ^[3] was based on three principles:

- (a) The addition of steel fibers should be accompanied by the addition of an amount of cement paste sufficient to coat the fibers and to ensure their

bond in the concrete mix.

(b) The added fibers and cement paste should be treated as a replacement for an equivalent volume of the plain concrete mix and.

(c) Water cement ratio in both plain and SFRC mixes remains unchanged.

The method is given in Appendix A

A holistic mix proportioning approach does not exist yet and the reason for this could be the large variety of steel fiber types available, as well as the high number of parameters influenced by the use of SFRC. In practice an indication of the mix proportioning is normally given. It has been recommended that large aggregates (38mm) are suitable for SFRC pavements bearing in mind that the steel fibers should have lengths greater than the largest aggregates ^[4]. The ACI committee has given the following guidelines to serve the purpose of SFRC mix design ^[8]:

- Coarse aggregates should be limited to 55% of the total aggregate.
- W/C should be kept below 0.55 (0.35 is recommended).
- Minimum cement content of 320 kg/m³ should be used.
- Reasonable sand content of 750 – 850 kg/m³ is recommended.
- The workability could be improved by increasing the cement paste, which is possible by addition of slag or fly ash to replace the cement.
- Maximum aggregate size is to be 19 mm.

2.4 Advantages and Disadvantages

Generally the increase of ductility, toughness, strength, fatigue endurance, deformation characteristics are the reasons for major saving in time, cost, and materials when using the SFRC ^{[9] [10] [11]}.

Despite of SFRC excellence and superiority, drawbacks exist. Loose fibers at the hardened surface might be blown onto aircraft engines or tyre, which leads to unsafe operation. Injury to personnel being scraped or cut by an exposed fiber while working on the concrete surface is also possible, however, no accident has been reported regarding any of the above two scares ^[4]. Packard et al ^[12] reported that, the residential street project was overlaid due to complaints from some residents because children suffered skin abrasions from falls on the pavements. Safety equipment is recommended to protect the personnel during construction ^[1], magnetic fields can be used to collect the loose fiber prior to opening to traffic ^[4] and finishing techniques

can be applied to knock fibers down while surfacing ^[13]. Another possible drawback, at aggressive exposure conditions, is that corrosion of the surface could take place, eventually influencing the appearance of the surface ^[14].

2.5 Practical aspects

Steel fibers should be dispersed with care to avoid clumping and non-homogeneity. Based on previous experience, possible non-problematic sequences were given by the ACI committee 544 ^[1]. The procedure is summarized in the diagram in figure 2-2.

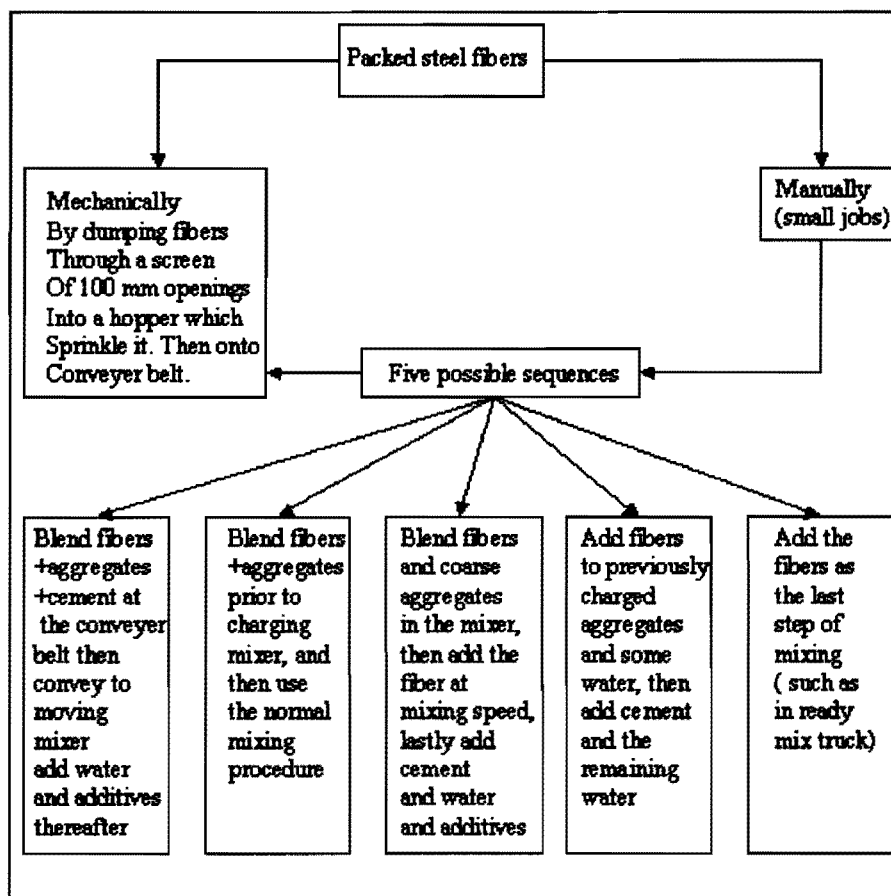


Figure 2-2: Mixing Sequences for SFRC

The addition of steel fibers to concrete reduces the workability, as additional water and cement are required to coat the surfaces of these steel fibers. Edgington et al found that the conventional slump test is unsatisfactory; they further recommended the V-B time method due to its merit in simulating field compaction ^[2]. ACI

Committee 544 recommended the use of inverted slump cone procedure. The test involves, the conventional cone inverted, centered and rigidly held by supports so that the small end of the cone is 4 inch (76 mm) above the bottom of a 1-cubic-foot (0.02832 cubic m) yield bucket. Concrete is to be placed in three un-compacted layers and the time required to empty the cone from the moment a vibrator has contacted the concrete up to the time of the slump cone first becomes empty is recorded. Inverted -slump-cone time should not be less than about 10 seconds or more than 30 seconds. Further details on the test can be found in ASTM C995 ^[15]. The conventional slump cone might however be beneficial to specify the consistency of the concrete. It was found that a slump range between 25 to 100 mm is satisfactory. It was also stated that the appearance of SFRC is deceiving, in other words, although the SFRC looks stiff and unworkable, it can still easily be placed when using the vibrator. Water should therefore not be added relying on the appearance of the concrete ^[8].

SFRC can be transported, placed, and finished using the same equipments and methods used for conventional concrete. In some cases the SFRC was found much easier to deal with for instance, pumping of SFRC is easier and less trouble than that of the plain concrete because of the greater paste content ^[8].

2.6 Mechanical properties

2.6.1 Toughness

Toughness as defined by the ACI committee 544 is the total energy absorbed prior the complete separation of the specimen ^[1]. It can be calculated as the area under the load-deflection curve plotted for beam specimen used in a flexure test. Although, it was well established that the steel fibers significantly improve concrete toughness and it is widely agreed that toughness can be used as a measure of the energy absorption of the material, there is a doubt about the way that SFRC toughness should be measured and used.

Two methods to interpret and calculate the toughness of SFRC are widely used. The ASTM C1018-97 method in which the energy absorbed up to a certain specified deflection is normalized by the energy up to a point of first cracking ^[15]. The Japanese Institute of Concrete standards interprets the toughness in absolute terms, as the energy required to deflect the beam specimen to a mid point deflection of 1/150 of its span ^[16].



The ASTM method evaluates the flexural performance of toughness parameters derived from SFRC in terms of areas under the load-deflection curve obtained by testing a simply supported beam under third-point loading. It provides for determination of a number of ratios called toughness indices that identify the pattern of material behaviour up to the selected deflection. These indices are determined by dividing the area under the load-deflection curve up to a specified deflection by the area up to the deflection at first crack. Schematic diagrams are given in figure 2-3 and figure 2-4 to illustrate the American and the Japanese methods respectively.

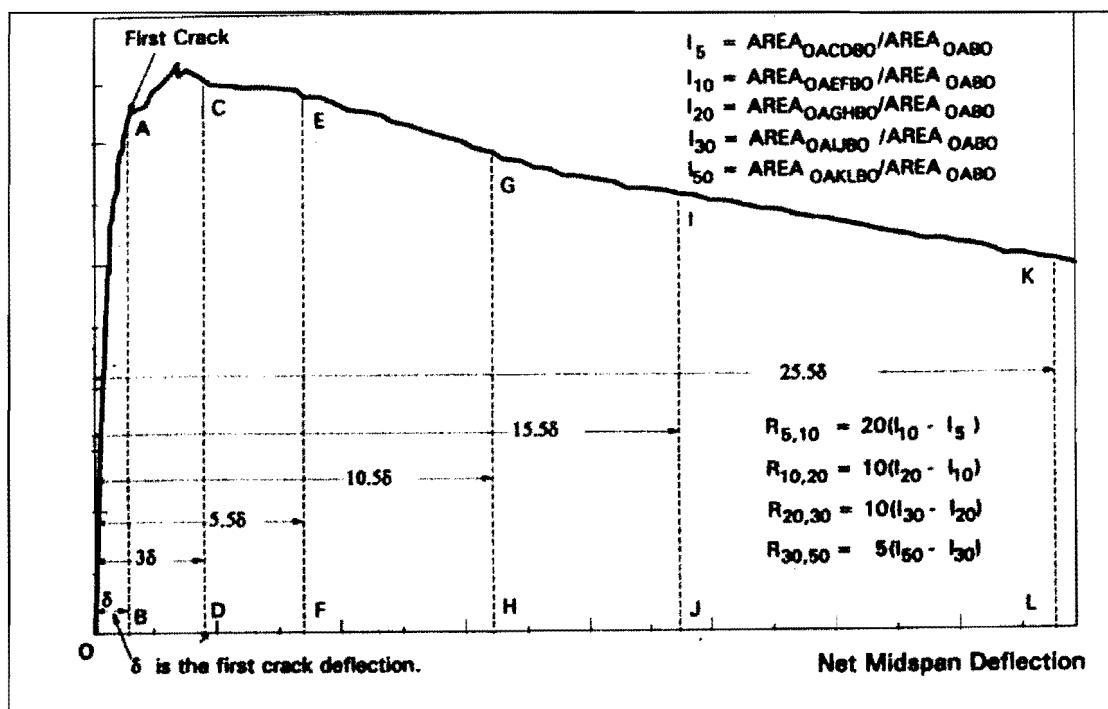


Figure 2-3: Schematic Diagram Showing (ASTM C1018) Toughness Parameters (Chen et al)

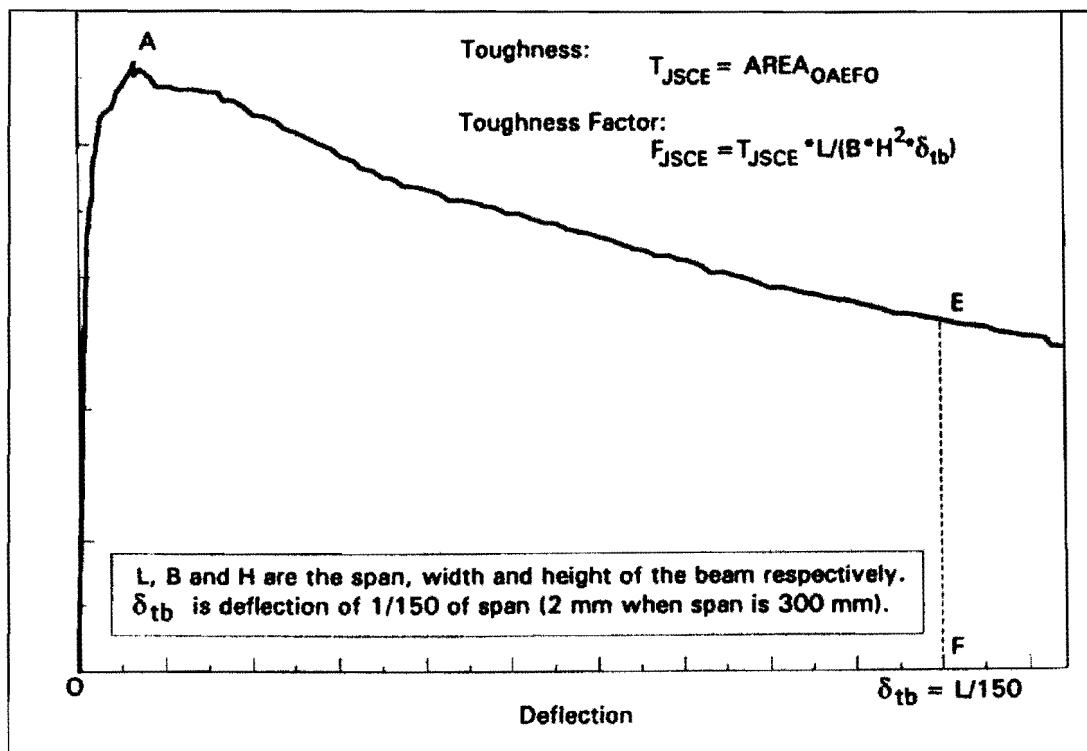


Figure 2-4: Schematic Diagram Showing the JSCE-SF4 Toughness Parameters (Chen et al)

Many criticisms have been directed at the ASTM method. Gopalaratnam et al carried out an investigation on about 750 beams. Two beam sizes (152x152x533 mm) and (102x102x356 mm); each with two different types of fibers and two different fiber contents were used. It was found that the ASTM C1018 is not sensitive to fiber content, fiber type and the size of the specimen. In addition to that the method is more dependent on the measurement accuracy of the deflection. The effect of the extraneous deformations are found to influence the first crack deflection significantly and its effect is less for greater values of deflection on the load-deflection curve, therefore an erroneous first crack deflections leads to unreal values for the area of the curve up to the first crack deflection and eventually an error in measuring the toughness indices. In contrast the JSCE-SF4 approach was found to be sensitive for the specimen size and fiber type and content, moreover, extraneous deformation problem is mitigated by considering higher deflection values (1/150 of the span). The study concluded that the JSCE-SF4 method is more reliable than the ASTM C1018 and recommendations were made for its usage ^[17]. Chen et al also came to the same conclusion, they further added that in some cases the first crack point is difficult to determine. Great uncertainty about the shape of the curve in the

vicinity of the first crack exist, hence indices with in the area (OAEF) as shown in figure 2-3 is questioned ^[18].

2.6.2 Flexural strength

The low flexural strength of plain concrete could possibly be over-come by the addition of steel fibers. A review of the literature on SFRC indicates that in general, the addition of short, randomly-oriented steel fibers increases the flexural strength of plain concrete by about 1.5 to 3.0 times, taking into account type and content of the steel fibers ^{[19] [2] [7]}.

The term flexural strength for SFRC is more complicated compared to that of the plain concrete. Flexural strength for plain concrete is the stress capacity determined through a third-point loading test, which strive to find the stress at maximum load that can be sustained by a prismatic beam. The situation is different when speaking about SFRC due to the after crack toughness imparted by the presence of the steel fibers. One should distinguish between the different terms viz, first crack strength, ultimate strength, and equivalent strength. These terms have different implications to the application of the SFRC and they are indicated in figure 2-5 and defined as follows:

- First crack flexural strength (or some times termed as the proportional limit): recognized as the stress at point at which the load-deflection curve first becomes non-linear.
- Ultimate flexural strength: defined as the stress at the point of maximum load that can be sustained during the third-point test.
- Equivalent flexural strength: It is the stress capacity derived at a point of specific mean load corresponding to specific deflection in a third-point loading test.

Considering a prismatic beam (150x150x450 mm), the values at a deflection of (span/300) and (span/150) ratios are being adopted; therefore, flexural strengths corresponding to these deflection values can be successfully used.

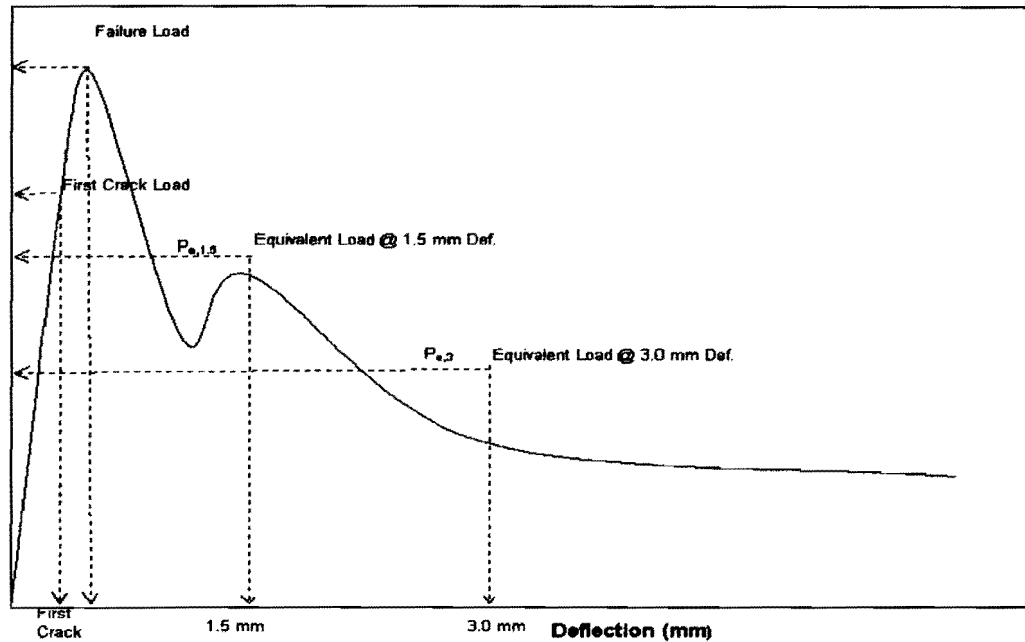


Figure 2-5: Schematic Load - Deflection Diagram

Main factors influencing the flexural strength of SFRC ^[19] are:

- Degree of consolidation of the matrix, which is a function of water to cement ratio, consolidation technique, and type and content of the steel fiber.
- Uniformity of fiber distribution, which is mainly influenced by the workability and mixing procedure used.
- The surface conditions of the steel fibers, which relates to the bond stresses generated between the steel fibers and the concrete, for instance a hydrophobic film on the steel fiber surface can prevent the development of an adequate fiber bond.

Theoretically, the improvement in flexural strength of SFRC is being brought by the crack arresting mechanism that the steel fiber provides. In fact, the steel fibers can sustain stress after cracking at strains beyond the normal for failure of plain concrete. Some sort of stress distribution is promoted which approaches the fully plastic condition in the tension zone, while remaining elastic in the compression zone. This mechanism causes the neutral axis of the section to move up, thus, the moment of resistance and ultimate load be increased significantly ^[20].

Due to the post cracking behavior of SFRC unlike plain concrete, the total flexural strength (design flexural strength) is to be taken as the sum of the flexural strength up to the point after which the elasticity zone of the material is exceeded (first crack strength) and the strength that resulted from the plastic phase (equivalent flexural strength). Equation 2-1, equation 2-2 and equation 2-3 can be used ^[11]:

$$f_d = f_{ct} \left(1 + R_{e,3} / 100 \right) \quad \Longrightarrow \quad \text{Eq.2-1}$$

$$f_d = f_{ct} + f_{e,3}$$

Where :

f_d = Design Flexural Strength.

f_{ct} = First Crack Strength.

$$f_{e,3} = P_{e,3} * \frac{L}{bh^2} \quad \Longrightarrow \quad \text{Eq.2-2}$$

$$R_{e,3} = \frac{f_{e,3}}{f_{ct}} * 100 \quad \Longrightarrow \quad \text{Eq. 2-3}$$

h, b = the depth and width of a uniform prismatic beam.

$P_{e,3}$ = Mean Load Over a Deflection of Length/150.

2.6.3 Fatigue Endurance

Fatigue endurance could be expressed by the so-called S-N curves, where S is the ratio of the maximum stress to the statistic strength and N is the number of the cycles at failure. The maximum value of S below, which no failure occurs, is known as endurance limit ^[21]. Previous investigations ^{[22][23]} have shown that the relationships are linear up to at least 2 million cycles; therefore, the term 2-million cycle endurance limit is commonly used to quantify the fatigue strength of SFRC.

Figure 2-6 shows results of fatigue tests conducted by Johnston et al ^[24] on prismatic specimens with nine different mixtures and varied fiber parameters (type, content, and aspect ratio). It was concluded that, the addition of steel fibers has improved the fatigue endurance of concrete and the improvement ranges between little and significant depending on the fiber parameters.

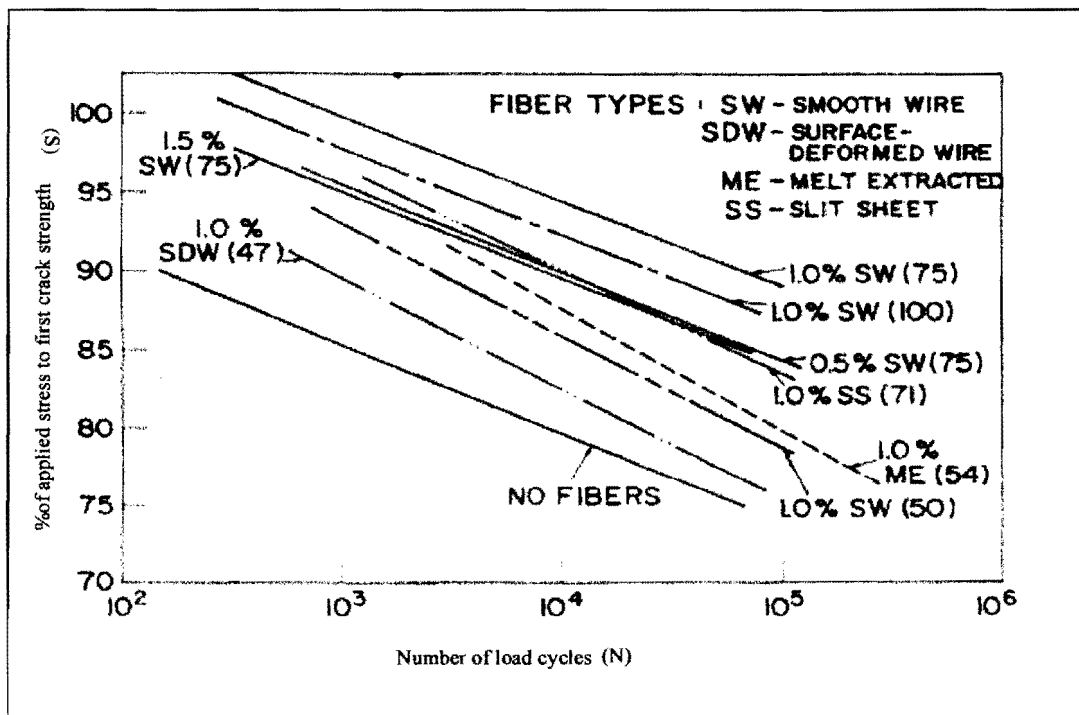


Figure 2-6: S-N relationship based on First Crack Strength (Johnston et al)

Hook-ended steel fibers appeared to have a superior influence in the 2 million-cycle endurance limit. An endurance limit of 76% and 80% were found for 0.5% and 1.0% volumes of hook-ended fibers respectively, whilst, 67% and 59% for similar volumes of slit sheet fibers [23].

The fatigue capacity of plain concrete is generally regarded as equivalent to an endurance limit equal to 50 to 55% of the static modulus of rupture [25]. Thus designs based on half the static strength is appropriate for conventional concrete [26]. By implication either thinner section is required to withstand the same load repetition or the same thickness could last for longer, and that is key benefit behind the usage of SFRC.

Bernard et al [27] suggested that fatigue performance for SFRC, expressed as an endurance limit can conservatively be taken as 65% of the stress to cause the first crack. Schrader [26] argued that the long term strength gain for SFRC is higher than that for the plain concrete, therefore, the fatigue performance should be improved as a result of strength compensation. Eventually it was stated that 85% of the ultimate strength has the same conservatism, as does 50% for conventional concrete.

2.6.4 Impact Strength

Pavements are in many cases subjected to dynamic load either due to the impact nature of the load itself or due to the high rate of gradual load applications. Runways are normally subjected to direct impact loads caused by the landing process and unevenness of aircrafts while roads are subjected to impacts in cases of unevenness, rutting, artificial bumps, and at faulting joints. It is seldom found that a pavement is thoroughly subjected to static loads during its useful life, even aprons and container terminals are subjected to dynamic loads prior to parking of aircrafts or containers respectively.

Although different type of tests and load application rates were employed by different researches, it is widely agreed that the addition of steel fibers improves the impact resistance of concrete. A significant increase was found by using the pendulum machine; the improvement was being especially favorable with crimped fibers ^[2]. Tests carried out using the ACI committee technique ¹ reported that SFRC has increased the impact resistance in order of three to four times relative to their un reinforced counterparts ^{[28] [29]}. In another set of test carried out on concrete slabs with and without steel fibers, supported on their edges, a falling weight was employed from different distanced to represent different energies. The results showed that the SFRC slabs absorbed about 4 times the impact energy of the plain concrete for equivalent damage ^[30].

Gopalaratnam et al ^[31] and Banthia et al ^[32], both came to conclusion that, the impact data is mostly sensitive to the stress-rate, in other words for different stress-rates there are different values for the impact strength. It was also agreed that the higher the rate of the load application the higher the impact resistance for both plain and SFRC, that can be seen from figure 2-6.

¹ The test involves dropping of 10 lb soil compaction hammer 18 inches onto a hardened steel ball placed in the center of the concrete specimen, which measures 6 inches in diameter and 2.5 inches thick. The number of blows required to crack the material is used to quantify the impact resistance of concrete

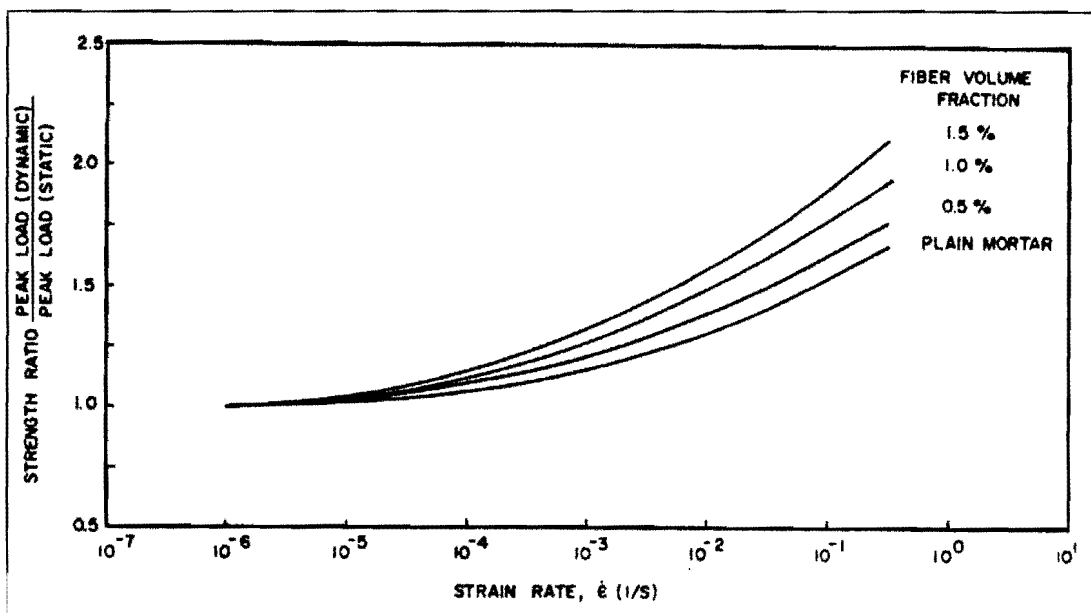


Figure 2-7: Effect of Strain-Rate and Fiber Content on Flexural Strength

(Gopalaratnam et al)

It is apparent from the above discussion that SFRC flexural strengths gained from relatively static load type of tests are less than those obtained from increased stress-rate tests. Designs based on static strengths are therefore satisfactory and safe.

2.6.5 Compressive strength

It has been found by many researchers that the inclusion of steel fiber in concrete increases its compressive strength value relative to the fiber content. Their findings ranged between marginal and significant increases in compressive strength.

Experimental work conducted in India, using straight steel fiber ($L/D = 46/0.91$ mm) and fiber content ranges between (0 and 3% by volume) found that, significant increase in compressive strength is achieved (about 40% increase when using 3% fiber content). More over, test results have shown a linear relation between the fiber content and the compressive strength of the concrete if fiber is being added. The following empirical equation was generated ^[33].

$$F_f = F_c(1 + K_1 P) = F_c * \alpha \quad \longrightarrow \quad \text{Eq.2-4}$$

Where:

F_f = Compressive strength of the SFRC.

F_c = Compressive strength of the parent concrete.

K_1 = Empirical constant (0.123).

P = Percentage of steel fiber (by volume)

α = Amplification factor.

Tests in Australia showed that, the addition of steel fiber to concrete matrix may produce marginal gains in compressive strength at constant water cement ratio. At steel fiber concentrations of (50 to 90 kg/m³) the increase in compressive strength is not usually statistically discernible [30].

Tests, on SFRC cubes made from same mix and containing bent fiber, carried out at the CSIR (South Africa), revealed that the addition of steel fibers with various contents may increase the compressive strength slightly (approximately 10%) and the highest increase occurred at low steel fiber contents (up to 20 kg/m³). In addition of that, specific limits exist after which a reduction or less increase on compressive strength is expected with addition of more steel fibers. In other words an excessive increase of fiber content will not affect the compressive strength as prior to that limit. This confirms that the addition of steel fibers is not a cost effective way of improving the compressive strength of concrete [34].

Results from cubes and cylinders tested in compression might differ significantly because the vibration tends to align the fibers in certain planes. In cylinders they tend to align perpendicular to the axis of loading where they could help to inhibit lateral bursting, while in cubes they tend to align parallel to the axis of loading [20].

According to Edgington et al, fibers in SFRC compacted by means of table vibration have a tendency to align themselves in planes at right angles to the direction of vibration. This indicates, that the method of compaction can be an important parameter influencing the compressive strength of SFRC [2].

Perrie argued that, since the failure is initially due to breakdown at the aggregate interface, fibers are expected to have little effect on compressive strength of concrete [20].

The author's opinion is that, the influence of steel fiber on the compressive strength should be taken as insignificant and the increase in compressive strength developed as the result of the presence of steel fibers should be considered to compensate for the variation of the testing results due to variation of fiber orientation and content in different specimens. Thus, the compressive strength of the parent plain mix should be considered as the target compressive strength.

2.6.6 Shear strength

Steel fibers are found to increase the shear capacity of concrete significantly ^[35] ^[36]. It was found that the inclusion of 1% by volume of hook-ended steel fibers could increase the shear strength of the SFRC by about 144% to 210% relative to the plain concrete depending on the aspect ratio of the steel fibers ^[37]. Punching shear tests show that the addition of 75 kg/m³ of steel fibers with enlarged ends increase the punching resistance by about 51% in comparison to plain concrete ^[30]. The mode of failure is also found to be changed due to the extra-enhanced shear capacity. Ductile failure was experienced instead of sudden diagonal failure ^[36] and in some cases the mode of failure changed from shear failure to a moment failure ^[37].

Shear strength capacity is important for pavements. Corner and edge break-off might occur as the result of exceeding the shear capacity of concrete; storage racking or raised storage legs can also punch on the floor. The knowledge of the shear capacity and behaviour of materials should therefore be applied to pavements. Grondziel ^[38] state that using SFRC at Frankfurt International Airport has virtually eliminated the joint shear failure due to its homogeneity and increased shear strength. He gave the model as shown in figure 2-7 to illustrate the benefit of using SFRC instead of conventionally reinforced concrete.

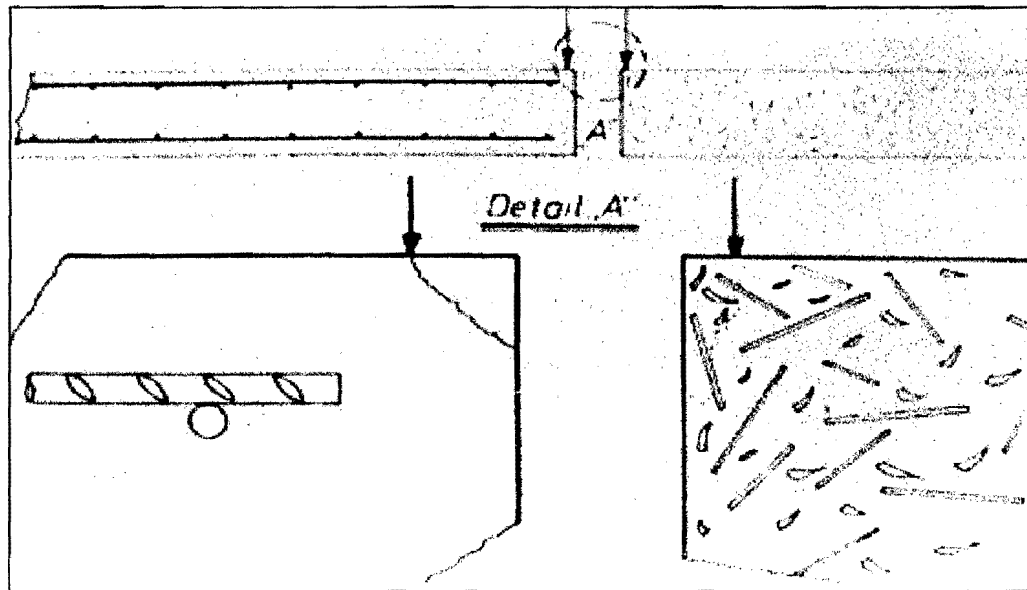


Figure 2-8: Shows the Influence of the Steel Fibers on Shear Capacity of Edges (Grondziel)

Despite the considerable laboratory data indicating that steel fiber is superior as far as the shear capacity and behaviour is concerned, design procedures are found not to consider that increase in shear strength of SFRC and the shear strength of plain concrete is still in use ^[39].

2.6.7 Modulus of Elasticity

The fact that the inclusion of steel fibers in concrete marginally influences the modulus of elasticity is widely agreed upon. Uniaxial tensile stress-strain measurements on (100x100x500 mm) plain and fiber reinforced specimens show an increase of 7.5% for the specimens having a dosage of 2.7% by volume of straight steel fibers ^[2]. Similar results were gained from a third-point test carried out on beam specimens, where it was found that the calculated modulus of elasticity increases very little relative to plain concrete ^[30]. The E-value is found to be in the same order of magnitude than the values for plain concrete from the parent mix ^[3]. Recent studies also show that 0.76% by weight of hook-ended and crimped steel fiber has a positive effect with increase in E-value ranging between 0% and 2.8% ^[40].

Modulus of elasticity could also be found from a third-point loading test as an alternative method to the standard cylinder compression test. It has the advantage that a number of material parameters can be calculated in a single test. The following

formula has been derived to calculate the modulus of elasticity ^[41].

$$E(\text{M.Pa}) = \frac{23}{1296} * \frac{F}{\delta} * \frac{l^3}{I} \left[1 + \frac{216}{115} * \left(\frac{d}{l} \right)^2 (1 + \mu) \right] * 10^3 \implies \text{Eq.2-5}$$

Where:

$\frac{F}{\delta}$ = the slope of the best - fit straight line drawn through the plotted points of the initial portion of the load - deflection curve (N/mm²).

l = support span, (mm).

I = second moment of area of the section $\left(\frac{bd^3}{12} \right)$.

b, d = width and depth of the prism section respectively (mm).

μ = poisson's Ratio

2.6.8 Poisson's Ratio

Poisson's Ratio is the ratio of the lateral strain to the vertical strain. Addition of steel fibers is found to have no or minimal effect on the value of Poisson's Ratio ^[30]. Value ranges between 0.15 and 0.21 are typical values assumed ^[42] or experimentally assessed ^{[30][43]} for SFRC ground floors.

2.7 Physical properties

2.7.1 Shrinkage

Shrinkage is the volume change exhibited by concrete bodies due to the loss of water. Two phases of shrinkage exist, the first one is the plastic shrinkage which takes place prior the final setting and the other one is the drying shrinkage which occurs in the long term ^[21]. Free and restrained are terms usually associated with shrinkage to define the constrain conditions of the concrete body under consideration.

Proof of the ability of steel fibers to limit the plastic shrinkage crack widths is widespread. Numerous investigations have shown that steel fibers reduce the plastic shrinkage crack widths relative to that of plain concrete ^{[44][45]}. Reduction in plastic shrinkage strain was reported to be as high as 20% relative to that of plain concrete ^[27]. Banthia et al have introduced a new concept to quantify shrinkage of concrete in their study on plastic shrinkage of SFRC. A fiber efficiency factor was adopted to compare the shrinkage capability of different concretes and this fibers efficiency

coefficient can be calculated as follows:

$$\text{Fiber Efficiency Factor} = L_c/W \implies \text{Eq.2-6}$$

Where

L_c = Cumulative crack length.

W = Cumulative crack width in the area under consideration

They further found the addition of 0.75 % by volume of crimped steel fibers will result in an effectiveness factor of 146.6 and 8 cracks while plain concrete yielded an effectiveness factor of 14.03 and one crack which proves that steel fibers can distribute cracks more evenly over the entire length resulting in closely spaced reduced widths cracks^[44].

Drying shrinkage strain is of considerable importance to pavement applications because it has a direct contribution to the spacing of the joints. There are conflicting evidences regarding the effectiveness of steel fibers in limiting both free and restrained drying shrinkage strain in SFRC. Edgington et al^[2] found that the shrinkage of concrete over a period of three months was unaffected by the presence of the straight steel fibers used. A study by Grzybowski et al^[46] found that steel fibers does not alter the free drying shrinkage properties of concrete, in the other hand many later investigations have proven that the steel fibers have a significant effect in improving the restrained shrinkage properties of concrete^{[47][48][49]}.

Work was conducted by Chern et al^[47] (on both beams and cylindrical specimens having crimped and straight steel fibers) to study the influence of steel fiber parameters testing age and ratio of the specimen volume to the exposed surface on shrinkage characteristics of concrete. It was found that, steel fibers restrain deformations more effectively at later ages due to the development of higher interfacial bond strength between fibers and matrix. Therefore, the older the SFRC the less shrinkage strains. It was also evident that both higher fiber content and aspect ratio was found to yield less shrinkage than those of lower values.

Despite the efforts directed towards developing a test method to examine shrinkage of slabs, which is more applicable to pavements, no published evidence exists that any substantive tests have been undertaken to quantify drying shrinkage strain in SFRC slabs. Most of the investigations mentioned, employed a ring or beam specimens with, at best, indirect relevance to concrete slabs, as the small cross-

sectional dimensions of the shrinkage moulds can result in preferential alignment of steel fibers in the direction of measured shrinkage. Standard size shrinkage specimens may therefore exhibit strains that are far different from the reality at which fibers are randomly oriented ^[27].

Literature on shrinkage provides different theoretical models to assess the plastic shrinkage strain ^[45], and crack spacing and widths resulting from drying shrinkage of SFRC ^[46] ^[50]. The author's view is that, these models should not be applied to pavements because of the above-mentioned reasons. Further work on shrinkage of slabs should be conducted.

2.7.2 Creep

Creep is the long-term deformation that a material exhibits under the application of a sustained load. Reasons for the concrete to creep are related to the movement of water out of the cement paste and more over, due to the prorogation of micro-cracks ^[21].

Creep studies in compression have been carried out at a number of applied stress-strength ratios ranging between 0.3 to 0.9 using cement paste, mortar and concrete mixes. Melt extract and hooked fibers with volume contents ranging between 0 and 3% (about 0 and 235 kg/m³) were added to the mixes that were used to cast prismatic specimens (150x150x500mm). The results after 90 days loading and 60 days unloading indicate that steel fibers have a significant (ranges between 15 and 24% reduction) influence in restraining the creep of specimens under uniaxial compression. More over, it was reported that, the restraint provided by steel fiber to the creep becomes more pronounced with increasing time under load ^[51].

Contradictory results were obtained on compressive creep test on concrete specimens having straight fibers with volumes ranging between 0 and 1.47 % (0 to 115 kg/m³). Specimens were loaded over 12 months. The results concluded that the effect of steel fibers on creep strains is negligible ^[21].

Flexural creep test on SFRC (75 kg/m³ enlarged end steel fibers) specimens (stress - strength ratios of 0.43 and 0.69), shows that the flexural creep is considerably less than for the identical concrete without steel fiber. The reported ratio of creep strain to load strain for plain concrete after 518 days loading was around 25% higher than for steel fiber reinforced concrete ^[30].

Another series of tests on flexural creep shows that creep strains are much less in the compression zone of a specimen than in tension zone ^[49]. Typically, with 1% percent by volume (about 78 kg/m³) steel fibers and flexural stress-strength ratio of 0.35, creep strains in the tension zone of the specimens ranged between 50 to 60% of the strains in the plain concrete specimens. The creep strains in the compression zone of the steel fiber specimens were 10 to 20% of the plain concrete specimens.

It can be seen that, the steel fibers has a negligible effect when low fiber content is added while a significant improvement is gained with larger amount of steel fibers. It should also be noted that flexural creep is more important than compression creep for ground slabs.

2.7.3 Durability

Porosity and permeability are primary factors affecting the durability of the concrete due to it's effect on alkali-acid reaction, leaching characteristics, resistance to chloride or sulphate attack, reinforcement corrosion, and freezing and thawing characteristics ^[7]. Initially SFRC mixes had high porosities and permeabilities due to the higher W/C used to increase the workability. Recently, reductions in W/C ratio are possible, which result in relatively low porosities and permeabilities. Tests indicated that the SFRC has permeability values typical of those for the plain concrete ^[30], therefore, apart from corrosion of steel fibers, the SFRC has the same durability (if not better) than the identical plain concrete.

Attention has to be given to the question of the corrosion of the steel fibers when added to concrete. Theoretically, one of the main problems associated with the use of steel fibers is their durability in concrete structures. In severe exposure condition, corrosion of steel fibers is more aggravated than that of steel bars, in other words, a significant decrease to the steel fibers diameter, contribute significantly to lessen the load capacity of the structure at service ^[52]. In contrast, unlike steel bars, only limited expansion force develops due to the corrosion of steel fibers ^[14], which means less paste disruption and eventually minimal breakdown and weathering rates in comparison to conventional concrete reinforced by steel bars ^[27].

There is ample evidence that in practice, in good quality concrete, fibers corrosion does not penetrate into the concrete. Laboratory studies have shown that, stainless steel fibers can perform well even in a very aggressive type of exposure conditions

while the carbon steel fibers invite the corrosion and cracks development ^[53]. SFRC specimens exposed to a marine environment for about 10 years, show that the corrosion of fibers is limited to the surface of the un-cracked specimens and no noticeable reduction in flexural strength was found, whilst, for cracked specimens, corrosion does occur through the depth of the crack and reduction on flexural strengths were encountered ^[54].

Under normal finishing processes very few fibers will be left exposed at the surface of slabs and any such fibers exposed to the surface is assumed to corrode and blow away under trafficking ^[39]. Schupack found that the corrosion depth is usually confined to the first 5 mm ^[54], therefore, designs should consider cover depths of about 10 mm apart from recommending the knocking down of steel fibers while finishing the concrete surface.

2.7.4 Abrasion and Skid Resistance

Knowledge of abrasion and wear resistance of concrete is essential especially for pavement due to the continuous nature of its loads. Difficulties might be encountered concerning of the wear and abrasion resistance, as the damaging action varies depending on the cause of wear, and no single test procedure is satisfactory in evaluating the resistance of concrete to the various conditions of wear ^[21].

Tests on hydraulic structures, which have the same effect of wear on slabs under traffic loads, revealed that the abrasion resistance of SFRC is not improved over that of the plain concrete ^[1]. Significant increases of abrasion resistance was found by other researchers, with about 15% higher resistance reported under drying, wet and frozen surface conditions ^[39]. Tests carried out to compare the abrasion resistance of plain concrete specimens (25 MPa) and SFRC having 75 kg/m³ enlarged end type of fibers, reported that the SFRC specimens have a LA (Los Angeles abrasion wearing test value: it includes milling specimens in the presence of steel and concrete balls for a certain number of revolutions. LA is the increase in the percentage of the material passing the 1.7 mm sieve) value of 50% greater than that of plain concrete specimens ^[30], which in turn proves the capability of steel fibers to resist abrasion and wear.

Wear tests were carried out using a pair of hardened steel wheels running in a circular path under load on flat specimen slabs. It was found that for specific number

of cycles, the SFRC exhibits average groove depths less than that of plain concrete, which in turn proves that the SFRC has a better wear resistance relative to an identical plain concrete ^[30].

The skid resistance of SFRC was found to be same as that of the plain concrete at early stages prior the deterioration of the surface. In later stages, where abrasion and erosion of the surface had to taken place, steel fiber reinforced concrete has an up to 15 % higher skid resistance relative to plain concrete ^[1].

It can be concluded that the SFRC has better performance regarding its erosion, abrasion and skid resistance, but how much better is dependent on the case of application.

2.7.5 Thermal Properties

There are three thermal properties that may be significant in the performance of concrete, viz, coefficient of thermal expansion, specific heat and conductivity ^[21]. To the author's knowledge little work on SFRC has been done in this area.

Thermal expansion is seen to be the most relevant to the ground slabs applications especially for concrete subjected to thawing and freezing action. Specific heat and conductivity are normally relative to applications whereby thermal insulations are provided ^[21], or other applications such as rocket launch facilities or mass structures ^[55].

The effect of steel fibers on coefficient of expansion factor was studied using beam specimens that have various steel fibers content (ranges between 0 and 2 % by volume). Specimens were subjected to temperatures ranges between 38 and 66 degree Celsius. Tests results indicate that the coefficient of thermal expansion factor was not significantly affected by fiber content ^[3]. Tests on relatively dry SFRC specimens at ages of about 220 to 250 days and 27 degree Celsius temperature rise, revealed that addition of steel fibers marginally influence the thermal expansion coefficient. Just to give an indication, for SFRC containing 75 kg/m³ of enlarged-end steel fibers, the typical expansion coefficient is found to be 8.2×10^{-6} per degree Celsius ^[30].

Thermal conductivity of SFRC is studied by Cook et al ^[55], they found that an increase of 25 % to 50% in thermal conductivity could be achieved with specimens

having straight steel fiber contents of 1% and 2%. Another contradictory study reported that with 0.5% to 1.5% by volume steel fiber, a small increase in thermal conductivity could be obtained ^[1].

It can be seen from the above discussion that the expansion of SFRC is the same (if not less) than plain concrete for identical mixes. The author's opinion is that, the only hazard is the expansion coefficient of the steel fibers, in other words, large differences between thermal coefficients of steel fibers and paste might cause the interface layers between them to damage and damage in many surfaces in different dimensions might weaken the entire matrix.

2.7.6 Electrical Conductivity

Steel fibers contents of up to 1% by volume (80 kg/m^3) has no significant effect on electrical conductivity ^{[30] [39]}, hence, wire guided vehicles may be operated without difficulties on SFRC floors, which can be taken as an advantage if compared with steel bars or mesh floors ^[39]. It can also be beneficial where traffic devices are needed e.g. vehicle detection loops for traffic counting and classification.

2.8 Conclusion

The following conclusions are drawn

- Although different types of steel fibers have been used, hook-ended steel fibers were found to perform better than the other types because of its hooked ends and/ or high tensile strength, which requires additional loads for pulling out and /or breaking.
- The mechanistic mix proportioning design approach for SFRC strives to adjust the additional paste required to coat the added steel fibers, therefore a some sort of coupling concept can be used, in other words, any of the plain concrete proportioning mix criterion can be used to design the mix and there after the mix can be adjusted for the added fibers.
- The normal transporting, placing and finishing methods used for plain concrete can also used for SFRC.
- Steel fiber has an effect ranging between little and significant on the mechanical properties. Endurance limit, impact strength and shear strength

are significantly improved while compressive strength, modulus of elasticity and Poisson's ratio improve slightly when the steel fiber is added. The flexural strength at first crack and maximum load is slightly improved, but on the other hand, the imparted toughness improves the equivalent strength (after crack) significantly (as high as 100%).

- The physical properties are also altered by the use of steel fibers. The steel fibers have a significant effect on the plastic shrinkage while little effect is found for the drying shrinkage. Methods used to measure the shrinkage are found not to simulate pavements. Creep is significantly influenced when using high dosage of steel fiber while little effect is found with low steel fiber dosages. The abrasion and skid resistance are also improved significantly. A negligible effect is found on the electrical conductivity. The thermal properties of the SFRC are not properly established and problems could be encountered as a result of the wide difference between the thermal expansion factor for the steel fiber and the other mixture constituents. Durability is not influenced by the use of steel fibers.

Chapter 3

Steel Fiber Reinforced Concrete Ground Slabs

3.1 Synopsis

The improved engineering properties of SFRC have implications for concrete pavement design criterion, as SFRC has improved fatigue performance and flexural strength. Apart from technical aspects, economy is usually the core aim that designs strive to. SFRC is found to have a significant impact on the economy of the pavements mainly due to the possibility of providing less thickness, longer joint spacing, less maintenance cost and longer useful life if compared to the plain concrete pavements.

In this section, published information on SFRC pavements is discussed and conclusions are drawn.

3.2 Design methods

Most of the accepted methods for conventional concrete pavement design have been used to design SFRC slabs^[56]. The main difference in designing for SFRC is the factor applied to the concrete flexural strength or slab thickness to take account for the improved ability of the SFRC to withstand impact and repetitive flexural loading^[30]. Generally, Westergaard formulas and its derivatives have been commonly used^[57]. Supporting design charts and formulas are available^{[11] [30] [39] [58]} for determining the thickness of SFRC warehouse floors. Airfield slab thickness for new designs can be obtained from charts developed for SFRC by the Corps of Engineers U.S.A.^{[56] [59]}. Heavy-duty port pavement design procedures and specifications are found in the manual developed by the British Ports and American Association of port authorities entitled "The Structural Design of Heavy Duty Pavements for Ports and other Industries", in which SFRC was considered^[9]. The plain concrete design criterion can be used to determine the design thickness for highways, but attention should be given to the failure criterion associated with SFRC as discussed later in this section.

The design parameters for SFRC are similar to those of plain concrete. Traffic loading, sub-grade reaction and static flexural strength and fatigue properties of the concrete are the design inputs to design charts. The required slab thickness is

determined as that necessary to limit the tensile stress in the slab to a such level that fatigue cracking will not occur until after the pavement have received the design number of stress repetitions ^[56]. Since the SFRC slabs are expected to yield thinner design thickness, it is necessary to ensure that the stress and strains induced in the foundation material do not exceed the strength of the sub grade, and that the deflection is within tolerable limits. Computer programs based on layered system theory and finite element analysis technique can be used to ensure that all criteria are met ^[58]. Data from plain and reinforced concrete was used to develop relationships between the elastic deflection and pavement performance using the available SFRC data a curve was drawn parallel to that of plain and conventionally reinforced concrete pavements, and this relationship was used to provide maximum acceptable deflections for entire pavement rather than providing limiting deflections ^[59].

Criticism has been leveled at some early and recent design procedures. Although SFRC has different fatigue and strength development characteristics, criterion in many cases was not altered to compensate for this difference and the fatigue properties of SFRC were considered to be similar to the fatigue properties of plain concrete ^[4]. The after crack flexural strength of the SFRC was not considered or considered indirectly, while, the first crack strength was used through Westergaard formulas (either directly on the formulas or proceeding through it's simplified design charts). In addition to that, these procedures lack or give little information regarding correlation between steel fiber parameters and the flexural strength and fatigue performance of SFRC in a design environment ^[27]. Some SFRC constrain the designer to a certain mix designs ^[30], which in many cases are not suitable for the required application. With the vast increase in use of SFRC, better experience is gained, and more refined design catalogues become available with time (for instance the steel fibers manufacturer design catalogues which considers the after cracking strength and clarify the correlation between fiber parameters and the flexural strength) ^[11].

3.3 Ground Slabs Distresses

Since pavement performance is a time dependant, the behaviour of materials cannot be predicted from stress analysis. It becomes evident that the structural performance involves more than stress analysis.

It is prudent to consider material related distresses at design stages in order to ensure better performance for the intended pavement. As discussed in previous sections, alteration on mechanical and physical properties brought to concrete by addition of steel fibers is seen to improve pavement performance.

Break-off and spalling of corners, edges, and joints usually results from excessive stresses, loss of support and curling^[60]. Investigations on SFRC airfield pavements in the U.S.A., found that although break-off is found in many locations, its effect on performance is minimal because the pieces remain held together with the rest of the slab and it was concluded that the normal routine maintenance could tackle the problem^[4]. As far as the spalling of concrete is concerned, laboratory tests and field investigation have shown that SFRC has much higher spalling endurance than the plain concrete^[29]. As a qualitative measure, results from dynamic and explosive test are used and it was found that SFRC does not disintegrate upon load application^[9]. To minimize the possible corner and edge break off, it was recommended that staggered transverse joints could be used resulting in two corners created instead of four corners^[61].

Edge punching is typical distress of continuously reinforced concrete pavements. The mechanism involves that, two adjacent cracks (about 1.2m apart) at the edge of the pavement, start to fault and spall slightly, which cause that portion of the slab to act as a cantilever beam. By that time more cracks are induced and pieces of concrete punch downward under load into the sub-base^[60]. Once again steel fibers can minimize this punching, because for the piece of concrete to punch fibers should either break down or pull out of concrete, which needs higher energy to be exerted.

Longitudinal cracks occurring parallel to the centerline of pavement slab are either due to loss of support or to the fatigue of concrete. SFRC can result in a reduction in the formation of fatigue related cracks, as the fatigue endurance of SFRC is better than that of plain concrete. Also if cracks are supposed to occur, it will be much narrower in SFRC preventing the ingress of water and deleterious material onto the underlying layers, thus reducing pumping.

Transverse cracks are usually caused by friction stresses between slab and sub-base, which causes tensile stresses on the slab. At some stage, these tensile stresses exceed the tensile strength of the slab and eventually transverse cracks occur ^[62]. Steel fibers in SFRC acts as discontinuous reinforcement, which to some extent restrain the drying shrinkage and expansion caused by moisture, in other words it reduces the action of the slab movement. As a result of this reduction, micro cracks are distributed through the slab instead of having one macro crack at approximately equal distances. Transverse crack spacing for SFRC pavements is expected to increase, which imply that savings could be achieved on transverse joints.

Curling stresses are the stresses caused by the temperature differential through the depth of the pavement. Downward curling occurs during the day due to the rise of temperature. The top of the slab tends to expand with respect to the neutral axis while the bottom tends to contract. However the weight of the slab restrains it from expansion and contraction, thus compressive stresses are induced at the top while tensile stresses occur at the bottom. At night the picture is reverse and upward curling has to occur ^[60]. Curling can be a serious impediment to satisfactory serviceability and thus the influence of steel fibers on curl must be established. The severity of curling on SFRC pavements is due to the fact that thinner section could possibly be provided, moreover, SFRC mixes have higher cement content which has a negative influence to the curling characteristics of the concrete ^[4]. Airfield investigation carried out in the U.S.A. concluded that, although some curling has occurred in SFRC pavement projects, distress associated with this curling has been minimal (in the form of corner cracking) and there has been very little need for maintenance. The investigation further recommended that curling and its effect should be minimized by adjusting the concrete mix through provision of lower cement content, use of water reducing admixtures, and use of retarding admixtures ^[61].

3.4 Insight Through Previous Projects

SFRC pavements have now been in use for about three decades. Question on how these pavements performed and the lesson learned is important for the future of the use of the steel fibers in this field.

Field investigation in 1982 ^[12] in the U.S.A. on SFRC pavements, reported that few of these pavements performed well and many developed defects in early stages

of their service life. The investigation concluded that additional research is needed in the areas of joint design and spacing, load transfer at joints, fiber content and thickness.

Another field study in 1989 ^[63] conducted in Belgium on overlays with SFRC stated that fairly good results are gained by using steel fibers in concrete. It was found that the bond condition between the old pavement and the overlay is fundamental. Further more direct resurfacing on concrete should only be considered when the condition of the old pavement is still relatively good. Suggestion was made for further research to address the problem of reflective cracks that were encountered at many locations in the project.

The decision was made to use SFRC to overlay two aprons at McCarran *International Airport /Las Vegas /USA* in 1976 and 1979 ^[64]. The first one is 152 mm deep built over an existing asphalt pavement to serve transient cargo aircraft. The SFRC mixture contained 95 kg/m³ of (0.25x0.56x25mm) straight steel fibers. Problems existed in overlaying the existing pavement, as the existing cargo building was already 0.6 to 0.9 m below the level of the ramp. Using conventional concrete would have added 381 to 406 mm to this difference, while SFRC allowed this thickness to be reduced to 152mm. In this project, transverse joints are spaced 15 m apart, longitudinal joints were spaced 7.6 m apart and keyway or tie bars were used (no dowels). A number of corner breaks was found and some of them were faulted and developed spalling, also some tight longitudinal cracks near the panel centerline were observed.

The second project was the new construction of 178 mm deep SFRC placed over 51 mm of new asphaltic concrete, which was on top of 305 mm of conventional concrete. The SFRC mixture had a cement content of 385 kg/ m³, a pozzolan content of 149 kg/m³, and fiber content of 50 kg/ m³ of (0.51x0.51mm) deformed steel fibers. Transverse joints (sawn 75 mm deep) were 15.2 m apart and longitudinal joints of 7.6 m apart were enhanced. Almost 10% of the panels had corner breaks and it was stated to be somewhat less than those of the 1976 apron. About half of the transverse contraction joints had not functioned resulting in wide-open joints at those that have functioned.

It was stated by Packard et al ^[12] that the problems associated with this project were:

- (a) Lack of load transfer to adjacent slab that was due the thinner SFRC slabs at which load transfer devices such as dowels had to be omitted.
- (b) Curling stresses influenced the edges and corners and.
- (c) Large amount of movement in some joints resulted in failures of the joint seal, therefore, water and debris filtered to the bottom layers causing more damage.

An old pavement at *J.F. Kennedy Airport /New York /USA* had a serious problem of “shoving” caused by aircrafts turning off the taxiway onto the runway ^{[56][64]}. Construction consisted of the removal of the old asphalt concrete wearing course, construction of 51 mm asphalt leveling course, placement of a double thickness of 0.15 mm thick polythene, and then construction of the SFRC overlay. The overlay was 140 mm thick, and used both keyway and doweled construction joints. The concrete mixture had a cement content of 445 kg/m³ and 104 kg/m³ of (0.64x64mm) straight steel fibers. One year later (1975) a survey indicated satisfactory performance and the repaired area were enlarged. Performance evaluation in 1984 stated that the paved area was still in service although there was some cracking and shattered corners at intersections.

Packard et al ^[12] stated that small apron areas in the same project were placed over asphalt where fuel spillage was causing serious “shoving” and rutting. These areas continue to settle badly. Some of the SFRC that was not jointed is cracking badly.

At *Ashland ramp /Ohio/USA* ^[64], an entrance to a truck weighing station was built as an experimental project to evaluate the use of SFRC in new pavement construction. Construction was completed in 1971 and opened to the estimated daily traffic of about 2400 to 3600 truck per day in the year 1973.

The ramp was 152 m long and 4.9 m wide having a depth of 102 mm and placed on top of an asphaltic concrete base. Ends were tapered to 229 mm over a 2.1m length. Doweled expansion joints were installed at either end. The concrete had a cement content of 500 kg/m³ and fiber content of 157 kg/m³ of (0.25x0.56x25mm) straight steel fibers. The maximum aggregate size was 9.5 mm.

The day following the placement, transverse cracks occurred approximately at midpoint of the slabs. The cracks varied in width from 3.2 to 12.7 mm. Four months

later a second transverse crack occurred 50 m from the first crack and 30m from one end. In 1973 a third transverse crack was found 30 m from the other end. An irregular longitudinal crack, hairline in nature, was also observed over a 12 m length at the center of the pavement beginning approximately 30m from the end of the pavement.

After it was opened to the traffic, spalling at areas of the transverse cracks occurred and these areas were resurfaced to full depth again. In 1976 the entire project was resurfaced.

An evaluation carried out by Packard et al ^[12], suggest that the problem was caused by a lack of load transfer through the transverse cracks, excessive deflection as a result of the thin section used and the heavy type of traffic was encountered. The ramp had corners break-off and slabs shattered.

A series of trails was conducted during 1970s on *bus lanes in Calgary /Canada* ^[65] to evaluate the usage of SFRC in new pavement construction. University bus route sections of conventional un-reinforced concrete were compared to similar thicknesses of SFRC containing 80 kg/m³ steel fibers. Pavement thicknesses of 76 mm, 102 mm, 152 mm, and 178mm were tested.

The result of this study showed that after four years and over 200 000 bus passed, the SFRC either greatly reduced the cracking for similar thicknesses or only 50 to 60% of the plain concrete thickness was required for equivalent performance. It was also stated that damage in conventional concrete slabs with thicknesses of 76 mm, 102 mm and 127 mm necessitate its replacement after just four weeks of trafficking whilst SFRC sections performed adequately over the four years.

SFRC slabs were used instead of double reinforced concrete slabs in *Burnssum Warehouse /Holland* ^[4]. This eliminated the conventional concrete and reduced the slab thickness from 200 mm to 180 mm. A concrete mixture containing 340 kg/m³ cement, 30 kg/m³ of hook-ended high tensile steel fibers, and a maximum aggregate size of 32 mm. Plasticisers were used to achieve low water content.

Although no mention was made regarding performance, it was stated that cost and shrinkage cracks were reduced; SFRC warehouse flooring became more common in other subsequent projects.



An experimental project was constructed during 1982 in *Maldegem /Belgium* ^[63] on a badly deteriorated concrete road, where pumping and stepping had taken place. The road was subjected to heavy traffic load.

Two overlay sections were constructed. The first section (1250 m long) had contraction joints 15 m apart following the pattern of the previous road, while the second section (500 m long) was constructed without contraction joints. The overlay thickness was between 100 and 120 mm. An asphalt separation course was used to prepare the surface.

The concrete mix had a cement content of 400 kg/m^3 , and 50 kg/m^3 of hook-ended 50 mm long and 0.5 mm thick steel fibers. A water cement ratio of 0.55 was used.

An evaluation in 1988 revealed that, in the 500 m section (without joints), cracks developed at an early age at distances between 10 and 60 m and they present slowly evolving distress for the entire overlay. On the other hand the section with contraction joints was not damaged at all, however, approximately 50% of the neoprene profiles utilized to fill the joints were loosened and 10% of the joints needed to be resealed.

In 1983 a concrete road in *Gent /Belgium* ^[63] that was heavily scaled but in good structural condition was overlaid. The old road was constructed on a crushed stone base and it had doweled contraction joints. It was serving a very heavy industrial type of traffic.

To ensure fully bonded overlay, surface preparations such as grouting, cleaning and milling to the old surface were performed prior the overlaying. A 100 mm deep layer with joints 10 m apart (coincide to the old pavement joints) was constructed. The mixture had a cement content of 400 kg/m^3 , water cement ratio of 0.53 and 40 kg/m^3 of hook-ended 0.5 mm diameter by 50 mm long steel fibers.

In 1988 the project was evaluated. The left lane exhibits relatively little damage, as the intense traffic utilize essentially the right lane. On that right lane, cracks developed at joints, indicating de-bonding at the interface. Obviously grouting had no positive effect especially at the high temperature reported during construction. The evaluation recommended that the right lane had to be resurfaced in the near future.

In some of these selected projects, the cement content was relatively high. The reason might be the additional paste required to coat the steel fibers. High cement content is normally associated with higher potential for curling and shrinkage ^[4]. Fly ash was used in the second project at Mccarran International Airport and it seems to work better as there was relatively less damage reported on the SFRC in that project. This agrees with the facts that fly ash does not only reduce the plastic shrinkage through the reduction of the heat of hydration at early curing ages, but it also improves workability and cost effectiveness ^[66].

High steel fiber content were used in some of the projects, for instance 157 kg/m³ straight steel fibers, was used in the Ashland ramp. The aim of that was probably to get very high flexural strength, thus very thin section was obtained. With the technology of to day, hook-ended steel fibers with high tensile strength have proven to yield better results and a reduction in the fiber content have become possible. Literature shows that fiber content of between 15 - 50 kg/m³ is satisfactory and more economical.

Performance evaluation stated that efforts to obtain the maximum economy had resulted in some designs that were on the un-conservative side, therewith, inadequate thicknesses were obtained and failure had taken place ^[12]. Pavement thickness should be considered for the deflection and curling of the slab as both these factors can cause edge breaking and shattering which was evident in some projects such as the Ashland ramp for the case of deflection and Maldegem overlay.

Joints spacing and load transfer devices were seen to cause major distresses in some projects. Inappropriate joint spacing caused cracks in middle of slab; moreover, these cracks are relatively wide. Transverse joint spacing of 15 m is found to perform well which agrees with the recommended spacing by some research corporations ^[56]. Inappropriate load transfer methods have contributed to the cause of damage in many SFRC pavements ^[4]. Thin slabs have led to the omission of keyways and dowels causing reduced joint efficiency and thus resulting in damage ^[12]. With better joint spacing and proper load transfer devices, middle crack effects could be reduced if not eliminated. In the case of narrow cracks the steel fibers could possibly acts as mini-dowels thus better load transfer could be achieved through cracks.

It was evident that steel fibers cannot be used as an alternative for the normal steel bars thus continuous road overlays cannot be constructed using SFRC even if much

high fiber content was used. Gent overlay and Ashland ramp were examples of failure of this application.

SFRC applications in warehouse floors have proven to result in massive savings and good performance. Many of the problems encountered with other pavements were not found in warehouse slabs and the probable reason for that is the exposure to weather condition for those floors are different to that of other mentioned pavements. The curling stresses and joint movement for warehouse floors are thus limited.

SFRC have proven good performance in many other applications such as bridge-decks, pipes, hydraulic structures, pre-cast elements and some others, which lies out of the scope of this research.

3.5 Economic Evaluation

Traditionally the decision between various alternative solutions to the problem of providing a pavement has been made on the basis of initial costs. This approach has some disadvantages in the way that the useful life span for different options and the maintenance cost are not considered. The concept of life cycle costs is found to be better in determining the most cost-effective option because the maintenance cost and useful life span are included ^[67].

Any new technology should, at the same level of performance, be cheaper than the one it substitutes; otherwise it will stay in the laboratory stage. SFRC is not cheaper than traditional techniques in many applications. Therefore it is very important to select and develop these applications where sufficient economics are guaranteed. Initial cost saving could be achieved in many cases where less thickness and longer joint spaces could be provided.

It was established by many researchers that saving could be made in different pavement components. Longer joints spacing could be used, 15 m for transverse joints and 7.5 m for longitudinal are applicable, thus massive saving could be attained due to the reduction of the number of joints to be used ^[56]. Saving in material is also possible and it's dependant on the type of application as presented in section 3.4. Also it has been established that in some projects, the SFRC shorten the construction period once again an indirect saving is made due to the earlier opening to the traffic ^[10].

Experience gained from previous projects has shown that massive initial cost saving could be made if SFRC is to be used. Saving was greatly recognized in airfield pavements, for instance, at Denver airport in the U.S.A., a saving of \$1.0 million (15.5% saving) was attained by using SFRC slabs having a depth of 203 mm instead of using 381 mm of plain concrete to with-stand the same load ^[68]. Saving was also acknowledged at container terminals where tremendous load growth has been experienced during the last two decades. SFRC is not only economical but it was also found to work perfectly and interruption caused by shorter maintenance intervals is no longer encountered. For the overlay at Ghent port in Belgium a saving of 40% in thickness and 50% of joint spacing was achieved in comparison to if conventional concrete was used ^[9]. SFRC roads in the past have been found not to be cost-effective when compared to plain concrete ^[69], as the small reduction in thickness on these pavements will probably not make SFRC economically feasible ^[12]. During projects constructed in the early 70s fiber supply capabilities and manufacturer were unable to meet the demand for any major projects, which could have been a fairer evaluator for such pavements ^[4]. On the other hand SFRC overlays and inlays have proven to be very cost-effective and reducing thickness by about 40% could make initial saving. SFRC have been widely used in industrial building floor with an economical advantage (saving in material and joints) of about 5 to 10 % initially gained and much of the concentrated heavy loads could be handled ^[70].

Where much thicker pavements are required for the heavier loads and higher tire pressure, SFRC may be more feasible ^[12].

The extra cost of adding fibers to the concrete mix and other additional cost is usually offset by the savings in cost of supplying and placing materials ^[10].

3.6 Conclusions

- Design methods for plain concrete pavements can be used for the SFRC pavements. Alteration to these methods is required to consider for the higher deflection values usually associated with the SFRC slabs due to the thinner sections.
- Distresses associated with wearing course are either be eliminated or reduced by the addition of steel fibers to concrete. Therefore, SFRC can have a performance superior to that of plain concrete pavements taking



into account all considerations of good applications, design and construction.

- The majority of the previous SFRC pavements are found not to perform as perfect as anticipated. The reasons for that are found to pivot around the inadequate designs, for instance, the thickness and the joints spacing.
- The SFRC for pavements is economically viable when compared to the plain concrete. A minimum of 10% to a maximum of 40% saving could be achieved in warehouse and overlay pavements respectively. It was further found that more saving could be perceived if the life cycle performance is considered for the evaluation of different pavement alternatives.
- Apart from the economy, SFRC could play the role to solve several technical problems, for example, the less required thickness can be beneficial in cases where headroom restrictions are found. Designers should however bear in mind that with reduced thickness, more curling stresses occur.



Chapter 4

Basic Analytical Theories and Similar Studies Conducted by other Agencies

4.1 Background

There are three groups of methods used to design concrete pavements. One group of methods is based upon observations of the performance of full-scale pavements. The other group of methods is generally based on stresses calculated in the pavements and compared to the flexural strength of concrete ^[67]. A third group of design procedures (mechanistic-empirical) are normally used by many design catalogues ^[60].

Most of the methods used for a mechanistic type of approach were based on the work done by Westergaard around 1925. Westergaard formulas were simplified by the provision of design charts and table ^[39].

Meyerhof developed another method in the early 1960s and this method is said to be well adjusted and correlated with full-scale field data. Falkner et al developed an equation by using three-dimensional finite elements and Shentu et al developed a finite element model in 1997.

4.2 Theoretical analysis approaches

4.2.1 Westergaard (1926)

Westergaard formula assumes that slab acts as a homogenous, isotropic, elastic solid in equilibrium and that the reactions of the foundations are vertical and proportional to deflections of the slab. Distinction between three cases of load was made viz interior, edge, and corner loads ^[71]. For the corner and edge loadings, the load is applied adjacent to the edges, thus the formula does not consider loads applied at a distance from the edges and corners. The following are convenient formats of Westergaard equations:

Internal Load :

$$\sigma_{\max} = \left[0.275(1 + \mu) \frac{P}{h^2} \right] * \log_{10} \left[0.36 \frac{Eh^3}{Kb^4} \right] \quad \Rightarrow \text{Eq.4-1}$$

$$Z_i = \frac{P}{8KI^2} \quad \Rightarrow \text{Eq.4-2}$$

Edge Load :

$$\sigma_{\max} = \left[0.529(1 + 0.54\mu) \frac{P}{h^2} \right] * \log_{10} \left[0.2 \frac{Eh^3}{Kb^4} \right] \quad \Rightarrow \text{Eq.4-3}$$

$$Z_e = \frac{1}{\sqrt{6}} (1 + 0.4\mu) \frac{P}{KI^2} \quad \Rightarrow \text{Eq.4-4}$$

Corner Load :

$$\sigma_{\max} = \frac{3P}{h^2} \left[1 - 1.41 \left[12(1 - \mu^2) \frac{Kb^4}{Eh^3} \right]^{0.25} \right] \quad \Rightarrow \text{Eq.4-5}$$

$$Z_c = \left(1.1 - 0.88 \frac{a_1}{l} \right) \frac{P}{KI^2} \quad \Rightarrow \text{Eq.4-6}$$

$$b = [1.6r + h] - 0.675h \text{ for } r < 1.72h$$

$$b = r \text{ for } r \geq 1.72h$$

$$l = \left[\frac{Eh^3}{12(1 - \mu^2)K} \right]^{0.25} \quad \Rightarrow \text{Eq.4-7}$$

where :

P = First crack load (N).

σ_{\max} = Maximum stress (N/mm²).

μ = Poisson's ratio (0.15 - 0.2).

h = Slab depth (mm).

E = Modulus of elasticity (N/mm²).

K = Modulus of foundation reaction (N/mm³).

l = Radius of relative stiffness (mm).

Z_i = Vertical deflection for interior load case (mm).

Z_e = Vertical deflection for edge load case (mm).

Z_c = Vertical deflection for corner load case (mm).

a_1 = Distance between load center and corner (mm).

4.2.2 Meyerhof (1962)

The Concrete Society Technical Report No. 34 suggested limit values for moment of resistance. It was assumed that limit moment of resistance formula for plain concrete should be considered for SFRC when dealing with corner cases of loading

[39]. On the other hand, steel fiber manufacturer design guidelines for designing SFRC ground slabs have included the effect of the steel fibers on the limit moment of resistance when dealing with corner loads [11]. Three cases of loading where given by Meyerhof as follows [72]:

Internal Load :

$$P_i = 6 \left[1 + \frac{2a}{l} \right] M_0 \quad \Longrightarrow \quad \text{Eq.4-8}$$

Edge Load :

$$P_e = 3.5 \left[1 + \frac{3a}{l} \right] M_0 \quad \Longrightarrow \quad \text{Eq.4-9}$$

Corner Load :

$$P_c = 2 \left[1 + \frac{4a}{l} \right] M_0 \quad \Longrightarrow \quad \text{Eq.4-10}$$

Where :

P_i = Ultimate interior load.

P_e = Ultimate edge load.

P_c = Ultimate corner load.

a = Contact radius of load.

M_0 = Limit moment of resistance of slab.

l = Radius of relative stiffness.

Formulas for resistance moment as given by steel fibers manufacturer design catalogue are as follows [11]:

For plain concrete :

$$M_0 = f_{cr} \frac{bh^2}{6} \quad \Longrightarrow \quad \text{Eq.4-11}$$

SFRC :

$$M_0 = \left[1 + \frac{R_{e,3}}{100} \right] * f_{cr} \frac{bh^2}{6} \quad \Longrightarrow \quad \text{Eq.4-12}$$

Where :

$R_{e,3}$ = Equivalent flexural factor of SFRC.

b = Unit width of slab.

l = Depth of slab.

f_{cr} = First crack strength.

Steel fiber manufactures have given the equivalent flexural strength factors $R_{e,3}$

for different steel fiber content relevant to their steel fiber. The values consider the steel fiber parameters ^[11]. In comparison with plain concrete (equation 4-11 and equation 4-12) $R_{e,3}$ is the amount of improvement associated with SFRC for a specific steel fiber content.

4.2.3 Falkner et al (1995)

A design proposal was generated by using a 3-D finite element model to assess the ultimate load capacity of a centrally loaded slab. The proposal was correlated with experimental data. The model is based on the plastic theory and takes into account two limit states, one is the first cracking load (Westergaard load) and the other is the ultimate load ^[73]. The following is the proposed model:

$$F'_u = P \left[1 + \left(\frac{K}{Eh^3} \right)^{0.25} W \frac{\sqrt{A}}{h} \right] \left[1 + \frac{R_{e,3}}{100} \right] \Rightarrow \text{Eq.4-13}$$

Where :

F'_u = Ultimate load capacity (N).

P = First crack load from Westergaard (N).

W = Width of slab (mm).

A = Area of load (mm²).

K = Modulus of foundation reaction (N/mm³).

E = Modulus of elasticity (N/mm²).

h = Slab depth (mm).

$R_{e,3}$ = Equivalent ratio.

The above model can be used to estimate the ultimate load capacity for concrete both with and without steel fiber. For plain concrete, the value of equivalent flexural factor is to be substituted as zero. The model has the limitation that it is not considering corner and edge cases of loading.

4.2.4 Shentu et al (1997)

In 1997, Shentu et al used a finite element model (ring-like elements with triangular cross sections) assuming a Winkler sub-grade to develop a simple formula to determine the ultimate load-carrying capacity of a plain concrete slab, with large plan dimensions subjected to an interior concentrated load. Shentu's model uses the uniaxial tensile strength in-lieu of the flexural strength. Models to assess the

equivalent tensile strength of SFRC do not yet exist and the model is considered of less use when dealing with SFRC. The model also has the limitation that it is not applicable to edge and corner load cases. The ultimate load capacity can be given as follows: ^[74].

$$P_{sh} = 1.72 \left[\left(\frac{Ka}{E} \right) * 10^4 + 3.6 \right] f'_t h^2 \implies \text{Eq.4-14}$$

Where :

P_{sh} = Ultimate bearing capacity (N).

f'_t = Uniaxial tensile strength of concrete (N/mm²).

K = Modulus of foundation reaction (N/mm³).

a = Radius of loaded area (mm²).

E = Modulus of elasticity (N/mm²).

h = Slab depth (mm).

4.3 Similar studies conducted by other agencies

Different researchers carried out full-scale test studies on slabs. A semi full-scale study was conducted by Kaushik et al in India in 1989. The study included the three critical load cases (interior, edge and corner) ^[75]. Beckett did a series of tests in 1990 to compare the load capacity of plain and SFRC slabs subjected to interior loading ^[76]. Later in 1999 he carried out an investigation to evaluate the load capacity of two slabs subjected to corner and edge loading ^[77]. Falkner et al performed a comparative study of strength and deformation behaviour of plain and SFRC slabs ^[73].

4.3.1 Kaushik et al (1989)

A semi full-scale test was conducted to compare the load capacity for plain and SFRC slabs. The effect of the steel fiber dosage on the load capacity of the interior, edge and corner load cases was evaluated. The result of the study is summarized in table 4-1.



Table 4-1: Results from Similar Previous Tests (Kaushik et al 1989)

Slabs	Fiber content % By volume	Interior		Edge		Corner	
		F.C (KN)	D. (mm)	F.C (KN)	D. (mm)	F.C (KN)	D. (mm)
P.C.	No Fibers	45.11	1.786	40.66	4.68	29.35	3.95
SFRC2	0.5	80	2.6	70	7.35	39	4.822
SFRC3	1.0	120	2.71	78.81	6.61	59.82	7.02
SFRC4	1.25	180	3.9	100		69.84	2.957
SFRC5	1.5	150	3.11	120	7.27	74.46	11.18
SFRC6	2.0	145		90.94	4.14	50	7.83

Slabs 1.8x1.8x0.1m/300 mm diameter loading plate/ (H) aspect ratio 80, diameter of 0.456 mm
(H.) Hook-ended steel fibers /F.C = First crack load/ D= Measured deflection

The study concluded that:

- The addition of the steel fibers changes the mode of failure of plain concrete from sudden failure (immediately after first crack) to a gradual relaxed failure.
- Fiber content between 0.5% and 2.0% by volume yields a significant improvement in the load carrying capacity of the SFRC pavements. The rate of increase in the load carrying capacity is significant up to 1.25% by volume (85 kg/m^3) beyond which the rate of gain in strength is not substantial, Fibers volume of 1.25% is therefore been observed to be an optimum steel fiber volume.

4.3.2 Beckett (1990)

The study was conducted to compare plain, fabric reinforced and SFRC slab subjected to an interior loading via a single load plate. The results relative to plain and SFRC slabs are presented in table 4-2. The readings in the fourth column indicated that either the jack capacity is exceeded prior the failure or something went wrong with the experiment.

Table 4-2: Results From Similar Previous Tests (Beckett 1990)

Slab	Fibers	Load at First crack (KN)	Load at failure (KN)
P.C.	No Fibers	180	200
SFRC1	(60/100) H. 20 kg/m^3	220	350
SFRC2	(60/80) H. 20 kg/m^3	260	390
SFRC3	(60/100) H. 30 kg/m^3	240	340
SFRC4	(60/80) H. 30 kg/m^3	290	>345
SFRC5	Mill cut 30 kg/m^3	180	200

Slabs 3.0x3.0x0.15m / Concrete grade 40 / 100x100 loading plate / K-value = 0.035 N/mm²
H. Hook-ended steel fibers



The following conclusions were given:

- The plain concrete and the mill cut fiber-reinforced slabs shows to have no significant post cracking behaviour.
- The performance of 60/80 hook-ended steel fiber reinforced slabs is superior to the 60/100 fiber reinforced slabs. Increasing the steel fiber dosage in both cases increases the post crack behaviour.
- Comparison of the measured results to the calculated results using Westergaard equations revealed that Westergaard's approach has its limitations if applied to SFRC.

4.3.3 Falkner et al (1995)

The study aimed to investigate and compare the strength and deformation behaviour of plain and SFRC subjected to interior load. A formula was generated using the tested results and finite element model. The study results are abstracted in table 4-3, while the formula is given in equation 4-13. The readings of the first crack at the second column are worrying. It might have to do with method used to calculate the first crack strength.

Table 4-3: Results From Similar Previous Tests (Falkner et al 1995)

		First crack		Failure		K-value (N/mm ³)
		Tested	Wester.*	Tested	Falkner*	
P1	No Fibers	80	100	180	160	Cork sub base 0.025
P2	Mill cut 30 kg/m ³	80	100	210	180	
P3	(60/80) H. 20kg/m ³	80	100	240	240	Rubber sub base 0.05
P4	(60/80) H. 30 kg/m ³	100	120	380	340	
P5	Mill cut 30 kg/m ³	100	120	235	260	
P6	No Fibers	100	120	220	220	
Slabs 3.0x3.0x0.15m / Concrete grade 35 /120x120 loading plate/ Interior load						
H. Hook-ended steel fibers						
Wester* Calculated first crack load using Westergaard equation.						
Falkner* Calculated ultimate load using Falkner et al equation.						

The study came to the following conclusions:

- The deformation behaviour of plain and SFRC slabs can be divided into three regions:
 - Region (i): The un-cracked state, where the slabs show linear-elastic behaviour.
 - Region (ii): The first radial crack occurs in the center of the slab, developing gradually till the main crack can be seen at the slab edge.
 - Region (iii): Presents the redistribution of stresses with in slab, while plastic hinge lines are formed along the main cracks and the slab develops final failure pattern.
- The main difference in the strength and deformation behaviour of the plain and SFRC slabs is seen in region (iii). While the plain concrete slab fails at an early age (by punching), the SFRC slab is able to distribute its stresses until the plastic hinges occur at main cracks. In this stage the SFRC slab can still maintain its slab action and the load can be increased until ultimate failure occurs.

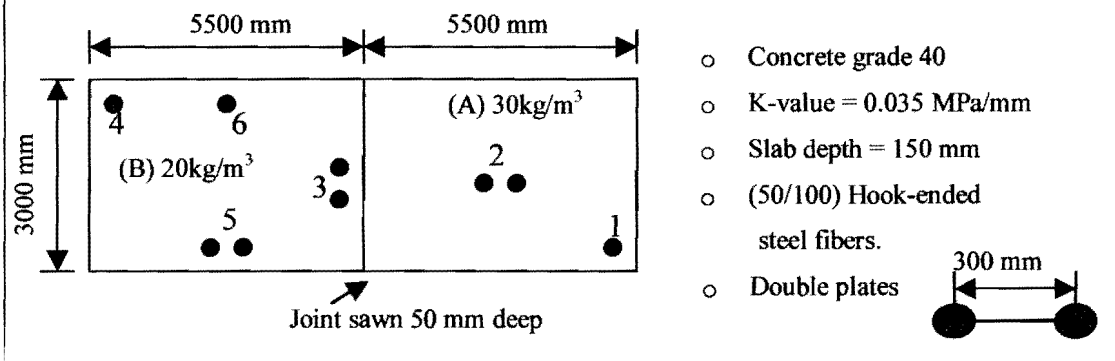
Table 4-3 show that the slab P3 with 60/80 hook-ended steel fibers has similar first crack load capacity value to the plain concrete slab. This results does not agree with the result gained by Beckett in table 4-2 (slab notified SFRC2), which shows the 60/80 hook-ended steel fiber slab to perform better than the slabs with other fiber parameters (bearing in mind that the same dosage was used).

4.3.4 Beckett (1999)

Test conducted (as a continuation of the 1990 tests) on two slabs constructed together and separated with a sawn joint as it can be seen in the sketch in table 4-4. The study aimed to investigate the corner and edge loadings of the SFRC using single and double loading plates. In addition to that, the tested values were compared to Meyerhof load and Westergaard load and deflection. Table 4-4 summarizes the results.

Table 4-4: Results From Similar Previous Tests (Beckett 1999)

Test Property	Corner 1	Internal 2	At joint 3	Corner 4	Edge 5	Edge 6
Loading plate (mmxmm)	100x100	2/(100x100)	2/(100x100)	100x100	2/(100x100)	100x100
First crack load (KN)	77.5	370	280	85	180	180
Maximum load (KN)	77.5	380	380	100	190	190
Meyerhof load (KN)	71.06	286.1	–	71.5	192.8	147.6
Westergaard load (KN)	58.9	105.1	–	59.2	79.15	55.5
Westergaard deflection (mm)	2.6	0.63	–	1.7	1.17	0.81
Test deflection for Westergaard load (mm)	2.1	1	–	1.8	1.6	1.6



- Concrete grade 40
- K-value = 0.035 MPa/mm
- Slab depth = 150 mm
- (50/100) Hook-ended steel fibers.
- Double plates 300 mm

It was concluded that:

- By increasing the plan dimension of the test slabs from (3x3 m) to (11x3 m), it was possible to develop negative partial circumferential yield lines in the top of the slab.
- The use of double load plates centered at 300mm apart does not appear to have an adverse effect on the load to first crack compared with tests using single loading plate.
- Tested deflections for Westergaard loads are approximately equal to the calculated ones using the same load.
- Meyerhof loads agreed with the maximum applied load.

It is noticeable that, the study does not compare plain and SFRC. Moreover, free edges were not compared.

4.4 Conclusion

- Although Westergaard's approach considers the three load cases, it is not suitable for applications involving SFRC. The theory was basically developed to consider the elastic behaviour of the material. Thus, it does not consider the after cracking strength of the SFRC. Comparison of measured results with the calculated results indicated that Westergaard approach has its limitation when used for the SFRC.
- Falkner and Shentu's approaches are found to consider the after cracking strength, but on the other hand they do not consider the three load cases. In addition, Shentu's model requires the measurement of the tensile strength using direct tensile testing, which is difficult to measure.
- Meyerhof's model is found to consider both the after cracking strength and the three cases of loading. It can be seen from the tabulated results in table (4-4) that the measured and calculated values agreed. The only drawback on the model is that it does not calculate the deflection and it is said that the deflection is checked indirectly through adjusting the model using existing plain concrete pavements.
- Hook-end steel fiber is once again proven to have the best performance. It was found that a significant increase in the load capacity is attainable with fiber dosage up to 1.25% by volume (approximately 95 kg/m³).
- Three phases for the failure pattern are found for both plain concrete and SFRC slabs viz: the un-cracked phase, the first radial crack and the final failure pattern. The effect of the steel fibers is apparent on the third phase. The fan pattern type of failure is not achievable with slab dimensions of 3.0x3.0 m while it is possible with a slab of 3.0x11.0 m, which indicates that the slab size has its influence to the pattern of failure.
- It can also be noticeable that fiber dosages less than 20kg/m³ were not considered. Tests to give the entire view were not conducted, in other words the corners and the edges were tested and compared independently of interior load. The only test using all three-load cases uses relatively small slabs, which might not be satisfactory to get a holistic view.

Chapter 5

Experimental Procedure

5.1 Introduction

The literature review revealed conflicting and / or gray areas in some aspect of SFRC. The influence of the steel fiber on compressive strength was not well established. Previously conducted flexural strength tests were not quite clear in describing the flexural strength of the SFRC, more over some studies once again did not agree on the influence of the steel fiber on the strength at first crack and at maximum load. Although there is a wide agreement about using the Japanese method to interpret and calculate the toughness of the SFRC ^[18], results published are limited.

Results for only a few full-scale tests were found. Some results of these tests were suspect either due to the testing equipments limitations or due to problems with the testing. The failure patterns were not clarified. Tests were conducted using steel fiber contents of 20kg/m³ and more, while the effect of low dosages was not tested. Above all, a full-scale study considering the three load conditions were not found. The only study found to consider these three load conditions was conducted on relatively small slabs.

In the light of the above-mentioned issues, a comparative study containing two elements has been conducted. The first is an experimental approach and the second an analytical approach. The behaviour of SFRC is compared to that of normal concrete containing no fibers.

5.2 Mix Composition

The concrete mixtures used in this investigation are based on the mixture shown in table 5-1. Six mixtures having steel fibers dosages of 0, 10, 15, 20, 25, 30 kg/m³ were manufactured respectively. Steel fibers (CHD 80/60 NB) used in this investigation were hook-ended wires with an aspect ratio of 80, length of 60 mm and a tensile strength of 1100 MPa. Fly ash was used as cement replacement to improve the workability of the mixture and to increase the mixture paste content.

Table 5-1: Constituents of the Used Mix

Material Content	Cement	Water	Pozzfil	Stones		Crusher Sand	Filler Sand
				19 mm	13 mm		
Mass (kg/m ³)	282	194	78	833	222	662	72

5.3 Effect of Steel Fiber Content on Properties of Concrete

The effect of steel fiber dosage on workability, compressive strength, modulus of rupture (MOR), modulus of elasticity, first crack strength and equivalent strength ratio ($R_{e,1.5}$) was studied. The following tests were conducted on the mixtures described in section 5.2:

- Standard slump test on all the mixes used in this investigation
- Standard compressive strength test after 7 and 28 days.
- MOR standard test on specimens tested after 28 days
- Third-point loading test with special setup on Material Testing System (MTS) on standard cast beams.
- Static modulus of elasticity test.

5.3.1 Standard Slump Test

Six mixtures containing steel fiber contents between 0 and 30 kg/m³ were tested to measure their workability. The standard apparatus was used and the standard procedure was followed as prescribed by (Standard Method: SABS Method 862:1994) ^[78].

5.3.2 Standard Compressive Strength Test

Compressive strength test was carried out after 7 and 28 days the standard cubes (150x150x150 mm). Three specimens (for every mixture) were tested after 7 days and three other specimens tested after 28 days. The procedure is prescribed by (Standard Method: SABS Method 863:1994) ^[79].

5.3.3 Standard Flexural Strength Test

Standard flexural strength tests were carried on three specimens according to Standard Method: SABS Method 864:1994 ^[80] (for every mixture). The beams were tested after 28 days on their side in relation to the as-cast position. The failure load is determined and modulus of rupture (MOR) is calculated on the basis of ordinary elastic theory viz:

$$MOR = \frac{PL}{bd^2} \implies \text{Eq.5-1}$$

Where :

MOR = Modulus of rupture.

P = Maximum load.

L = Span.

b = Width of the beam.

d = Depth of the beam.

5.3.4 Standard Modulus of Elasticity Test

Static compression standard test was conducted on two cylindrical specimens for each mix (mixtures in section 5-1). The procedure given by the ASTM C 469-94a was followed ^[81].

5.3.5 Third-Point Loading Test on Standard Beams

Three standard beam specimens for each mix (150x150x500 mm) were tested after 28 days to determine their first crack flexural strength and toughness characteristics.

A Closed-Loop Material Testing System (MTS) was used in displacement control to apply the load, measure the applied load and record deflection. Displacement was applied in a rate of 0.02mm/sec and 10 readings per second were recorded. The test setup is shown in figure 5-1. Mid-span deflection was measured by using two Linear Voltage Displacement Transducer (LVDTs) (mounted on a rig) reading against a clamp fixed to the specimen in a way that minimizes the error. The rig was fixed to the beam's neutral axis (assumed zero stresses surface) by means of 4 screws adjusted on the centerline of the two supports. Swiveling rollers were used at one of the supports and one loading point to accommodate any probable specimen

deformations prior testing.

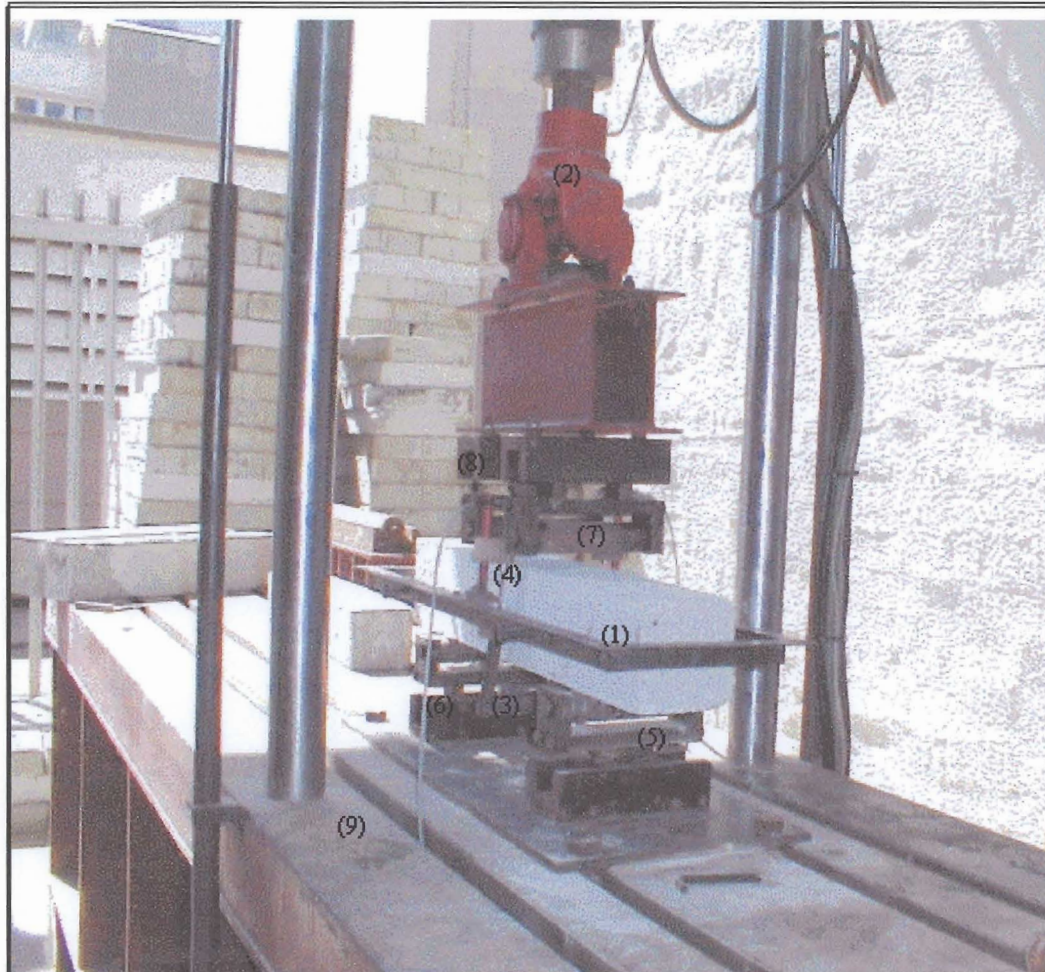
The load was applied by using two bearing rollers (one of them a swiveling roller) 150 mm apart with their center lines 75 mm from center of the beam. The beam supports were bolted to the (MTS) body and set 450 mm apart.

The number of steel fibers at the cracked section was counted to ensure that the steel fibers were well distributed in the specimen under consideration.

First crack load was estimated as the load point at which the load-deflection curve deviate from linearity. The technique used is described in Appendix C. The first crack strength was calculated by substituting the first crack load in equation 5-1.

Japanese standard method (JSCE-SF4) was used to calculate equivalent strength and equivalent strength ratio. The following steps were followed:

- Area under the load-deflection curve up to deflections of 1.5 mm (tested span is 450 mm) was calculated. Numerical approach (trapezoidal method) was used, by dividing the area under the curve into trapezoids. The area up to a certain deflection is the sum of the trapezoids area up to that deflection.
- The Equivalent load is then calculated by dividing the area by the deflection up to which the area is calculated.
- The equivalent strength and equivalent flexural ratio were calculated using equation 2-2 and equation 2-3 presented in section 2.1.2.



- | | |
|--------------------------------------|---------------------------------|
| (1) Steel rig. | (5) Swiveling support. |
| (2) M.T.S loading arm. | (6) Fixed support. |
| (3) Gripping clamp. | (7) Fixed loading cylinder. |
| (4) LVDT 's clamp (held on the rig). | (8) Swiveling loading cylinder. |
| (9) M.T.S. body. | |

Figure 5-1: Test Set-up: Third-Point Loading Test

5.4 Slab Test

The test contains four elements:

- Major test on two full-scale slabs subjected to interior, edge, corner loaded at 150 mm from its angle bisector and corner loaded at 300 mm from its angle bisector.
- Plate-bearing test.

- Compressive strength test on cores drilled from the two slabs.
- Third-point loading test on beam specimens sawn from the two slabs.

5.4.1 Full-scale Test

Endeavoring to get similar behaviour for the two slabs, the depth of the SFRC slab was reduced by 16.6% in comparison with the plain concrete. According to steel fiber manufacturer design tables (refer to tables in Appendix B) the flexural strength of the SFRC slab is improved by 42% relative to plain concrete strength. Hence the SFRC depth should be reduced in order to get similar behaviour for both slabs. The following criteria were followed:

$$f = \frac{M}{Z} \quad \Longrightarrow \quad \text{Eq.5-2}$$

$$Z = \frac{bd^2}{6}$$

Where :

f = Flexural strength.

M = Moment of resistance.

Z = Modulus of section.

b = Width.

d = Depth.

Equation 5-2 was used to calculate for both slabs the following:

For SFRC slab :

$$f + 0.42f = \frac{6M_s}{(d_s)^2} \quad \Longrightarrow \quad \text{Eq.5-3}$$

For plain concrete slab :

$$f = \frac{6M_p}{(d_p)^2} \quad \Longrightarrow \quad \text{Eq.5-4}$$

Where :

M_s M_p = Moment of resistance of SFRC and plain concrete slab respectively.

d_s d_p = Depth of SFRC and plain concrete slabs respectively.

f = Flexural strength of plain concrete.

By equating equation 5-3 and equation 5-4, the two slabs yield equal moment of resistance. Therefore similar behaviour:

$$\sqrt{(d_p)^2} = 1.42(d_s)^2 \implies \text{Eq.5-5}$$

It is obvious from equation 5-5 that, 125.8 mm depth for SFRC slab is equivalent to 150 mm plain concrete slab.

Full-scale tests were conducted on two ground slabs subjected to interior, edge and corner loading. The first slab was SFRC (3.0x3.0x0.125m) and the second plain concrete (3.0x3.0x0.15m). The interior points were tested after 28 days and the edges and corners tested after 90 days. A 150 mm thick foamed concrete subbase cast on top of 1000 mm deep solid concrete floor.

The SFRC slab has identical mixture to that of the plain concrete slab refer (table 5-1). 15 kg/m³ of steel fibers was added to the plain concrete mixture to cast the SFRC slab.

A closed-loop material testing system was used in displacement control (1.5 mm/min.) to apply the load through a hydraulic twin jack and record the data (100 readings/sec) from LVDTs sited at certain spots. A single steel loading plate (100x100x50mm) was placed centrally beneath the jack's load transferring plate. The devices and instruments used in the test can be seen in figure 5-2 and figure 5-3. Eight different test setups were used in this investigation and details of the different setups can be seen in figure 5-4. The setup for four load cases is considered:

5.4.1.1 Interior load (Test 1)

Seven LVDT's were used to measure the deflection at loading point and six other locations. One LVDT was adjusted and located to measure the vertical displacement beneath the loading point while the other six LVDTs were located at 300 mm intervals as shown in figure 5-4/Test 1. The LVDTs were clamped on a steel beam simply supported next to the foamed concrete sub base. Figure 5-2 shows the general setup for the interior load case.

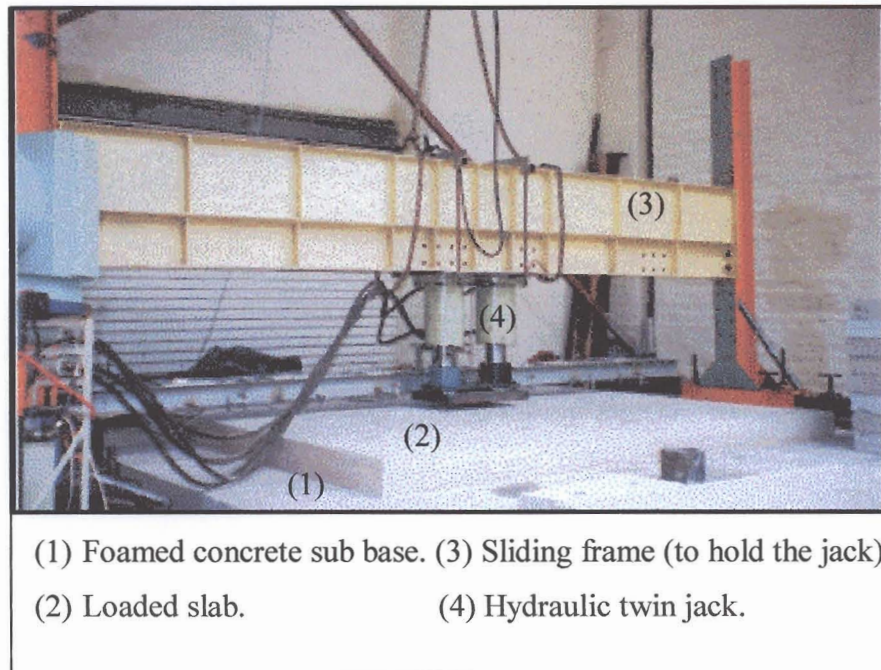


Figure 5-2: Photo Shows the General Test Setting: Full-scale Test (Interior load)

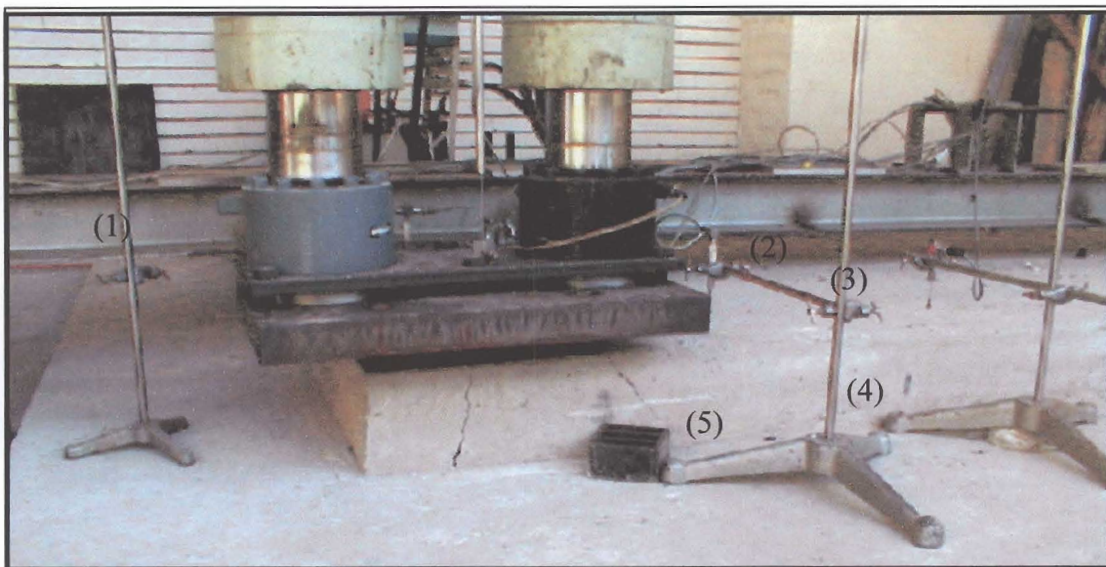
5.4.1.2 Edge load (Test 2)

Six LVDTs were used as shown in figure 5-4/ Test 2. The Procedure is described in section 5.4.1.1. The practicality of moving the jack around the slabs limited the possible test positions to one set of edges.

5.4.1.3 Corner load (Test 3 and 4)

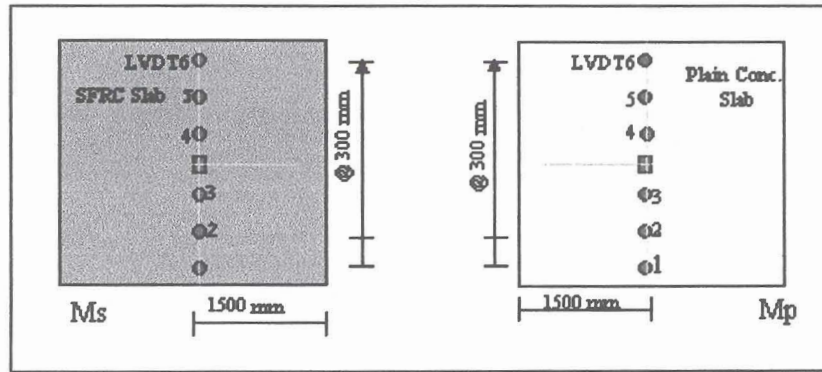
Two sets of corners were tested. The loading points were chosen at 150 mm and 300 mm from the corner angle bisector for each set of corners respectively. See figure 5-4/Test 3 for corner at 150 mm and figure 5-4/Test 4 for corner loaded at 300 mm. It was aimed to evaluate the influence of the loading position relative to the corner.

Figure 5-3 shows the general test setup for corner load. Three LVDTs were clamped on a steel beam, having the same setting as in section 5.4.1.1 above. The other three LVDTs were mounted on a clamp fixed to a steel footing. One LVDT was adjusted and located to measure the vertical displacement beneath the loading point while the rest were located at points where failure is likely to be detected.

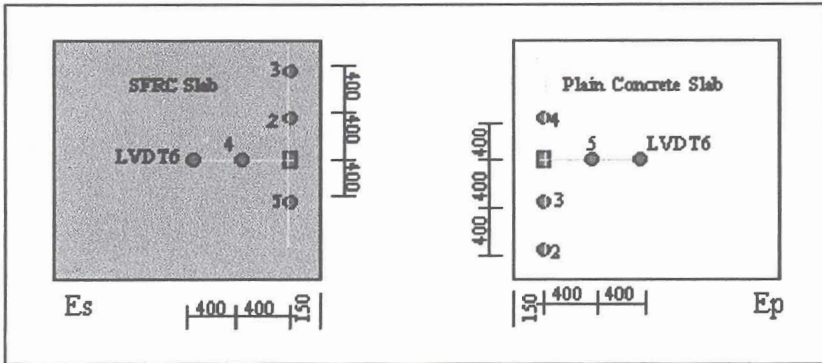


- (1) Steel beam (used to hold LVDTs). (2) LVDT. (3) Clamp.
(4) Steel footing. (5) Loading plate.

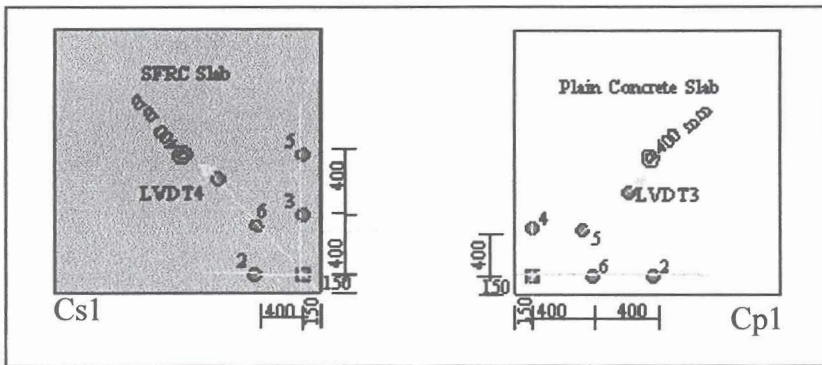
Figure 5-3: Photo Shows the General Test Setting: Full-scale Test (Corner Load)



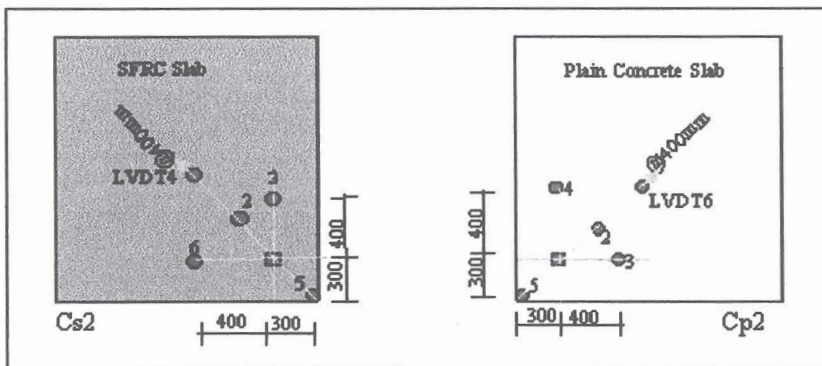
*Interior loading
Test 1*



*Edge loading
Test 2*



*Corner loading
@ 150 mm
Test 3*



*Corner loading
@ 300 mm
Test 4*

Figure 5-4: Loading and Measuring Points: Full-scale Test

The load-deflection relation was established for the two slabs for each case of loading. Spot readings every 10 KN were used to eliminate the effect of noise recorded. The first crack was estimated as the point at which the load-deflection curve first deviates from linearity. Differentiation techniques were used to estimate the first crack (sample of its assessment is found in Appendix C). The highest recorded load is assumed to be the maximum or “failure load”. The readings of the LVDTs at first crack and “failure” were used to establish a deflection profile for each set of test. Mode of failure for each test was visually established during testing

5.4.1.4 Comments on the Slab Setup

The test setup used for the full-scale test has the following shortcomings and limitations:

- The foam concrete sub base was very hard and might not simulate the field conditions. The measured K-value is very high compared to those used for the normal pavements. The deformation behaviour might also differ. The negative pressure associated with the normal compacted layer is not possible or not likely to take place with the foamed concrete, because of the high compressibility due to high void ratio found in the foamed concretes.
- Slabs were constructed adjacent to each other and the sub base was cast as one unit. Therefore the effect of the loading on the first slabs might extend to create a residual stresses and strains on the sub base of the second slab, which can affect the load capacity of that second slab.
- Three LVDTs were mounted on steel footings and these steel footings were put on the foamed concrete sub base. The readings of these LVDTs might be affected while the specific slab was under loading.
- The LVDT needles were rested freely on the top surface on the slabs to measure the vertical deflection. These needles should have glued to the slabs to eliminate the effect to surface roughness. This mistake was duplicated in all tests; therefore its effect might not have a significant influence in comparing the slabs.
- The practicality of moving the jack around the slabs limited the possible test positions to one set of edges and two sets of corners.
- The two slabs were cast on an enclosed environment having walls on three

sides while the fourth side was open. The SFRC slab was cast closer to the open side. The two slabs therefore did not have identical curing conditions. The SFRC slab had a longer sun exposure time and more exposed to the rain than the plain concrete slab. That might slightly affects the results.

- The available space for testing was limited; therefore, larger slabs were not possible.
- Only semi static load (low rate loading application) was applied and no provision was made for the cyclic loading.

5.4.2 Plate-Bearing Test

A plat-bearing test was conducted after 28 days to estimate the modulus of reaction for the foamed concrete sub base. The closed-loop system used in section 5.4.1 was used to apply the load and measure the deflection at the loading point. A loading plate having 250 mm diameter was used as a bearing plate. The following steps were followed to calculate the K-value as required by Westergaard ⁽¹¹⁾:

- A stress-deflection curve was established and the stress at a deflection of 1.25 mm was obtained from the curve.
- K_{250} is calculated by dividing the obtained stress by 1.25.
- The recommended bearing-plate diameter is 750 mm. Therefore; a correction factor was applied to convert K_{250} into K_{750} . The experimental diagram of Stratton in figure 5-5 was used to read off the correction factor corresponding to the plate diameter of 250 mm (Factor = 2.55).

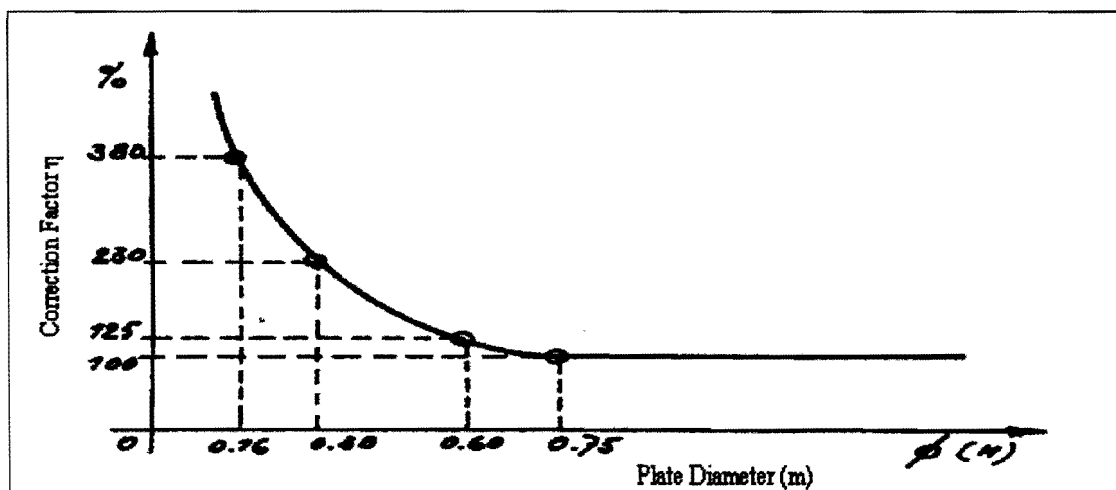


Figure 5-5: Diagram of Stratton to Correct for Bearing-Plate Size

- The following formulas are used to calculate K-value

$$K_{250} = \frac{\sigma_{1.25}}{1.25} \quad \Longrightarrow \quad \text{Eq.5-6}$$

$$K_{750} = \frac{K_{250}}{\eta} \quad \Longrightarrow \quad \text{Eq.5-7}$$

Where :

K_{250} = Modulus of subgrade reaction using bearing - plate of 250 mm diameter.

$\sigma_{1.25}$ = Stress at deflection of 1.25 mm.

K_{750} = Corrected modulus of subgrade reaction for bearing - plate of 750 mm diameter.

η = Stratton correction factor.

The bearing-plate test was only performed after 28 days and it would have been better if the test was repeated after 90 days to calculate K-value (at 90 days) for the theoretical analysis of the edge and corner load cases.

5.4.3 Core Test

Twelve cores of 100mm diameter were taken at 60 days from the two slabs (six cores each slab). The cores were drilled and capped according to SABS Method 865^[82]. The cores were capped to approximately 100mm length and stored in a constant room temperature (22C^o) and subjected to a standard compressive strength test after 90 days (the time at which the slabs were tested). This core strength was converted to actual and potential standard cube strength using the conversion formula given in the British Concrete Society Technical Report No. 11^[21]. The following are the formulas:

$$f_{act} = \frac{2.3f_{\lambda}}{1.5 + \frac{1}{\lambda}} \quad \Longrightarrow \quad \text{Eq.5-8}$$

$$f_{pot} = \frac{3.0f_{\lambda}}{1.5 + \frac{1}{\lambda}} \quad \Longrightarrow \quad \text{Eq.5-9}$$

Where :

f_{act} = Actual cube strength.

f_{pot} = Potential cube strength.

f_{λ} = Core strength.

λ = Ratio of length to diameter of the core

5.4.4 Third-Point Loading Test on Sawn Beams

Similar test setup that in section 5.3.3 was used to test four sawn specimens (two from each slab). Specimens were stored in a constant temperature room for three weeks; thereafter, third-point loading tests were conducted. Endeavoring to simulate the field curing conditions and loading direction, the four specimens were tested dry and loaded on the casting side.

The load-deflection relation was established for each individual tested specimen. The first crack load was estimated as the load at which the load-deflection curve deviates from linearity. (Refer to appendix C for sample of calculation). The highest recorded reading for the load is considered as a maximum load “failure load”. The first crack strength was calculated by substituting the first crack load in equation 5-1. Equivalent flexural load, strength and equivalent flexural ratio were calculated using the Japanese method as described in section 5.3.2. In addition to that, modulus of elasticity was calculated using equation 2-5 in section 2.1.7 sample of calculation is given in Appendix D.

5.5 Theoretical Analysis

To compare the theory and practice, the following theoretical models were used:

- Westergaard for the first crack load and elastic deflection.
- Meyerhof for the ultimate load capacity.
- Falkner et al for the ultimate load capacity.
- Shentu et al for the ultimate load capacity.

The slab properties were measured, calculated or assumed. The casting depth was taken as the slab thickness. The first crack strength and equivalent strength ratio were measured from the third-point tests conducted after 28 days on beam specimens. Modulus of elasticity was calculated from a third-point test described in section 5.4.4. For the purpose of this research, Poisson’s ratio and direct tensile strength were estimated to be equal for both SFRC and plain concrete. The K-value after 28 days was measured as described in section 5.4.2. After 90 days (edge and corner tests) greater K-value was estimated. The higher estimated K-value is because of the expected growth of its value because of the pozzolanic material contained in the foam concrete sub base.



The above-mentioned properties were used as inputs to Westergaard, Meyerhof, Falkner et al and Shentu et al to calculate the interior load capacity for the two slabs. Westergaard and Meyerhof were further used to calculate edge and corner load. Westergaard formulas for interior, edge and corner deflection were used to calculate the elastic deflection relevant to Westergaard load. Models are given in chapter 4.

Further calculations were performed considering various K-values. K-values ranging between 0.015 and 0.4 MPa/mm were assumed and used together with the slab's properties to calculate the load capacity and deflection as described thereof. Sample of calculations are presented in appendix E.



Chapter 6

Effect of Steel Fiber Content on Properties of Concrete

6.1 Background

The effect of the steel fiber content on workability, compressive strength, modulus of rupture, modulus of elasticity and toughness characteristics is studied.

6.2 Results

Table 6-1 shows the results of the slump test, compressive strength test on standard cubes to measure the failure load after 7 and 28 days, standard third-point loading test, third-point loading and standard E- value test (compression test). The number of fibers at the crack section of the beams are counted and presented for the different fiber dosages. The equivalent flexural strength ratio at a deflection of 1.5 mm is also calculated using the JSCE-SF4.

Table 6-1: Effect of Steel Fiber Dosage on Properties of Concrete

Content	Steel Fibers Dosage (kg/m ³)					
	0	10	15	20	25	30
Property						
Slump (mm)	135	135	145	100	80	90
Cube 7 days (MPa)	29.4	35.9	31.4	31.1	32	32.1
Cube 28days (MPa)	43.8	48.5	47.2	44.3	44.7	46.4
MOR (MPa)	4.1	4.9	4.8	5	5.3	5
Fibers counted Nr.	0	40	66	83	86	98
E-value (GPa)	25.3	24.2	26.7	26.6	27.3	24.4
First Crack (MPa)	4.1	5.2	5.2	5.4	4.9	5.2
Equivalent Strength (MPa)	0	2.0	1.9	2.4	2.7	3.8
Re 1.5	0	38.5	36.5	44.4	55.1	73.1
(80/60) Hook-ended steel fibers / 150x150x150 mm cubes / 150x150x500mm beams						

6.3 Discussion

6.3.1 Workability

Figure 6-1 shows the effect of the steel fibers dosage on workability of the concrete mixtures. The dotted line shows the general trend for the effect of steel fiber content on workability. It shows that addition of steel fiber has a minimum effect for low dosage while it has a significant effect for higher dosages.

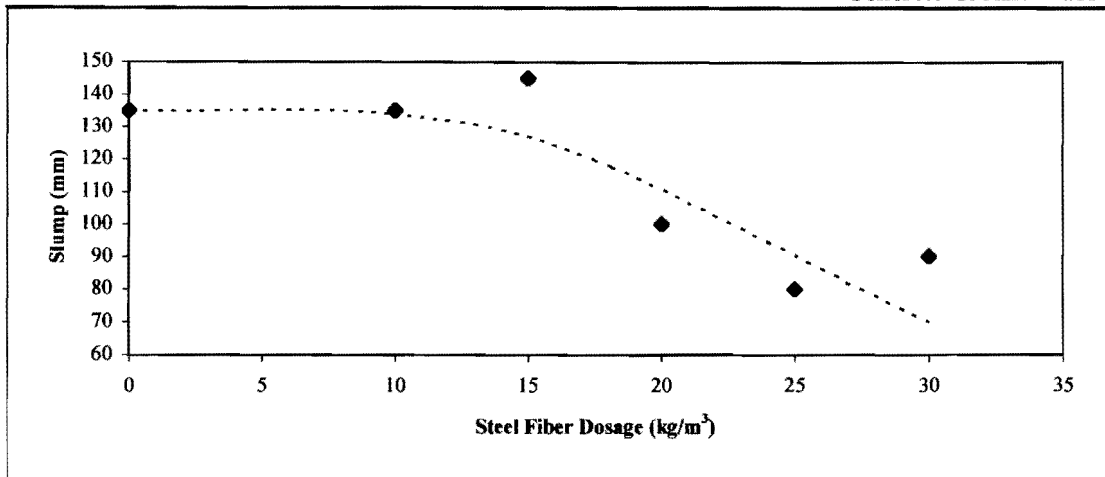


Figure 6-1: Effect of Steel Fibers Dosage on Workability

6.3.2 Compressive Strength

Figure 6-2 and figure 6-3 show that the steel fiber has a minimum effect on the compressive strength of the concrete mixture. An increase of minimum 1% to a maximum of 10% for different dosages is gained. It should also be noticeable that, the 7 days and the 28 days curves are approximately following the same patterns, which in turn means that some sort of consistency is normally associated with the strength growth characteristics of the SFRC.

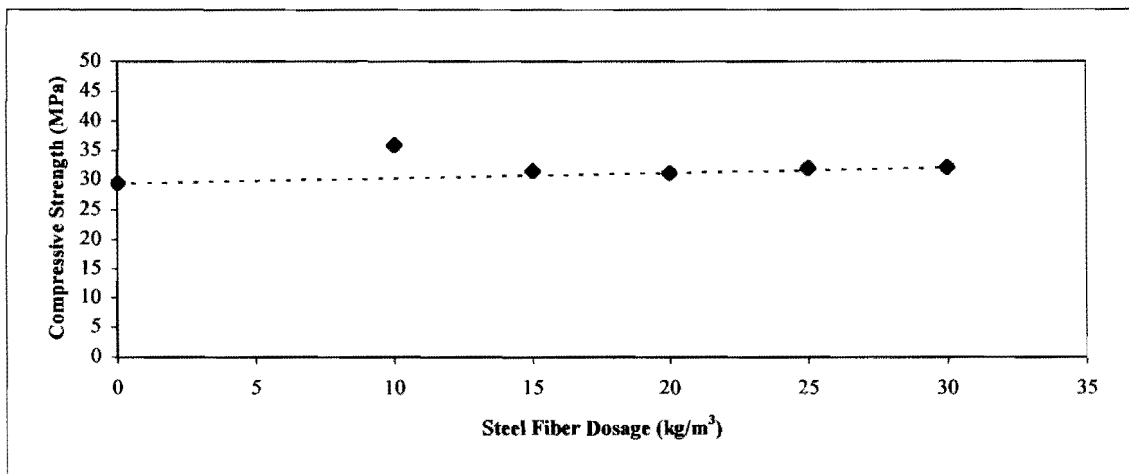


Figure 6-2: Effect of Steel Fibers Dosage on Compressive Strength at 7 days

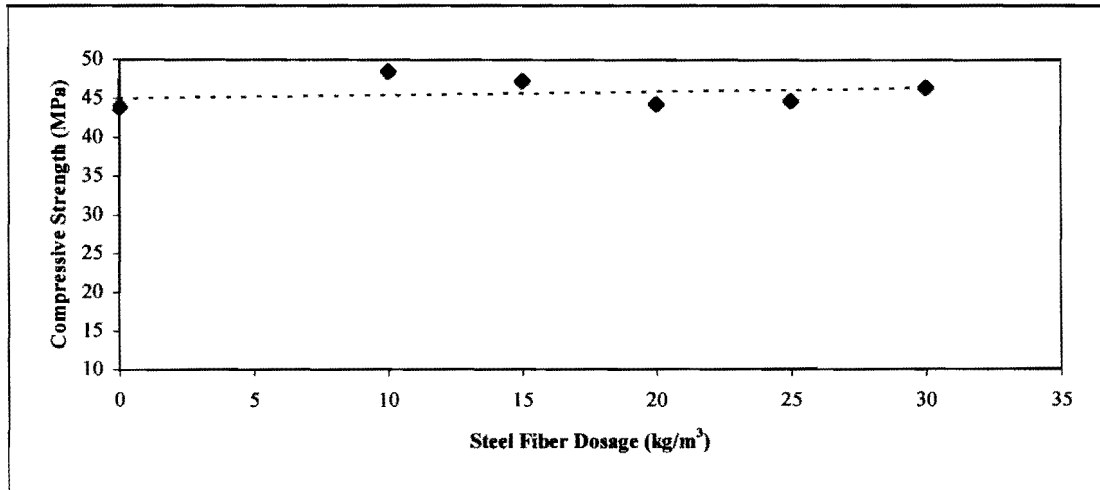


Figure 6-3: Effect of Steel Fibers Dosage on Compressive Strength at 28 days

6.3.3 Modulus of Rupture

Figure 6-4 shows the effect of the steel fiber dosage on modulus of rupture (MOR). It shows that about 19% increase is found for concrete containing steel fibers of 25kg/m³. The orientation of the individual steel fibers might profoundly affect the measured strength using beam specimens. This is obvious from the strength reading at steel fiber dosage 30 kg/m³ at which the MOR drops instead of increasing.

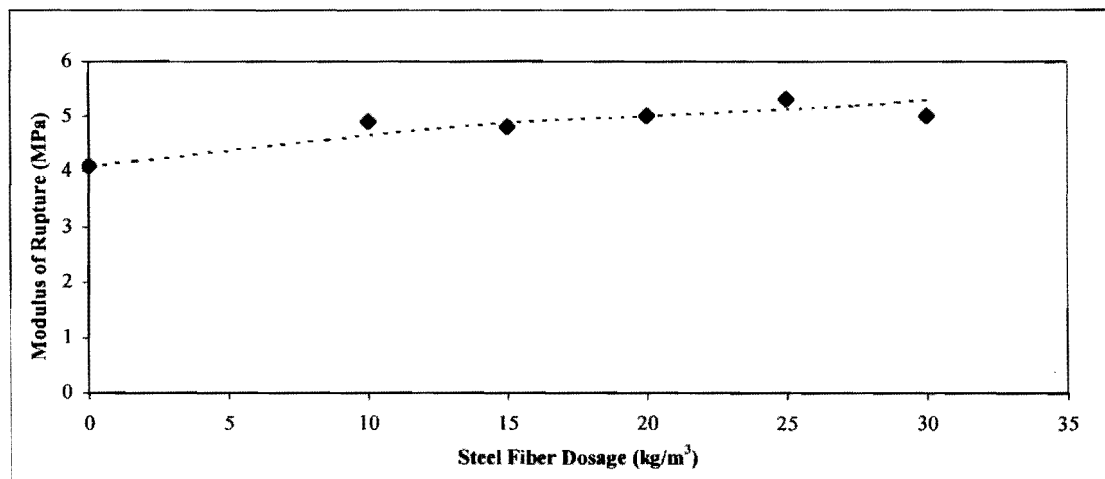


Figure 6-4: Effect of Steel Fibers Dosage on Modulus of Rupture

6.3.4 Modulus of Elasticity

Figure 6-5 shows the effect of steel fibers on the modulus of elasticity. Although the general trend of the curve shows a slight increase in its value with the increasing of the steel fiber dosage, this increase is insignificant.

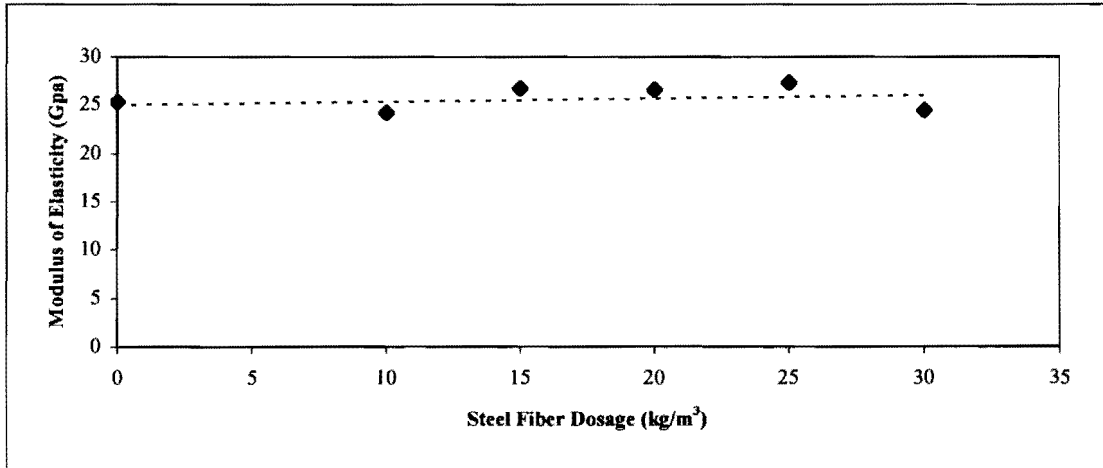


Figure 6-5: Effect of Modulus Steel Fibers Dosage on Modulus of Elasticity

6.3.5 Toughness

Figure 6-6 shows the effect of steel fiber dosage on first crack strength. The highest increase found was 25% with dosage 20kg/m³. The general trend shows that the steel fiber dosage has an insignificant effect on first crack strength at 28 days.

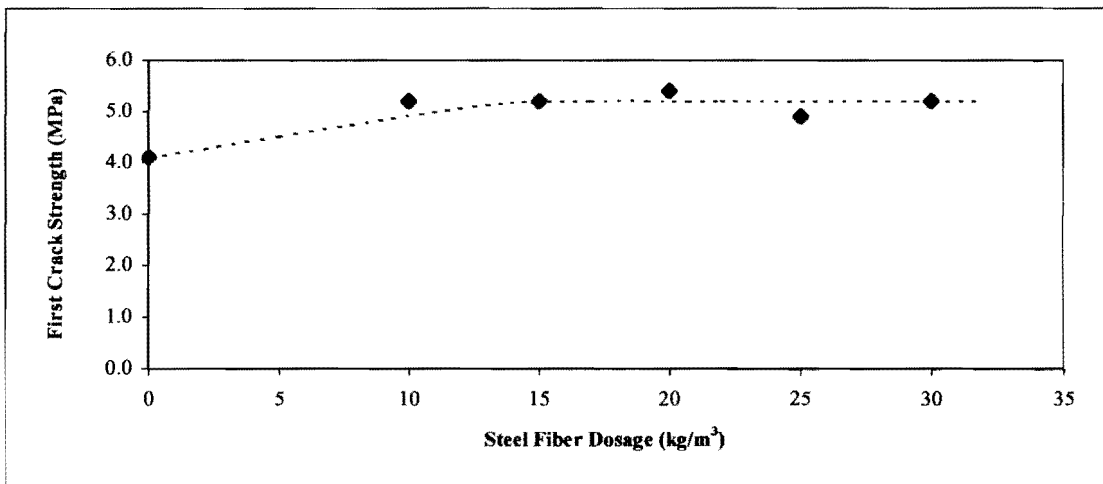


Figure 6-6: Effect of Steel Fibers Dosage on First Crack strength

Figure 6-7 shows the strength equivalent ratio (at a deflection equal to span/300) as a function of steel fiber dosage. From the graph it is noticeable that the addition of the steel fibers to concrete increases the toughness of the concrete by more than 70% at steel fiber contents such as 30 kg/m³. The general trend shows that a significant increase in toughness is gained by adding even low steel fiber dosage.

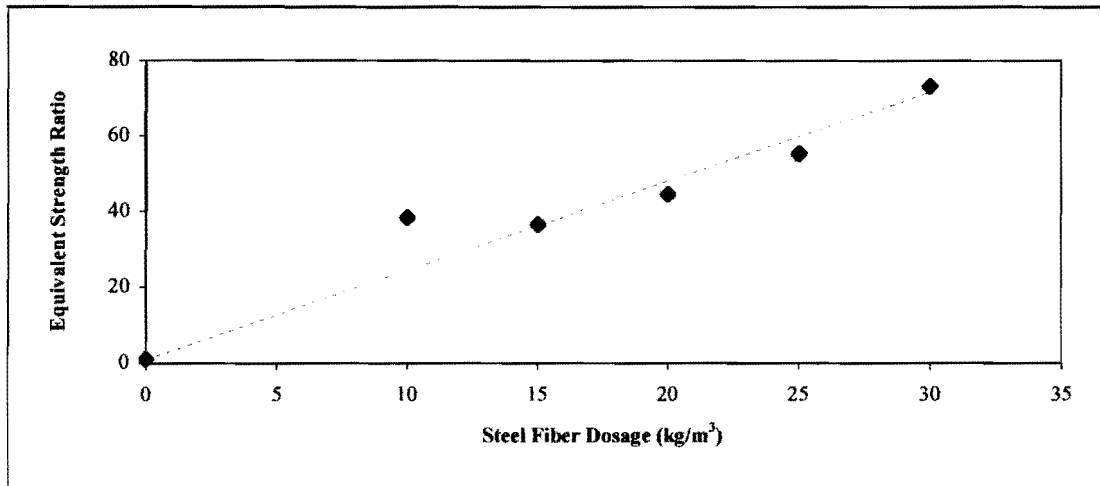


Figure 6-7: Effect of Steel Fibers Dosage on Toughness

6.4 Conclusions

The steel fiber dosage was found to influence the workability, compressive strength, MOR, modulus of elasticity, and toughness characteristics as following:

- The workability is less sensitive to low dosage and the sensitivity increases with the increase of dosage. As an indication, with steel fiber dosage of 25 kg/m³ the workability decrease by about 40% compared to plain concrete.
- The steel fiber dosage has a negligible influence on the compressive strength at 7 and 28 days.
- At 28 days, steel fiber dosage has insignificant influence on MOR. As an indication, for steel fiber dosage of 25 kg/m³ an increase of approximately 19% in the MOR was obtained (relevant to plain concrete).
- At 28 days the general trend is found that the steel fiber slightly increases the modulus of elasticity. This increase is considered insignificant.
- At 28 days, the addition of steel fibers with various contents increases the first crack strength by about 25 % (relative to plain concrete) and the most rapid increase occurred at low steel fiber dosage (up to 15 kg/m³).
- Steel fiber dosage has a significant influence on toughness characteristics. As an indication, it increases the after crack strength by more than 70% with steel fiber dosage of 30 kg/m³.

Chapter 7

Results of Slab Test

7.1 Background

In this section, results and the observations from the slab tests are presented and discussed. The discussion includes the full-scale slab test, cores and sawn beams.

7.2 Full-scale Slab Test

The results and the observations of the full-scale test are discussed. The discussion includes load capacity, deflection characteristics and failure patterns.

7.2.1 Results

Cubes and beams were cast using concrete mix identical to that of the two slabs. The results are summarized in table 7-1. (Refer to Appendix F).

Table 7-1: Strength Properties of the Slabs Mix

Property	Cube Strength (MPa)		First Crack Strength (MPa)	MOR (MPa)	Equivalent Strength (MPa)	Equivalent Ratio
	7 Days	28 Days				
SFRC	18.1	33.6	4.6	5.3	1.86	34.9
Plain Concrete	17.4	33.6	4.2	5.3		

Table 7-2 shows the full-scale test results for first crack and maximum load and its corresponding deflections. The given deflections are measured at loading points.

Table 7-2: Full-Scale Test Results

Impact Points	@ First Crack		@ Failure	
	Load (KN)	Deflection (mm)	Load (KN)	Deflection (mm)
Interior Loading (Test 1)				
Ms	383.80	1.48	656.70	4.50
Mp	398.40	1.36	731.0	3.94
Edge Loading (Test 2)				
Es	181	6.34	538.0	14.13
Ep	184	6.50	513.0	13.60
Corner Loading @ 150 mm diagonally from the corner angle bisector (Test 3)				
Cs1	193	7.35	413.0	13.26
Cp1	202	6.70	437.5	14.6
Corner Loading @ 300 mm diagonally from the corner angle bisector (Test 4)				
Cs2	485	10.73	568	12.12
Cp2	487	14.60	598	17.23

7.2.2 Comparison Between the Slabs

The two slabs were designed to have similar strength. The after cracking strength used (42% according to steel fibers manufacturers tables) was not achieved for the specified mix with the specified steel fiber content. The actual measured value was 34.9%; therefore a marginal difference of about 7.4% might be obtained.

The theoretical relation between the SFRC and plain concrete slab is shown in figure 7-1. Theoretically, a depth reduction of 16.6% can be achieved by adding 15kg/m^3 of hook-ended steel fiber to the parent concrete mix. With this steel fiber dose, the percentage of reduction is constant (i.e. Considering a plain concrete slab having 200 mm depth, the equivalent SFRC slab depth is 167.8, thus the reduction in depth is 16.6%).

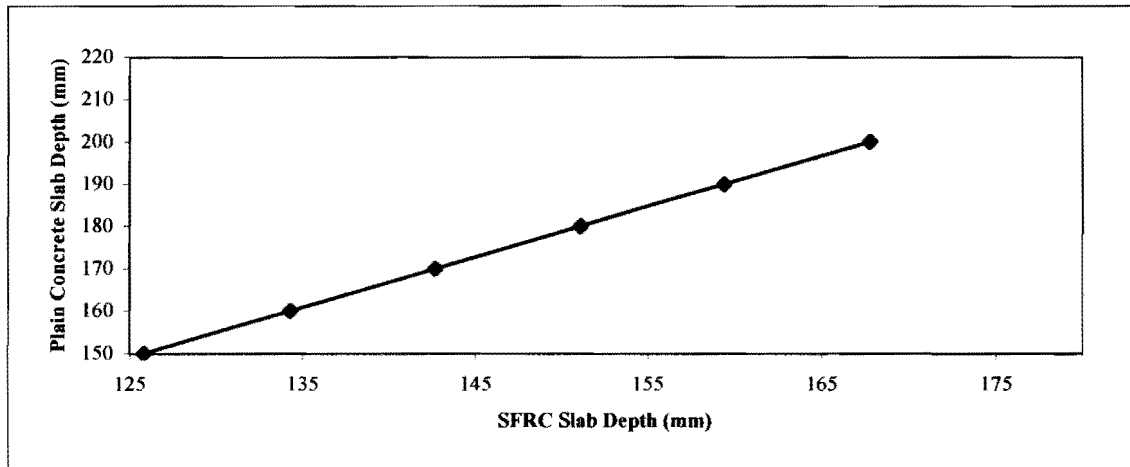


Figure 7-1: Relationship Between Depth of SFRC and Plain Concrete Slabs

Figure 7-2, figure 7-3, figure 7-4 and figure 7-5 show the load-deflection diagrams developed from the normalized measured datum for interior, edge, corner at 150 mm and corner at 300 mm respectively. It's appear from these figures that the first crack point is difficult to estimate and a different researcher can deem different cracking point for same load-deflection relationship. Therefore, the determination of the toughness factor at a limiting deflection value can better justify the slabs. So it can be seen from the graphs that both slabs can absorb approximately equal energy, which indicate that their load capacities are equal. In these figures, the first portion of the load-deflection relation is curved and that is due to the initial seating for the loading plate (due to surface roughness) during the starting stage of the load application.

Figure 7-2 shows that, although the plain concrete slab has slightly higher load capacity, both slabs have the same pattern of load–deflection curve. Which imply that the two slabs have the same structural behaviour when considering the bearing capacity for the interior load case. Sudden failure anticipated for the plain concrete slab is not prominent. (See discussion on failure modes in section 7.2.2.3).

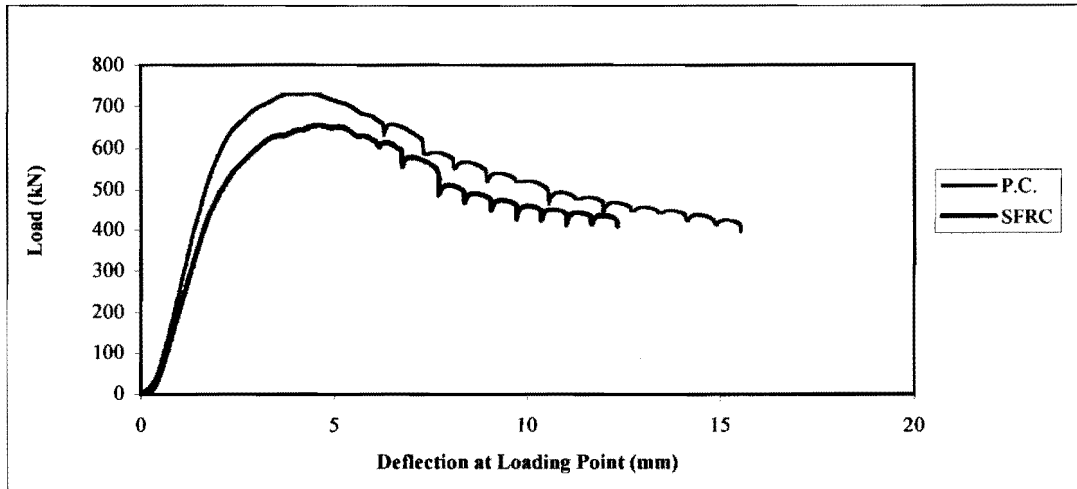


Figure 7-2: Full-scale: Test Load-Deflection Diagram (Interior Loading-Test 1)

Figure 7-3 shows the SFRC edge to have higher toughness and that the two edges have similar deflection at the ultimate failure. Apart from the localized reinforcement, the homogeneity of the SFRC tends to distribute the load in a larger area. The structural behaviour and failure characteristics of both slabs are again similar.

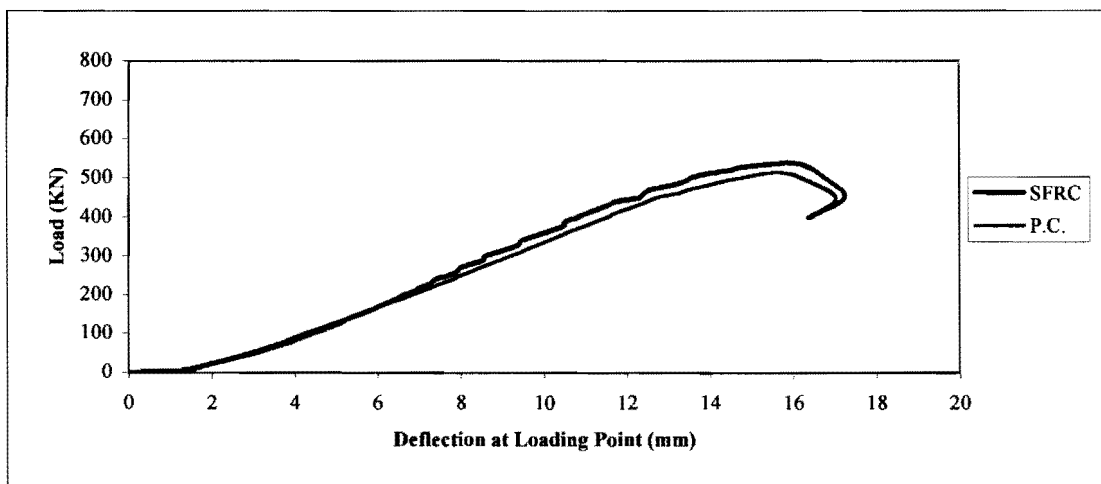


Figure 7-3: Full-scale Test: Load-Deflection Diagram (Edges Loading-Test 2)

Figure 7-4 shows that the behaviour of the two corners are approximately equal. They have different patterns of load-deflection curve, therefore, their structural behaviour is deemed to be slightly different. The ultimate failure for the SFRC corner was found at higher deflection but for low load capacity, while the plain concrete, fails at less deflection but at higher load. This can be taken as an advantage, because higher strains can be withstood with the SFRC than that of the plain concrete. Thus the brittle behaviour of the plain concrete corner is altered to a more elastic behaviour.

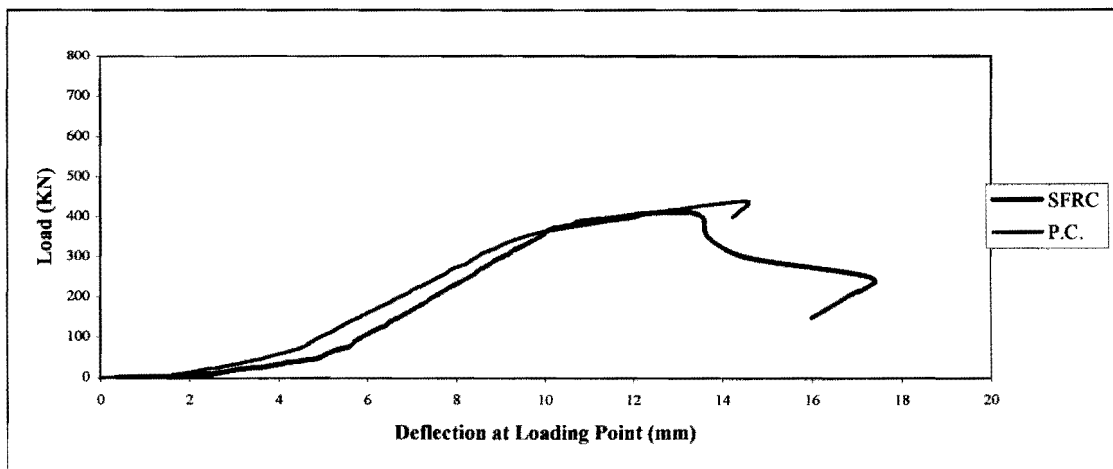


Figure 7-4: Full-scale Test: Load-Deflection Diagram (Load @150 mm-Test 3)

Figure 7-5 shows that the corner behaviour is completely dependent on the location of the load from its angle bisector. When corners are loaded at 300 mm from its angle bisector, the resulting load-deflection diagram is different to that for corner loaded at 150 mm (adjacent to the edges).

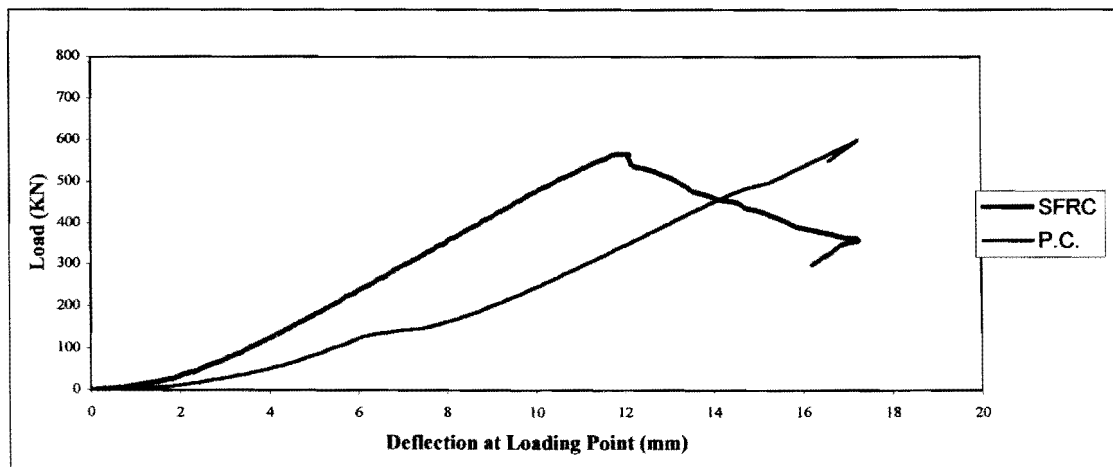


Figure 7-5: Full-scale Test: Load-Deflection Diagram (Load @300mm-Test 4)

7.2.2.1 Load Capacity

Figure 7-6 shows that, for interior, corners loaded at 150mm, corners loaded at 300 mm, and edge loading, the plain concrete was found to have 3.8%, 1.7%, 4.7%, and 0.4% greater first crack strength than the SFRC respectively. In comparison to the interior load, the corners loaded at 300 mm seems to yield very high first crack load. These relatively high values could be explained by the fact that these tests were conducted 90 days after casting the slab while the interior tests were conducted after 28 days. Other reason could be that something went wrong with the corners at 300 mm.

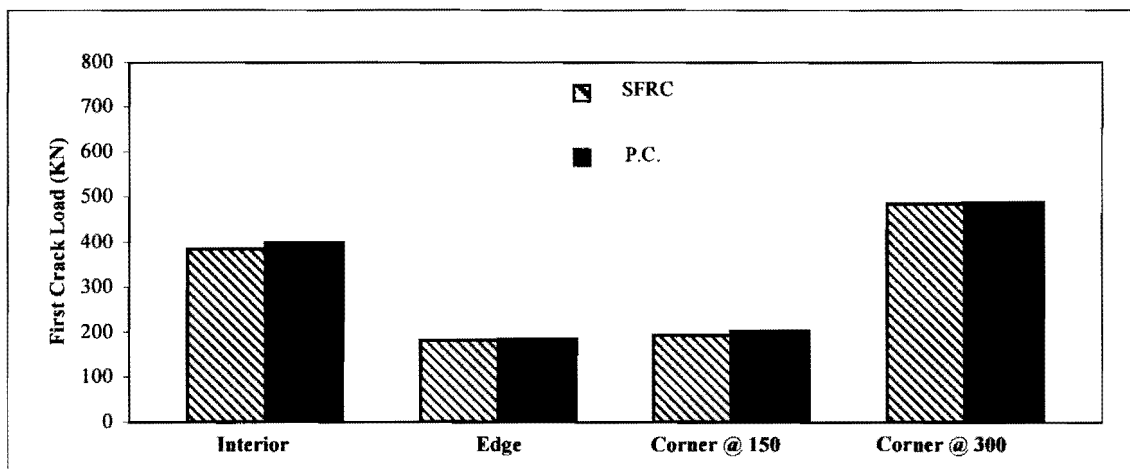


Figure 7-6: Load Capacity of the Slabs at First Crack

Figure 7-7 shows that, at maximum load the interior and corners of the plain concrete slab were found to have 11.3% and 5.5% greater values while the edge of the SFRC slab was found to be 5% stronger than the plain concrete slab. The edge of the SFRC slab shows higher load capacity than the edge of the plain concrete slab which is not the case at the first crack load as seen in figure 7-6. However the increase is negligible, but it can be an indication of the effect of the localized fiber orientation at that edge which cause the edge to sustain higher maximum load before its load capacity drops down.

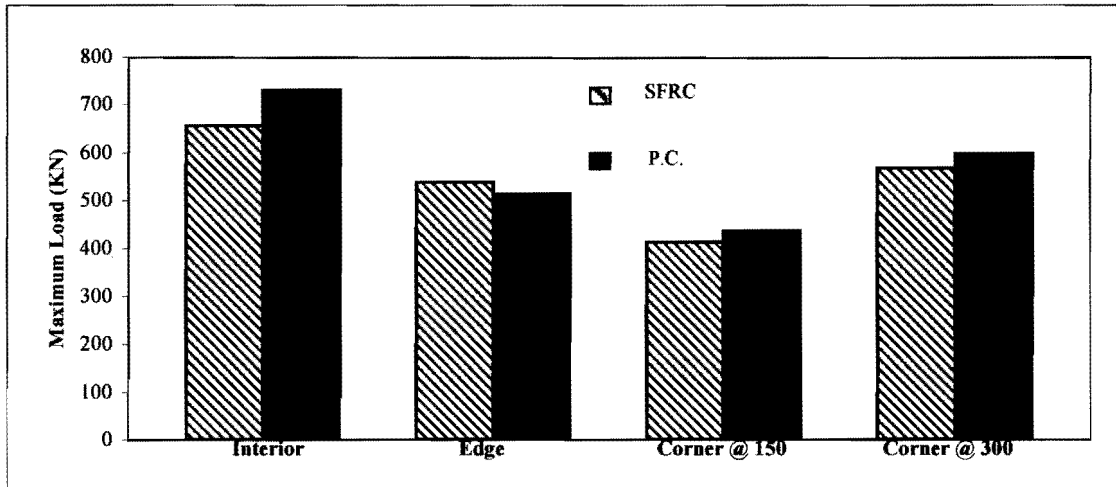


Figure 7-7: Load Capacity of the Slabs at Maximum. Load

The full-scale loading test showed that the two slabs are approximately equal in terms of first crack and maximum (termed failure) load capacities (Bearing in mind that the SFRC slab has 16.6 % less depth than the plain concrete slab).

7.2.2.2 Deflection Characteristics

Figure 7-8 shows the first crack deflection under load point for interior edge and corners of the SFRC and plain concrete slabs. The SFRC interior and corners at 150 mm was found to have 8.8% and 9.7% greater deflection respectively while edges and corners at 300 mm were found to have 2.5% and 36.1% less deflection respectively. Difference in deflection for the corners at 300 mm is huge.

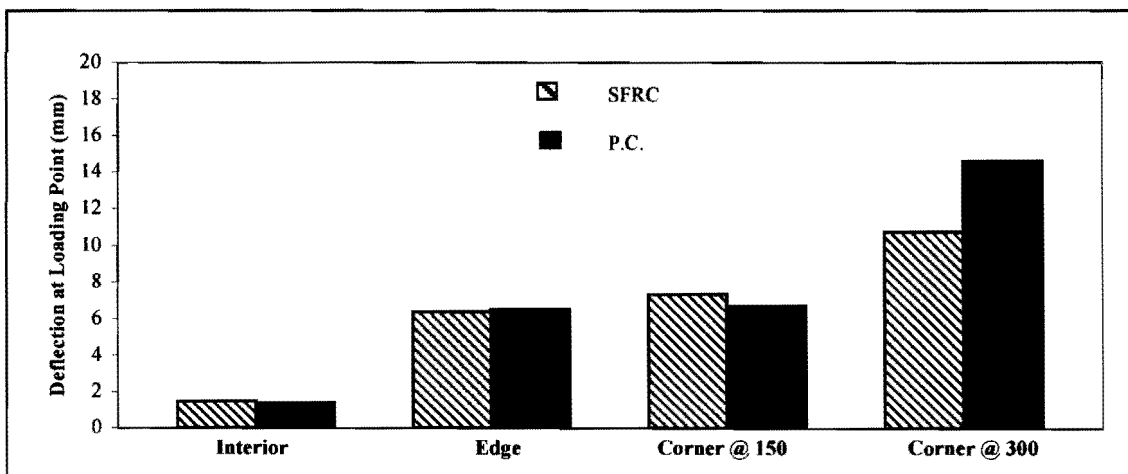


Figure 7-8: Deflection at Loading Point (at first crack load)

Figure 7-9 shows the deflection under load point at maximum load for interior, edge and corners of SFRC and plain concrete slabs. The SFRC interior and edge was found to have 14.3% and 3 % less deflection respectively. On the other hand, the SFRC corners at 150mm and at 300mm were found to have 10% and 42% greater deflection than plain concrete respectively. Difference in deflection for the corner at 300 mm is huge.

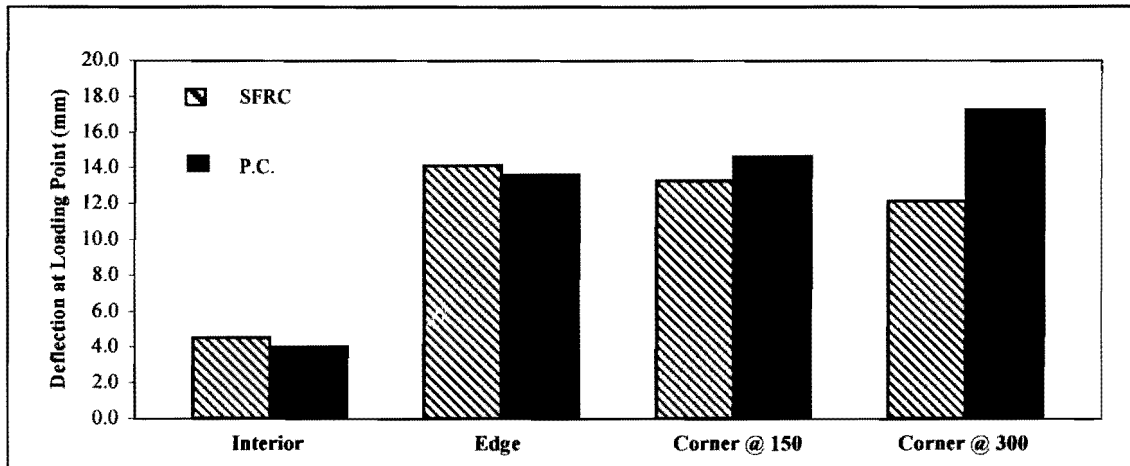


Figure 7-9: Deflection at Loading Point (at maximum load)

Figures from figure 7-10 to figure 7-17 shows the deflection profile for each case of load for both slabs. The deflection profile for each pair seems to have same pattern. It can be seen that for the most of the load conditions, the settlement is not that great relative to plain concrete which agrees with the study of Kaushik et al 1989, which stated that the settlement values of SFRC slab are less than or equal to that of plain concrete slab having same depth. Excessive deflection values associated with the free corners can cause densification or/and shearing of the underlying layers. Although free corners are rare in the reality of the pavement (usually doweled to the next corner), one should check that the resulting deflection doesn't exceed the underlying materials' vertical strain capacity for all critical load conditions.

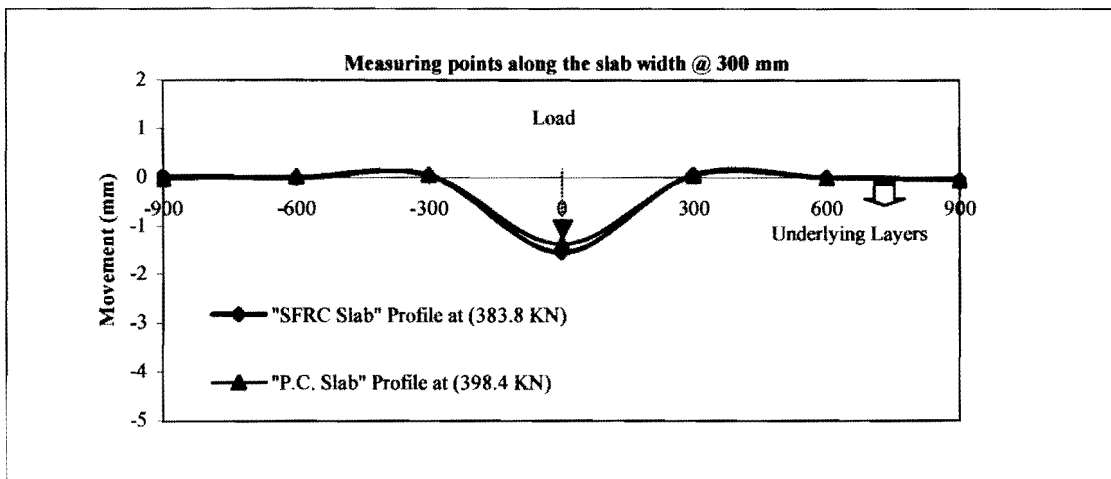


Figure 7-10: Deflection Profile at First Crack (Interior Loading-Test 1)

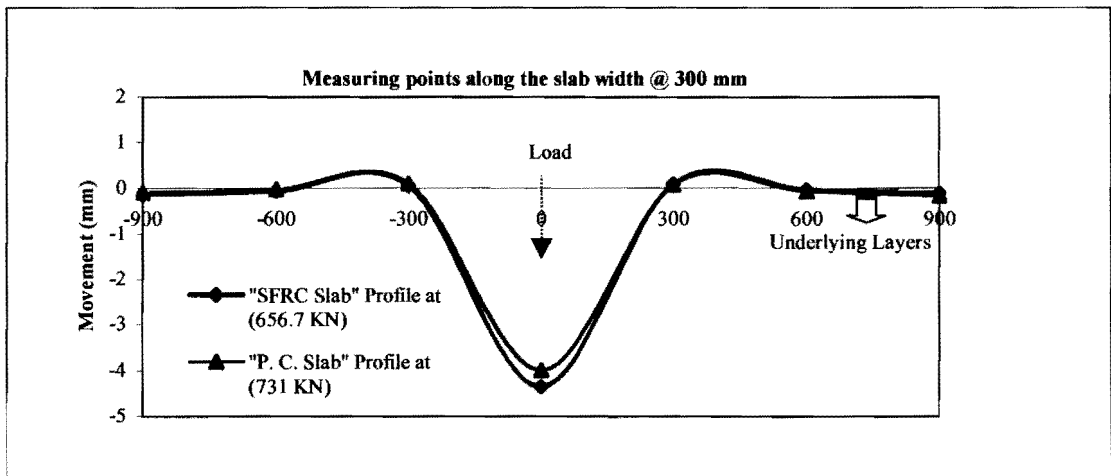


Figure 7-11: Deflection Profile at Maximum Load (Interior Loading-Test 1)

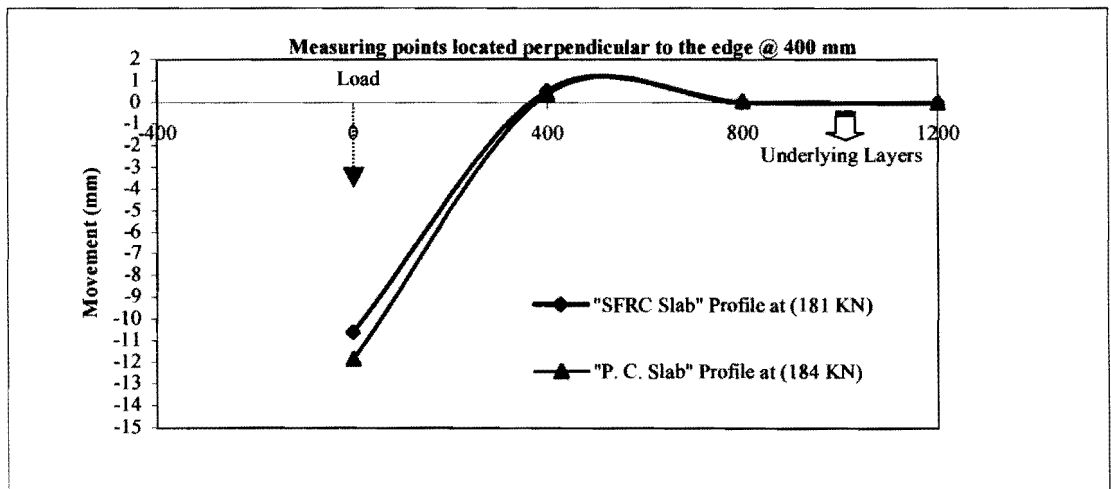


Figure 7-12: Deflection Profile at First Crack (Edge Loading-Test 2)

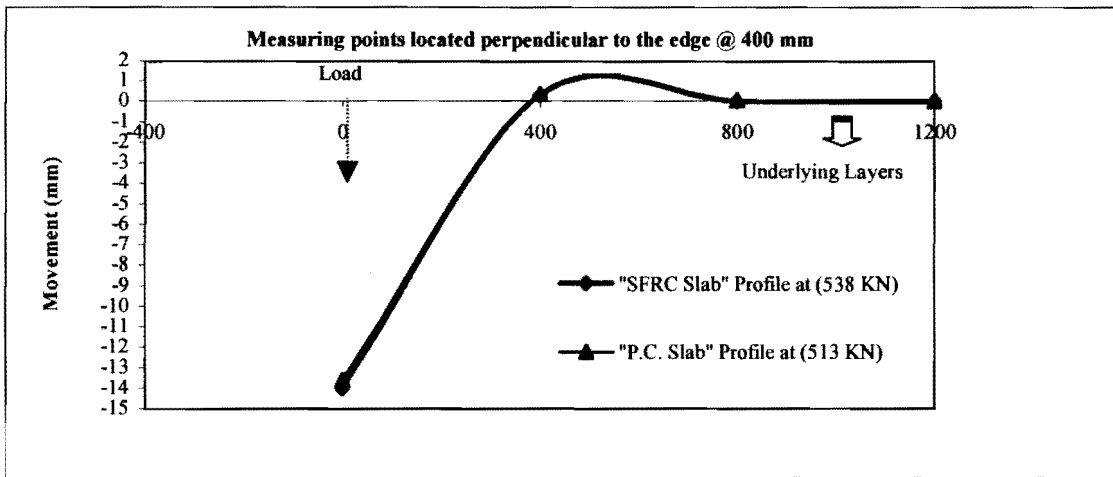


Figure 7-13: Deflection Profile at Maximum Load (Edge Loading Test 2)

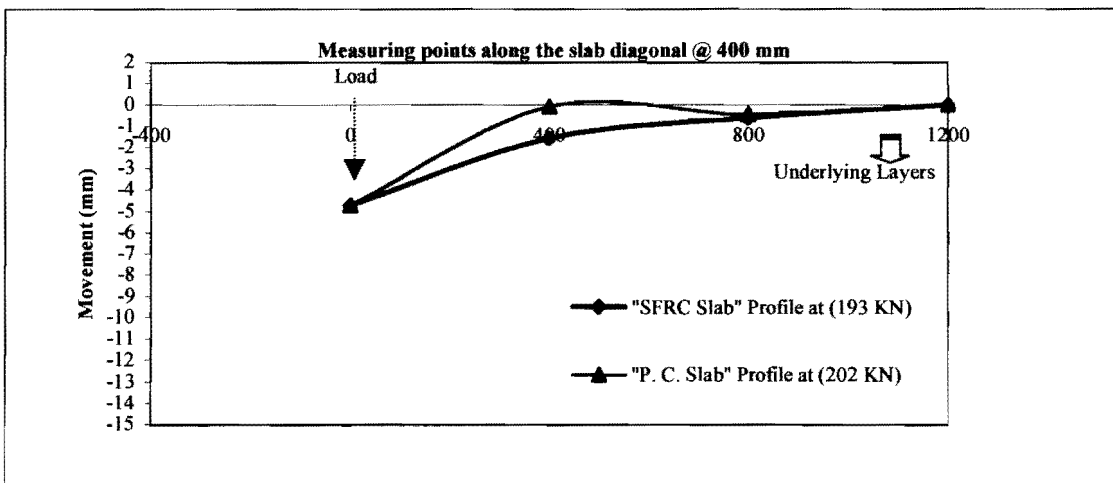


Figure 7-14: Deflection Profile First Crack (Corner at 150 mm-Test 3)

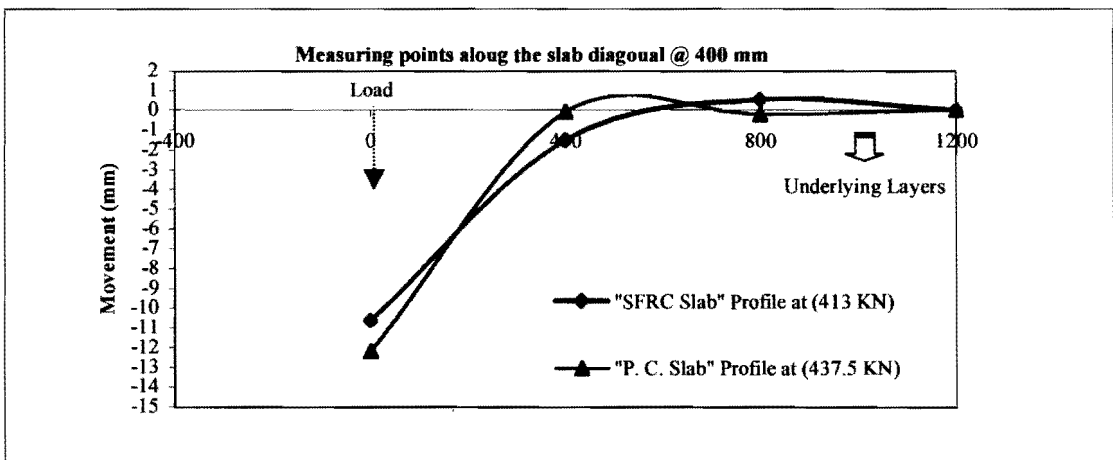


Figure 7-15: Deflection Profile at Maximum Load (Corner at 150mm-Test 3)

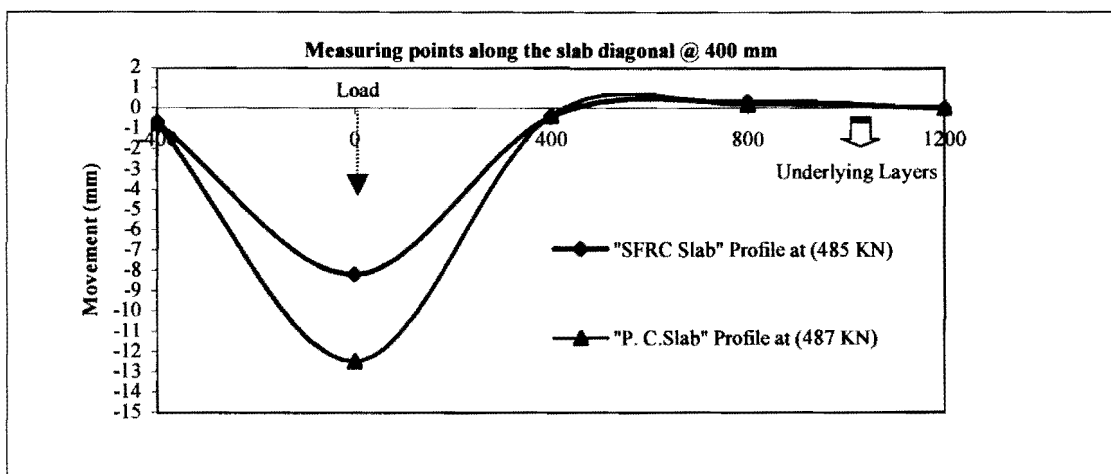


Figure 7-16: Deflection Profile at First Crack (Corner at 300 mm-Test 4)

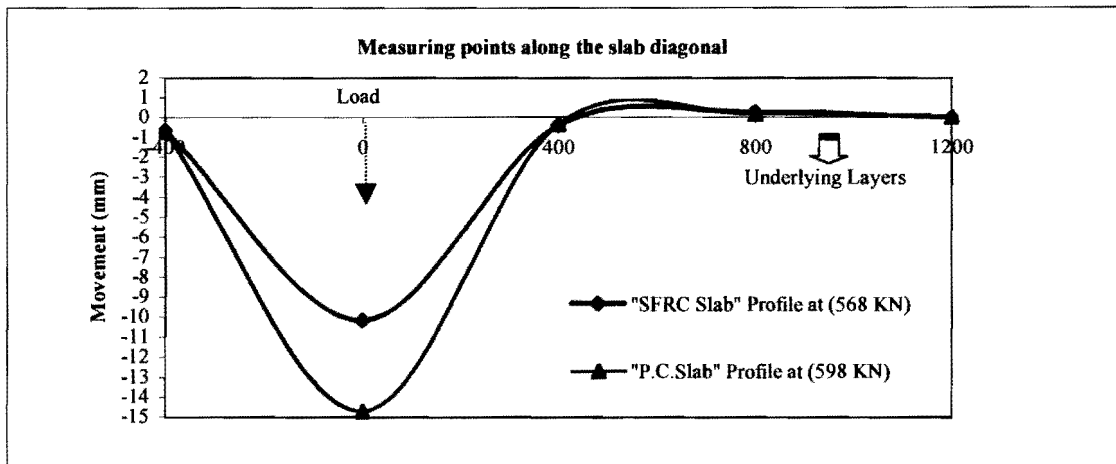


Figure 7-17: Deflection Profile at Maximum Load (Corner at 300 mm-Test 4)

Once again (excluding the results for corners tested at 300) the slabs are approximately equal in terms of deflection.

7.2.2.3 Failure Characteristics

Based on experimental work and test observation, the mode of failure for edges and corners was not altered and the SFRC shows integrity and consistency compared to the plain concrete. Although corners loaded at 150 mm from angle bisector and edges for both slabs were sheared, the steel fiber ones held together with the slab while the plain concrete ones punched down about 10 mm deep into the sub-base. Corners loaded at 300 mm failed in bending. Cracking of the SFRC corner occurred at a distance from the angle bisector, which is greater than that of the plain concrete. This confirms that the SFRC slab distributes the load to a bigger area than that of the plain concrete slab. While spalling occurred along the crack at the edge and around

the loading plate print at the corner of the plain concrete slab, the SFRC slab has shown no spalling.

Circumferential cracking with the “full fan” type associated with the interior load case as described in previous similar tests ^[83] was not observed on top of the two slabs. The settlement profile in figures 7-10 figure 7-11 shows the possibility that tiny circumferential cracking might have taken place at a distance of 400 mm from the center of the load. The reason behind tiny circumferential or no visible crack could possibly be the high K-value associated with the foamed concrete sub-base. It was also observed that the loading plate punched deeper by about 30 mm into the plain concrete slab while it punched about less than 10 mm into the SFRC. This might be attributed to the localized steel fiber reinforcement under and around the loading plate.

7.3 Compressive Strength Test on Cores

The compressive strength test on core specimens is discussed for the following:

- Variation on strength among the tested specimens.
- Mode of failure.
- Strength gain (results of the 28 days compared to those of 90 days).
- Conversion formula (formula to convert core strength into cube strength and formula to convert cube strength into flexural strength).

7.3.1 Results

Table 7-3: Compressive Strength Test on the Cores Taken from the Slabs.

Cores	L/D	Density (Kg/m ³)	Failure Load (KN)	Core Strength (MPa)	Actual Strength (MPa)	Potential Strength (MPa)
Steel Fiber Reinforced Concrete Cores						
S1	104/99	2299.6	318.6	41.41	38.6	50.3
S2	106/99	2305.2	293.1	38.1	36	47
S3	101/99.5	2267.7	368.6	47.4	43.9	57.2
S4	98/99	2281.2	339.5	44.1	40.4	52.7
S5	102.5/97.5	2353.3	317	42.5	39.9	52
S6	99/99	2258.2	349	45.3	41.7	54.4
Average				42.8	40.1	52.3
Plain Concrete Cores						
P1	105/99	2302.41	259.3	33.7	31.7	41.4
P2	106/99.5	2282.1	271.4	34.9	32.9	43
P3	101.5/100	2007.1	314.6	40	36.9	48.2
P4	98/98.1	2295.1	335	44.3	40.8	53.2
P5	102/99	2267	344	44.7	41.6	54.3
P6	99/98.5	2412.5	280.5	36.8	33.9	44.2
Average				39.1	36.3	47.4

7.3.2 Strength Variation

The variation of the compressive strength of the SFRC core specimens is expected to be higher than plain concrete ones, due to the randomness of the quantity and orientation of steel fibers in SFRC specimen. In spite of that, lower standard deviation of 3.5 was found for the SFRC specimens while a standard deviation of 5.4 was calculated for plain concrete specimens. The reason for that can be attributed the normal variation in concrete due to mixing, coring, casting, curing...etc.

7.3.3 Mode of Failure

Fracture mechanism for SFRC and plain concrete core specimens (under compression) was observed to fairly agree with that described by Neville and Brooks [21]. Under uniaxial compression, four stages were observed. The first stage was the formation of tension cracks parallel to the direction of load, second inclined cracks start to propagate and then noticeable disintegration to the specimens was seen and in the last stage failure took place. The only difference between SFRC specimens and plain concrete specimens was the last stage; at which the plain concrete specimens burst suddenly while the SFRC ones had a relatively gradual failure.

7.3.4 Strength Gain

After 90 days, 55.7% and 41.1 % are the gain in compressive strength for the SFRC and plain concrete cores relative to the 28 days strength. The extra strength for SFRC cores was anticipated and can be attributed to the after crack behaviour associated with SFRC. The failure of concrete specimens under uniaxial compression is mainly due to the formation of tensile cracks parallel to the direction of loading. Inclusion of randomly oriented steel fibers in the specimens arrest the propagation of tension cracks, there by apparently increases the compressive strength of concrete. This mechanism not only contributes to generate higher compressive strength for the SFRC specimens, but also contributes to the relaxed mode of failure. Figure 7-18 shows that the SFRC has a higher rate of strength growth than plain concrete.

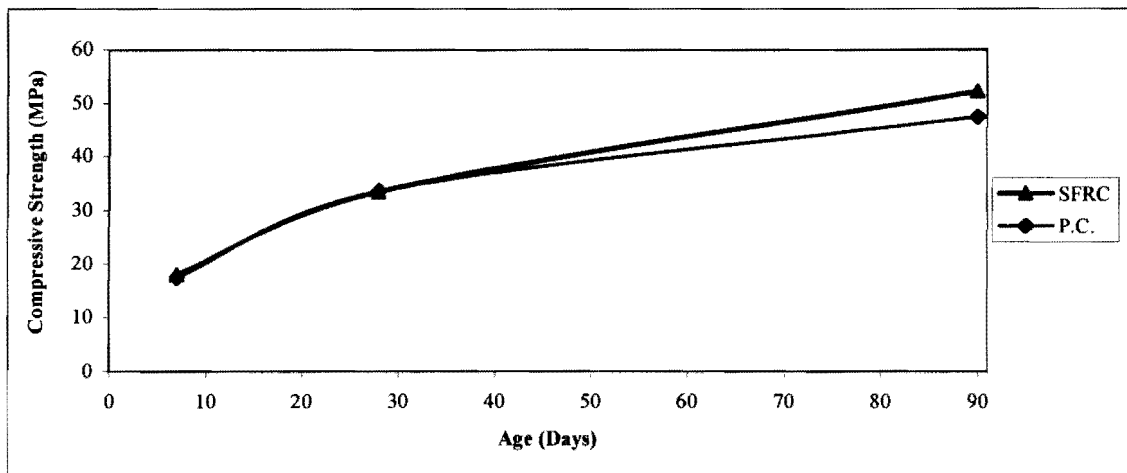


Figure 7-18: Strength Gain for SFRC and Plain Concrete

It was found that, potential strengths (derived for cores tested at 90 days) are greater by about 55.7% and 41.1% than the cube strength (assessed from crushing cubes at 28 days) for SFRC and plain concrete specimens respectively. It can be seen that an average of about 14.6% greater gain in strength is found for the SFRC specimens. The continued cement/ fly ash hydration causes both type of concrete to gain strength, but it has greater influence to the SFRC. Additional strength to the cement paste can also increase the interfacial bond between that paste and the steel fibers, which in turn contributes to more increase in the strength of the entire concrete. Another reason could be that the steel fibers acts to reduce the deterioration of the strength due to shrinkage cracks resulting from the dryness of the concrete. Previous tests show substantial increase in strength gain rate with high steel fibers

dosages ^[24]. Although the difference in strength gain found by this test is marginal compared to the plain concrete, it can contribute to more economical pavement design especially when the pavement will not be loaded until many months after it has been placed.

7.3.5 Conversion Formula

Empirical formulas prescribed by BS1881: Part 120; 1983 and adapted from Neville and Brooks ^[21] were used to assess potential strength for both SFRC and plain concrete core specimens. The potential strength results in table 7-3 were compared to results from cubes having identical mix tested after 28 days. Comparison between compressive strength derived from cores and 28 days cube strength revealed that the conversion formulas are satisfactory and applicable to evaluate compressive strength for SFRC cores. Formulas that convert for cores with steel bars are not considered due to difficulties in finding the cross sectional area of steel fibers and to random orientation of these fibers.

7.4 Third-Point Loading Test on Sawn Beams

The results of the third-point loading test on the sawn beam specimens are discussed from the following angles:

- Capacity comparison between the SFRC and plain concrete,
- Toughness characteristics.
- Failure mode.
- Modulus of elasticity.

7.4.1 Results

Table 7-4 shows the results of the sawn beam specimens. Results of load, strength and deflection at first crack and at maximum load are presented. The equivalent load, strength and strength ratio are calculated according to the JSCE-SF4 method. Modulus of elasticity is calculated on the bases of elasticity theory using the load-deflection curve obtained from the third-point loading test.

Table 7-4: Sawn Beams Taken from the Slabs: The JSCE-SF4 Characteristics

Property		Beams	IS	OS	IP	OP
Dimensions (hxbxL mm)			131x122x544	130x118x556	155x158x563	158x154x560
At First Crack	Load (KN)		19.8	18.3	26	24.5
	Strength (MPa)		4.3	4.2	3	2.9
	Deflection (mm)		0.04	0.04	0.03	0.03
At Maximum Load	Load (KN)		22.48	21.61	31	27.7
	Strength (MPa)		4.8	4.9	3.7	3.4
	Deflection (mm)		0.08	0.08	0.06	0.07
Japanese Standard JSCE-SF4 Properties	Equivalent Load (KN)	Pe,3	10.24	11.01	—	—
		Pe,1.5	13.11	16.01	—	—
	Equivalent Strength (MPa)	f _{e,3}	2.2	2.49	—	—
		f _{e,1.5}	2.82	3.61	—	—
	Equivalent Strength Ratio	Re,3	51.2	60.6	1	1
		Re,1.5	65.6	88	1	1
Modulus of Elasticity (MPa)			28x10 ³	27x10 ³	23.4x10 ³	24.6x10 ³

7.4.2 Capacity

Table 7-4 shows that the load capacities of the sawn plain concrete beams are greater than those for the SFRC beams bearing in mind that smaller section are loaded for the last. On the other hand the flexural strength capacity of the SFRC beam is greater by 40 and 35% for first crack and maximum load respectively, which agrees with many other results reported elsewhere. It can also be seen that the smaller depths for the SFRC beams cause them to yield higher deflection, which agrees with the results obtained from the full-scale slab testing.

The higher flexural strength capacity found for the sawn SFRC beams can be explained by the upward movement for the beam's neutral axis which implies that greater portion of the beam's section is involved in resisting the applied flexural stress.

7.4.3 Toughness Characteristics

First crack flexural strength calculated at 90 days from sawn beam specimens is found less than the one calculated from beam specimens tested at 28 days. The sawing action might be the reason for that. First crack strength estimated from load deflection test is approximately equal to the modulus of rupture for the same concrete, therefore, for design purposes the term f_{ct} in equation 2-1 can be substituted with the modulus of rupture or it can be assessed from the compressive strength as discussed later. The modulus of rupture is convenient and easy to assess compared to the first crack strength

The equivalent flexural strength ratios presented in table 7-4 show that the after crack strength is equal to about 50 to 60 % of the first crack strength when considering 3mm deflection and equal to about 65 to 88% of the first crack when 1.5 mm deflection is considered. This means higher flexural strength can be gained when considering less deflection. It can be argued that the flexural strength assessment still needs further investigation, because with limiting the unfavourable deflection to a lower values higher flexural strength could be obtained which in turn reduced the section of structural elements. The situation is aggravated when speaking about ground slabs. Further work is required to prove that the $L/150$ (L =length) free deflection will yield deflection values that are not very small compared with the tolerated limits for ground slabs. The $L/300$ deflection limit could be considered for the pavements and that the extra strength could be utilized.

Figure 7-19 and figure 7-20 show that the load-deflection curve for the SFRC beams has a straight portion immediately after the maximum load. That portion is also reported elsewhere and known as the region of instability. That straight portion is because the sequences of its occurrence are faster than the response of the measuring devices. In fact that is one of the reasons for using the JSCE-SF4 method instead of the ASTM C1018. Apart from difficulties in assessing the first crack strength, the toughness factors and their relative residual strength ratios calculated within this zone are erroneous.

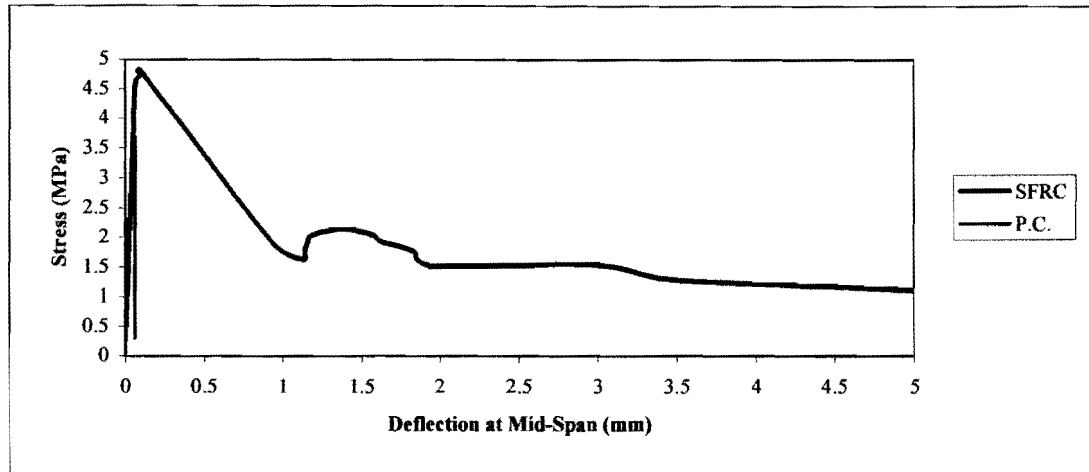


Figure 7-19: Stress-Deflection Diagram (IS & IP-inner beams)

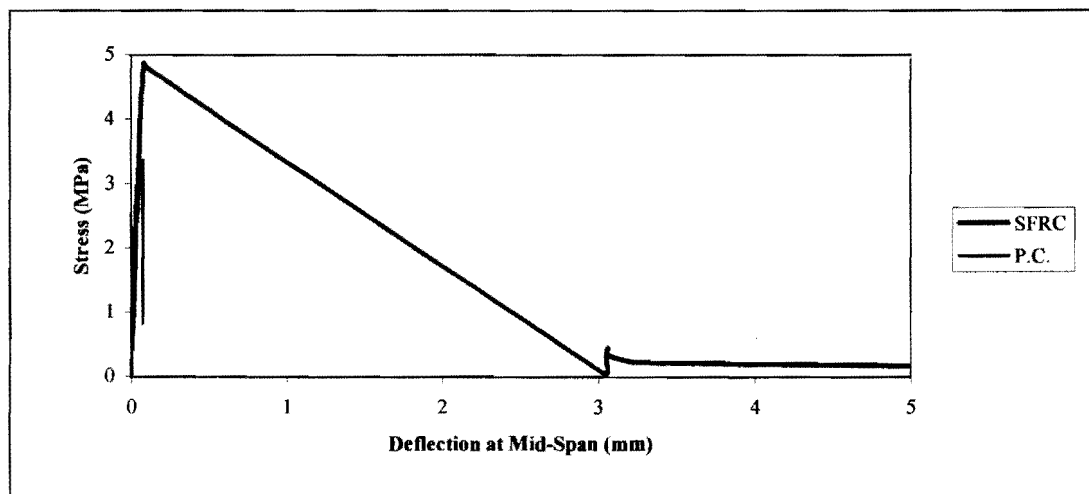


Figure 7-20: Stress-Deflection Diagram (OS & OP-outer beams)

Values for 28 days equivalent strength ratios ($R_{e,3}$) derived from steel fibers manufacturer's tables are found to be high by about 7.1% compared to the measured values (at 28 days) (refer to table 7-1). The average measured value from the sawn beams tested after 90 days is 56. Thus, the 90 days strength derived from the sawn beams is 14% greater than that derived from the steel fiber manufacturer tables. Some of that difference might be allocated to the strength growth either due to the hydration of the pozzolanic material contained in the mixture or to the increase of bond between steel fibers and concrete paste. These tables are found to be satisfactory for design purposes.

7.4.4 Modulus of Elasticity

E-values calculated from the third-point loading test are shown in table 7-4. The calculated values from sawn beams tested after 90 days agree with those found from cylinders under compressive strength tested after 28 days. The first method is believed to be better than the second one, because with one test many other properties can be assessed.

7.4.5 Mode of Failure

Figures 7-19 and figure 7-20 shows that the plain concrete beams fail suddenly while the SFRC beams fail slowly. The after-crack toughness can be explained from the multiple peaks associated with the load deflection curve for the SFRC. The sequence of the multiple peaks involves, that the steel fibers at the very bottom beam fibers initially hinder the first crack from growing to upper fibers. With increasing the load these steel fibers break down by either stretching or pulling out and the crack will grow to an upper level through the beam depth, once again another steel fiber does same above and so on till the beam fails completely. The breaking down of the steel fibers was evident from the breaking sounds heard during the test.

7.4.6 Empirical Formula for First Crack Strength

A number of empirical formulae have been suggested to relate flexural strength (f_{ct}) and compressive strength (f_{cu}). The following formula at Eq.7-1 is given by many design catalogues ^{[11][39]}

$$f_{ct} = 0.393(f_{cu})^{2/3} \quad \Longrightarrow \quad \text{Eq.7-1}$$

Where :

f_{ct} = Flexural strength.

f_{cu} = Compressive strength

From compressive strength data after 28 days and after 90 days, it is found that the equation is over estimating the flexural strength by about 5.7% and 25.5% of the SFRC and plain concrete respectively. Obviously the equation can be used for design purposes to estimate the flexural strength of the SFRC, which is beneficial in the sense that the compressive strength test is easy to conduct and cheap compared to the third-point loading test.

7.5 Conclusions

7.5.1 Full-scale Slabs

- For plain concrete ground slabs with a depth of 150 mm a theoretical reduction of 16.6% in depth could be achieved by adding (15kg/m^3) steel fibers to its mix. Theoretically the reduction (16.6%) is constant. Further practical tests are required to investigate the consistency of that reduction with other depths.
- Keeping in mind that the SFRC is thinner by 16.6%, the measured load capacity and deflection and the observed failure of the SFRC and plain concrete slabs for the interior, edge, and corners at 150 mm are found to be approximately equal.
- The results obtained from corners loaded at 300 mm are suspicious. Further tests should be conducted to investigate its load capacity and deflection characteristics.
- The mode of failure characteristics of the SFRC slab is marginally affected by the addition of steel fibers. The brittle behaviour of the plain concrete corner is altered to a more elastic behaviour when adding the steel fiber to concrete. This could have influence on concrete ground slabs, because the breaking off and shattering of corners could then be reduced if not completely overcome by using SFRC. Further investigation is required.
- Results could be affected by the foamed concrete support stiffness and failure mode. Further investigation is required.

7.5.2 Cores

- The strength variation among SFRC cores was expected to be higher than that for the plain concrete. Tests revealed that variation is higher among the plain concrete specimens, therefore higher consistency was achieved for SFRC than that for plain concrete.
- Gradual mode of failure is found for the compressed SFRC specimens, while brittle failure is found for the plain concrete ones.
- 14.5% greater strength gain in compressive strength was found after 90 days for the SFRC cores compared to plain concrete cores. The gain is due to the increasing of the bond between steel fibers and the concrete paste at the interfacial surface.

- Conversion formulas (for cores without steel bars) developed for plain concrete to convert core strength into cube strength is found applicable to the SFRC. Further tests should however be conducted to refine the formula.

7.5.3 Sawn Beams

- After 90 days the first crack flexural strength and strength at maximum load of the SFRC was found 40 and 35% greater respectively compared to plain concrete.
- The equivalent strength ratio derived from sawn beams tested at 90 days and beam specimens tested at 28 days were 60 and 35 respectively. The manufacture values at same fiber type and content is 42%. Reason for late strength development might be attributed to the pozzolanic material used in the mix. The manufactures tables are considered satisfactory for design purposes.
- The Japanese standard for determination of the SFRC toughness is deemed to give satisfactory and reliable results.
- Test results indicate that the modulus of elasticity calculated from data developed by third-point loading test is satisfactory.
- Gradual type of failure is observed for SFRC (unlike the plain concrete).
- Conversion formula to convert cube strength into flexural strength for plain concrete is found applicable to the SFRC. Further tests should however be conducted to refine the formula.

Chapter 8

Comparison Between Theory and Practice

8.1 Background

Theoretical analysis results are discussed in conjunction with the measured values to evaluate the use of the models for SFRC and further compare the two slabs.

8.2 Results

8.2.1 Westergaard K-value

Figure 8-1 shows the stress-deflection relation for the bearing-plate test conducted on the foamed concrete subbase.

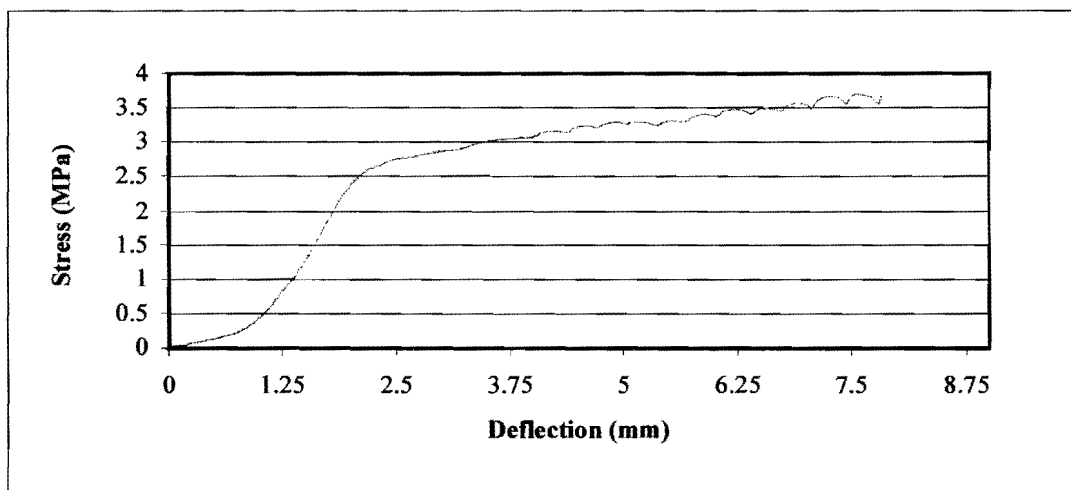


Figure 8-1: Stress-Deflection Diagram: Plate-Bearing Test on Foamed Concrete Sub base.

Based on figure 8-1, the stress at 1.25 mm deflection is 0.8 MPa. Thus K-value relative to 250 mm plate is $0.8/1.25$, which equal 0.64 MPa/mm. The correction factor is used to rectify for the plate size and the K-value as given by Westergaard is $(0.64/2.55)$ that is 0.25 MPa/mm.

8.2.2 Characters Used for Analysis

Table 8-1 shows the concrete properties as required by Westergaard, Meyerhof, Falkner et al and Shentu et al models to assess the load capacity and /or the vertical deflection at loading points.

Table 8-1: Properties of the Slabs Mix

Property	Units	P.C. Slab	SFRC Slab	Remark
Nominal thickness	mm	150	125	Casting depths
First crack strength (f_{ct})	MPa	4.1	4.8	Measured from Third-Point loading test
After crack strength ($f_{e,3}$)	MPa		1.9	Calculated from third-point loading test data.
Equivalent strength ratio ($R_{e,3}$)	%		39.6	Calculated from third-point loading test data.
E-value	MPa	24000	27500	Calculated from a third-point loading test.
Poisson's ratio		0.15	0.15	Estimated (has very little influence)
Uniaxial tensile strength.	MPa	2.2	2.2	Estimated
K-value (28 days)	MPa/mm	0.25	0.25	Measured from bearing plate test
(90 days)	MPa/mm	0.3	0.3	Estimated

8.2.3 Interior Load Capacity

Table 8-2 shows the results of calculation of interior load capacity of the two slabs by using Westergaard, Meyerhof, Falkner et al and Shentu et al. The calculation was performed using the properties as indicated in table 8-1. Apart from the measured K-value, various other K-values were assumed and the relevant load capacities were calculated.

Table 8-2: Calculated Interior Load Capacity for Various K-values

K (N/mm ³)	Plain Concrete Slab (150 mm thickness) (KN)				SFRC Slab (125 mm thickness) (KN)			
	Westerg.	Meyerhof	Falkner	Shentu	Westerg.	Meyerhof	Falkner	Shentu
0.015	57.9	104.9	133.8	336.5	47.3	122.4	181.2	231
0.035	62.44	107.9	163.7	376.5	51.1	126.2	225.1	255.3
0.05	64.6	109.3	179.1	406.6	52.9	128	247.9	273.5
0.1	69.2	112.6	215.1	506.6	56.6	132.2	300.5	334.1
0.15	72.21	114.7	240.7	606.7	59.1	134.9	338.4	394.8
0.2	74.5	116.4	261.3	706.7	61	137.1	369	455.4
(1)*0.25	76.4	117.8	278.9	806.8	62.6	138.8	395.4	516.1
0.3	78	119	294.5	906.8	63.9	140.4	418.3	576.7
0.35	79.4	120	308.5	1006.9	65.1	141.7	439.3	637.3
0.4	80.7	121	321.4	1107	66.1	142.9	458.1	698

(1)* Find sample of calculations in Appendix (E)



8.2.4 Edge and Corner Load Capacity

Table 8-3 shows the results of calculation of edge and corner load capacity of the two slabs by using Westergaard, Meyerhof. The calculation was performed using the properties indicated in table 8-1. Apart from the measured K-value, other K-values were assumed and the relevant load capacities were calculated.

Table 8-3: Calculated Edge and Corner Load for Various K-values

K (N/mm ³)	Plain Concrete Slab (150 mm Thickness)				SFRC Slab (125 mm Thickness)			
	Edge		Corner		Edge		Corner	
	Westerg.	Meyerhof	Westerg.	Meyerhof	Westerg.	Meyerhof	Westerg.	Meyerhof
0.015	33.7	64.9	34.6	39.2	27.6	76.1	28.2	46.2
0.035	36.5	67.5	36.6	41.2	29.9	79.4	29.1	48.7
0.05	37.9	68.8	36.2	42.1	31	81.1	29.5	49.9
0.1	40.7	71.6	37.4	44.3	33.4	84.7	30.5	52.7
0.15	42.6	73.5	38.3	45.7	34.9	87.1	31.3	54.5
0.2	44.1	74.9	39	46.9	36	88.9	31.9	56
0.25	45.3	76.2	39.7	47.8	37.1	90.5	32.4	57.1
(2)* 0.3	46.3	77.2	40.2	48.6	38	91.8	32.8	58.2
0.35	47.2	78.1	40.7	49.3	38.7	93	33.3	59.1
0.4	48	78.9	41.1	49.9	39.4	94.1	33.6	59.9

(2)* Find sample of calculations in Appendix (E)

8.2.5 Deflection

Table 8-4 shows the results of calculating vertical interior, edge and corner deflection using relevant Westergaard load for the two slabs. The calculation was performed using Westergaard formulas. Apart from the measured K-value, other K-values were assumed and the relevant deflections were calculated.

Table 8-4 Deflections for Various K-values (Calculated by using Westergaard)

K- Values (N/mm ³)	Plain Concrete Slab (150 mm)			SFRC Slab (125 mm)		
	Interior (mm)	Edge (mm)	Corner (mm)	Interior (mm)	Edge (mm)	Corner (mm)
0.015	0.71	1.43	2.97	0.71	1.44	2.89
0.035	0.50	1.02	1.88	0.5	1.02	1.18
0.05	0.43	0.88	1.55	0.44	0.89	1.48
0.10	0.33	0.67	1.05	0.33	0.68	0.99
0.15	0.28	0.57	0.83	0.28	0.58	0.78
0.20	0.25	0.51	0.7	0.25	0.52	0.65
0.25	0.23	0.47	0.61	0.23	0.47	0.57
(3)* 0.30	0.21	0.44	0.55	0.22	0.44	0.5
0.35	0.20	0.42	0.50	0.2	0.42	0.46
0.40	0.19	0.40	0.46	0.19	0.40	0.42

(3)* Find sample of calculations in Appendix (E)

8.3 Comparison Between Theory and Practice

8.3.1 Westergaard

8.3.1.1 Load Capacity

Load capacities calculated using Westergaard model are compared to the *loads at first crack* because Westergaard formulas assume an *elastic* behaviour. The after crack toughness of SFRC cannot be considered; therefore the influence of the steel fiber can be considered only when it contributes to increase the first crack strength if any.

Figure 8-2 shows a comparison between actual measured first crack load and the calculated load using Westergaard for the SFRC slab. It was found that the actual measured values are greater than calculated values by about 510%, 375% and 490% for interior, edge and corner loads respectively.

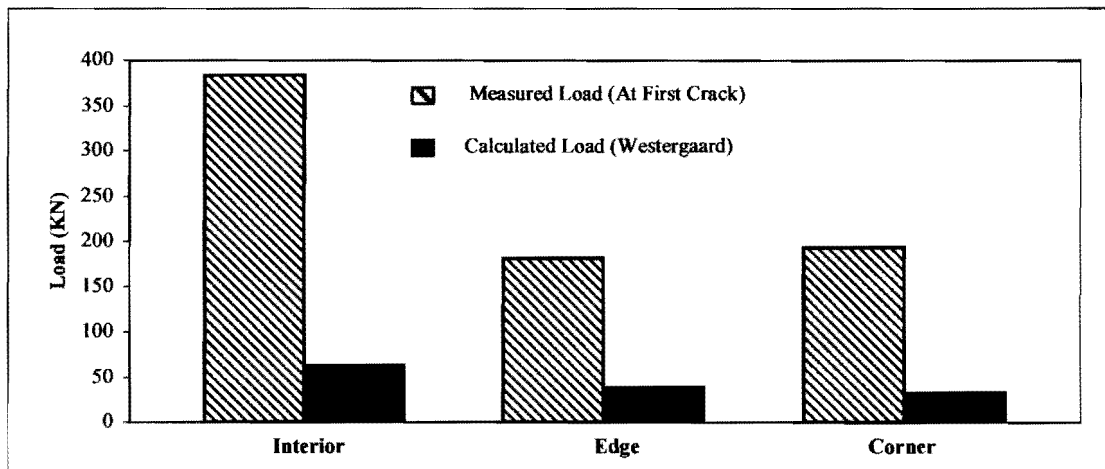


Figure (8-2): Measured Load and Westergaard Load for SFRC Slab

Figure 8-3 shows a comparison between actual measured first crack load and the calculated load using Westergaard for the plain concrete slab. It was found that the actual measured values are greater than calculated values by about 420%, 300% and 400% for interior, edge and corner loads respectively.

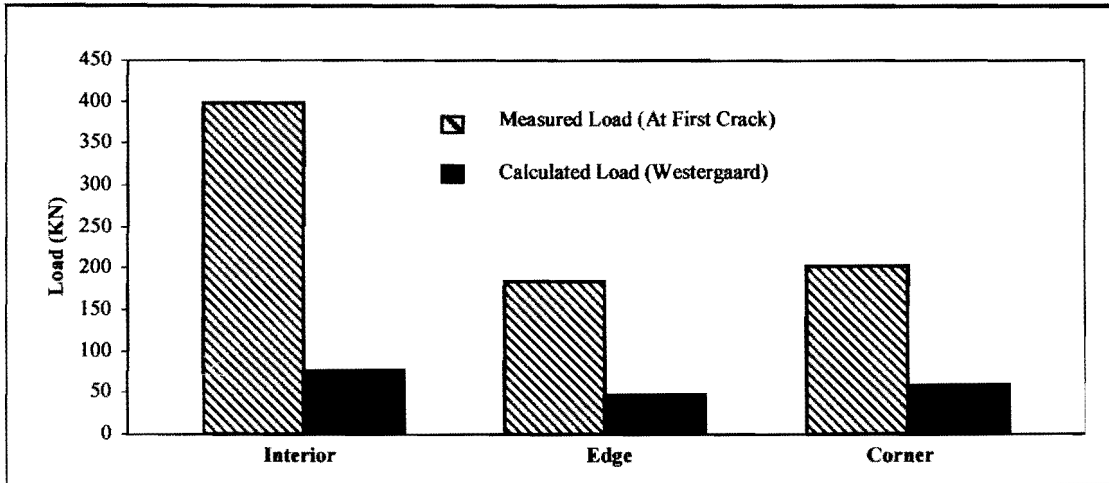


Figure 8-3: Measured Load and Westergaard Load for Plain Concrete Slab

The measured load capacities are very far from the calculated loads and this result correlates with results obtained by other researchers ^[77].

The hard foamed concrete subbase might influence the result. Figure 8-4 shows the relation between K-value and calculated load capacity. It is evident that there is a certain limit of K-value beyond which the increase in its value does not increase the calculated load capacity significantly. The reality might be different, because with increasing the sub grade reaction the slab and underlying layers tend to act as one unit thus increasing the load capacity dramatically.

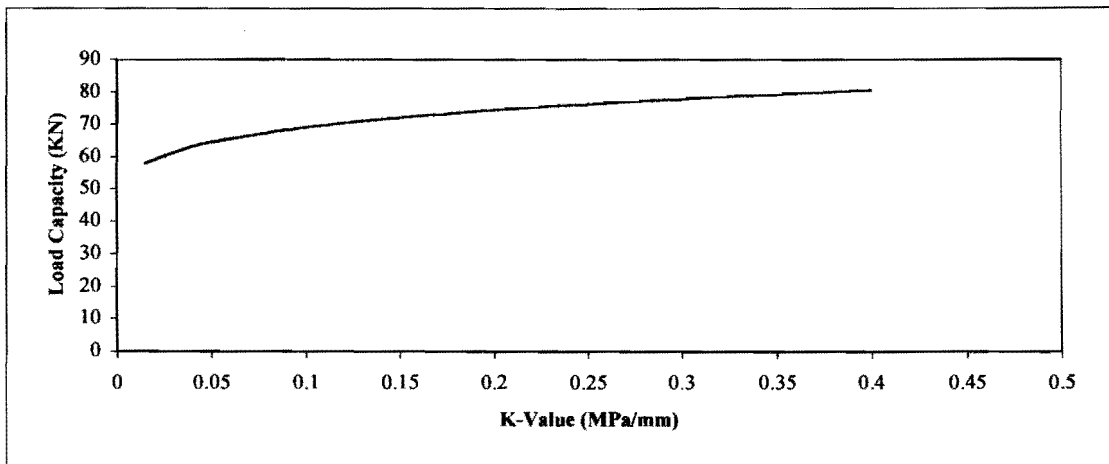


Figure 8-4: Sub grade Reaction-Load Capacity Relationship (Westergaard)

The theory of Westergaard was based on infinite slab. The dimensions of slabs used for this investigation might not be suitable for the comparison between Westergaard load and actual measured loads. There may be a certain minimum dimension required for the slabs for which better correlation could be obtained.

The first crack determination might also cause some disagreement. The first crack as defined (point at which load-deflection curve deviate from linearity) was not clearly found because the point of first crack as defined does not exist in the most of the cases. Therefore the estimated value might not be the real first crack.

The theoretical load capacity for the plain concrete slab is at most 18% more than the theoretical capacity for the SFRC slab while the measured loads were found to be approximately equal. This shows that the actual structural behaviour of the SFRC is different to that of plain concrete even prior to cracking. Westergaard formula doesn't seem to consider that behaviour and the SFRC is considered as plain concrete having higher first crack strength and less depth.

8.3.1.2 Deflection

The deflection calculated using Westergaard model is compared to the *deflection at first crack* as Westergaard formulas assume an *elastic* behaviour. The measured deflections were corrected by subtracting the seating deflections at the start of the load-deflection curve.

Figure 8-5 shows a comparison between actual measured first crack deflection at Westergaard load and the calculated deflection using Westergaard load for the SFRC slab. It was found that the actual measured values are greater than calculated values by about 150%, 60% and 115% for interior edge and corner loads respectively.

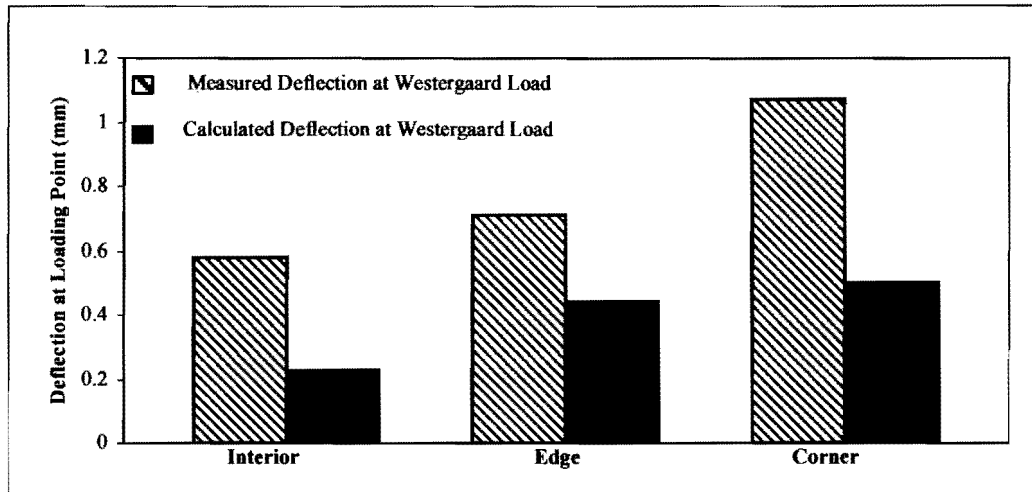


Figure 8-5: Calculated and Measured Deflections at Westergaard Load for the SFRC Slab.

Figure 8-6 shows a comparison between actual measured first crack deflection at Westergaard load and the calculated deflection using Westergaard load for the plain concrete slab. It was found that the actual measured values are greater than calculated values by about 130%, 130% and 75% for interior, edge and corner loads respectively.

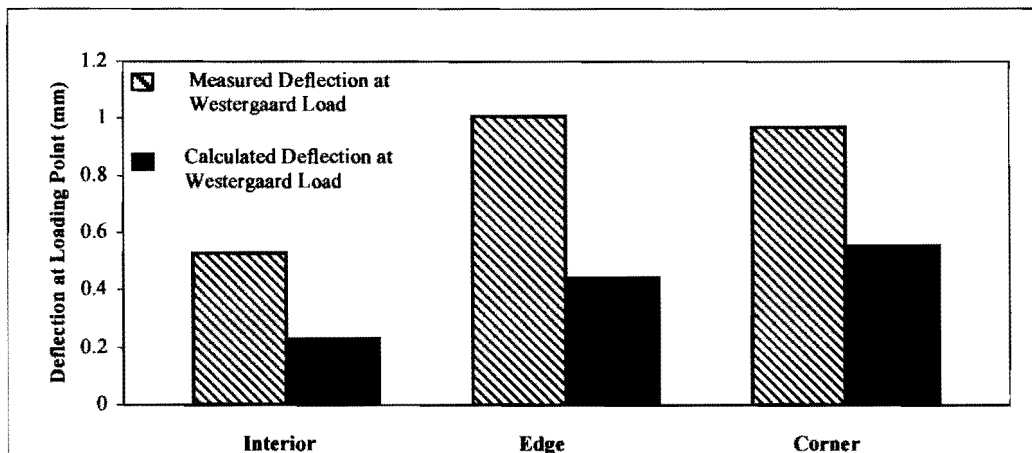


Figure 8-6: Calculated and Measured Deflections at Westergaard Load for the Plain Concrete Slab

For both slabs, the deflection values calculated using Westergaard is far less than that measured. This result was partially confirmed from the finite element analysis developed by Ioannides et al ^[83] which shows that slab requires certain dimension to yield deflections approximately equal to that of Westergaard. He found that the ratio of the least dimension to the radius of relative stiffness (L/l) should be equal or greater than a value of 8.0 for interior and edge loads and 5.0 for corner load. For smaller ratios, larger deflection values will take place with slab load testing. L/l are calculated as 8.2 (3000/367.9) and 7.4 (3000/407.4) for the SFRC and plain concrete slab respectively. These values indicate that limitations of Ioannides might needs further adjustment. In addition to that, the SFRC has different behaviour than that of plain concrete.

Table 8-4 shows that the elastic deflection calculated using Westergaard formula are approximately equal for both slabs, even they have different depths. Due to it's reduced thickness; the SFRC slab was expected to yield higher calculated deflection values. Once again, one could realize that Westergaard formulas are not suitable for the SFRC in the way that it underestimates the loads and corresponding deflection.

The K-value influences the calculated deflection for both the SFRC and plain concrete slabs. Both slabs were found to have approximately the same sensitivity to the K-value and that can be seen from table 8-4. Also it can be seen that increasing K-values in lower ranges results in a higher reduction to deflection than that of the higher range of K-values. Corner conditions were found to be the most sensitive to the above-mentioned phenomenon. For instance, an increase of K-value from 0.015 to 0.4 MPa/mm decreasing the corners deflection by about 7 times while the same increase in K-values results in a reduction of 3.5 times as to edge and interior deflection of both slabs.

8.3.1.3 Failure Characteristics

For interior loading, Westergaard estimated the radius of circumferential crack to be 1.9 of the slab radius of relative stiffness, which is about 700 and 774mm for the SFRC and plain concrete slabs respectively. The deflection profiles discussed in the previous chapter shows that the radius of crack is about 400 and 350mm for the SFRC and plain concrete slabs respectively, which is far less than that given by Westergaard

It was also found that the crack location for the corners loaded at 150 mm from its angle bisector is about 280 and 260 mm from the corner bisector for SFRC and plain concrete respectively. This again less by 16% and 26% from the calculated values for SFRC and plain concrete respectively. The following formula was given by Westergaard to give the radius of the crack from corner angle bisector ^[85]:

$$r = 2.38\sqrt{al} \implies \text{Eq.8-1}$$

Where :

r = Crack radius.

a = Radius of loading plate.

l = Radius of relative stiffness.

8.3.2 Meyerhof

8.3.2.1 Load Capacity

Load capacities calculated using Meyerhof model is compared to the *Maximum loads "at failure"* because Meyerhof formulas assume an *elastic-plastic* behaviour for concrete. The after crack toughness of SFRC can now be taken into account.

Figure 8-7 shows a comparison between actual measured ultimate load and the calculated load using Meyerhof for the SFRC slab. It was found that the actual measured values are greater than calculated values by about 370%, 485% and 560% for interior, edge and corner loads respectively.

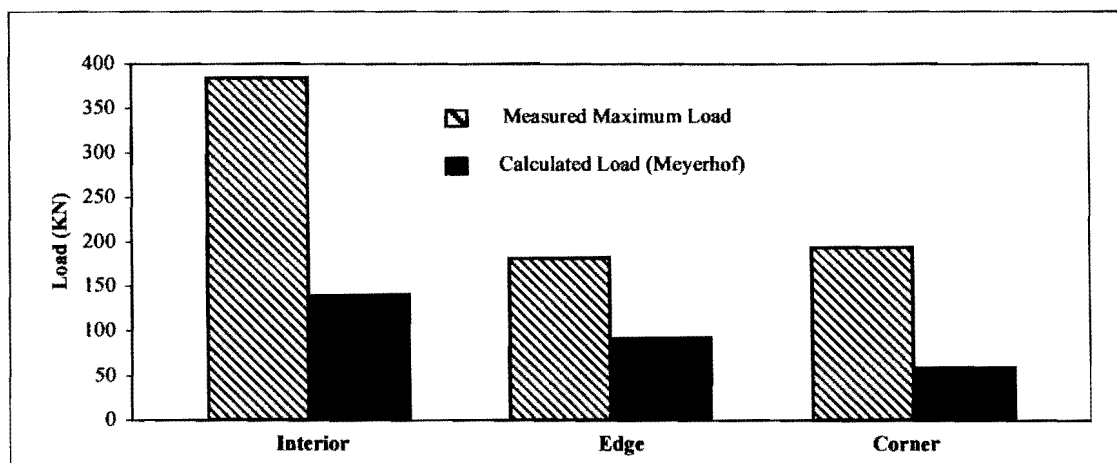


Figure 8-7: Measured Load and Meyerhof Load for SFRC Slab

Figure 8-8 shows a comparison between the actual measured ultimate load and the calculated load using Meyerhof for the plain concrete slab. It was found that the actual measured values are greater than calculated values by about 520%, 560% and 800% for interior edge and corner respectively.

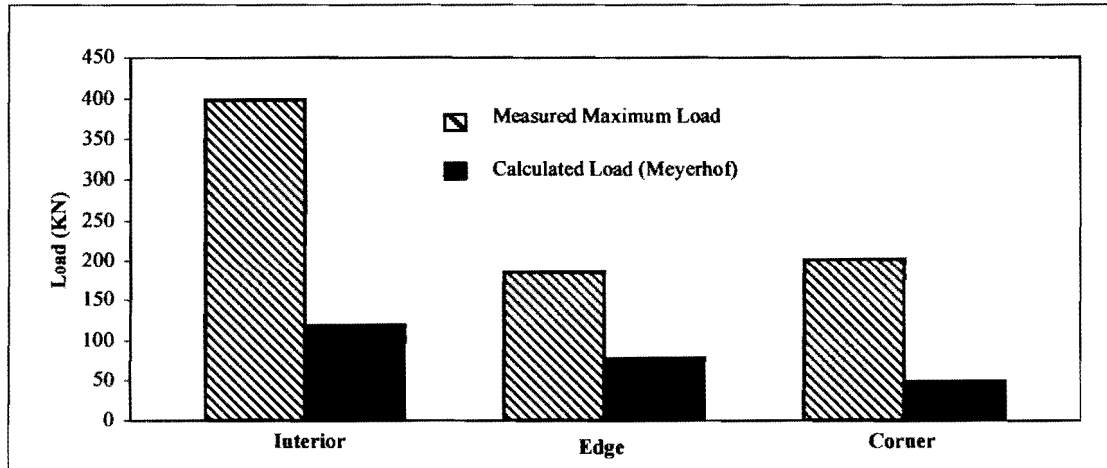


Figure 8-8: Measured Load and Meyerhof Load for Plain Concrete Slab

Obviously, the measured load capacities are far from agreement with the calculated loads. Although the difference between the calculated load and measured loads is significant, the difference is smaller for the SFRC slab.

For corner load, the British Concrete Society Technical Report No. 34 [39] does not consider the after crack toughness of the SFRC and the following equation was used to calculate the moment of resistance for both plain concrete and SFRC slabs.

$$M_o = \frac{f_{ct}bh^2}{6} \implies \text{Eq.8-2}$$

Where :

M_o = Moment of resistance.

f_{ct} = Flexural strength.

b, h = Width and depth respectively.

Steel fiber manufacturer design catalogues [11] suggests the inclusion of the SFRC toughness by changing the f_{ct} to be $f_{ct} [1+R_{e,3}]$. Doing this for the SFRC slab improves the correlation between calculated and measured values, but the difference is still far from acceptable.

The calculated load capacity increases with the increase of the K-value, which implies similar limitations to that, discussed for Westergaard in section 8.3.1.1.

8.3.2.2 Deflection

Although Meyerhof did not give deflection formulas, the model was developed and adjusted using data from existing airfield pavements. The calculated deflection corresponding to the Meyerhof load should agree with actual deflection corresponding to that load. Deflection in the case of Meyerhof model is elastic-plastic deflection.

Actual deflections *at Meyerhof load* are read-off from the load-deflection curves. For the SFRC slab the deflections corresponding Meyerhof's interior, edge and corner are 0.61, 2.1 and 2.1 mm respectively while deflections for plain concrete slab are 0.68, 1.4 and 1.4mm for interior edge and corner respectively.

8.3.2.3 Failure Characteristics

Figure 8-9 shows the failure mechanism considered by Meyerhof model ^[86]. This mode of failure "fan failure" is assumed for a large slab resting on linear elastic (Winkler) subgrade (imply complete contact between slab and sub grade). For the slabs under consideration, the mode of failure in figure 8-9 was not observed. This might be the reason for the disagreement between the calculated loads using Meyerhof model and actual measured loads. Once again, the hard subgrade might have influenced that.

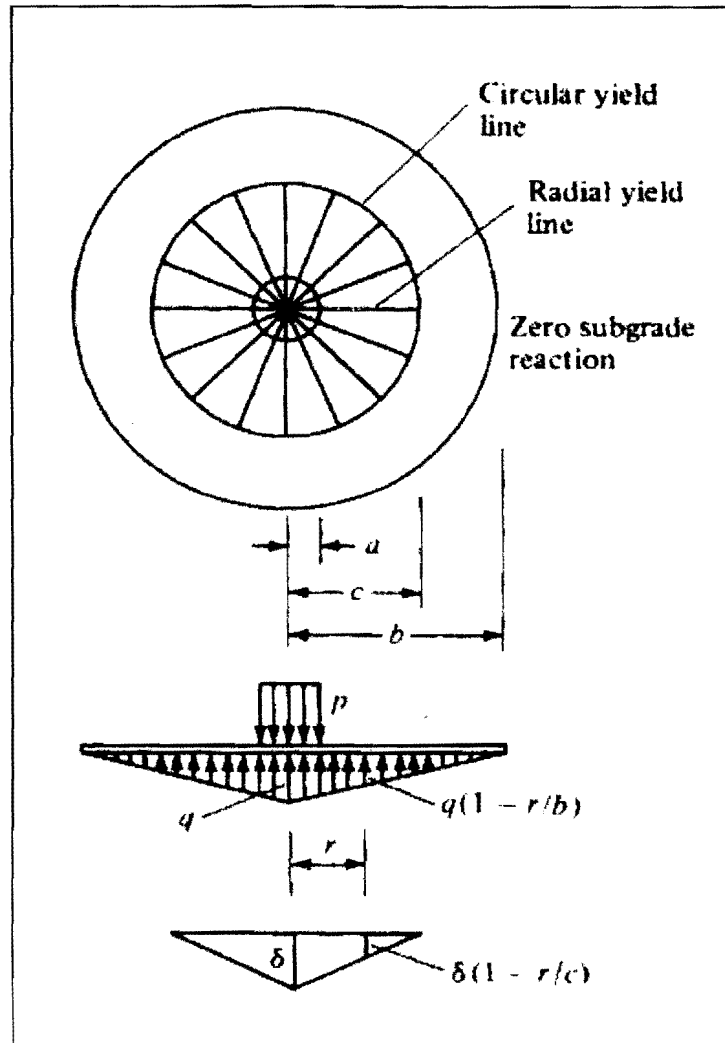


Figure 8-9 Failure Mechanism for Meyerhof Model

Although the “fan failure” was not observed, the deflection profiles obtained for both slabs indicate that a tiny crack might have taken place and that the radius of that crack is 400 and 350 mm for the SFRC and plain concrete slabs respectively. The following equation was given by Meyerhof to calculate the theoretical radius of circumferential crack ^[85]:

$$r = 1.63\sqrt{al} \quad \longrightarrow \quad \text{Eq.8-3}$$

Where :

r = Crack radius.

a = Radius of loading plate.

l = Radius of relative stiffness.

The calculated radius is equal to 230 for the SFRC slab and 240 for plain concrete slab. This is still less than the actual values but it is a better estimation than that given by Westergaard.

8.3.3 Falkner et al

8.3.3.1 Load Capacity

Load capacities calculated using the model of Falkner et al are compared to the *Maximum loads "at failure"* because the formulas assumed by Falkner et al are based on two limit states. One is the limit state of cracking and the other is the ultimate failure state. For the calculation of the first cracking load, Westergaard equation was used. For the plastic behaviour (after cracking) the plastic design principles were used.

Figure 8-10 shows a comparison between actual measured ultimate load and the calculated load using Falkner et al for the SFRC and plain concrete slabs. It was found that the actual measured values are greater than calculated values by about 66% and 160% for the SFRC and plain concrete slabs respectively.

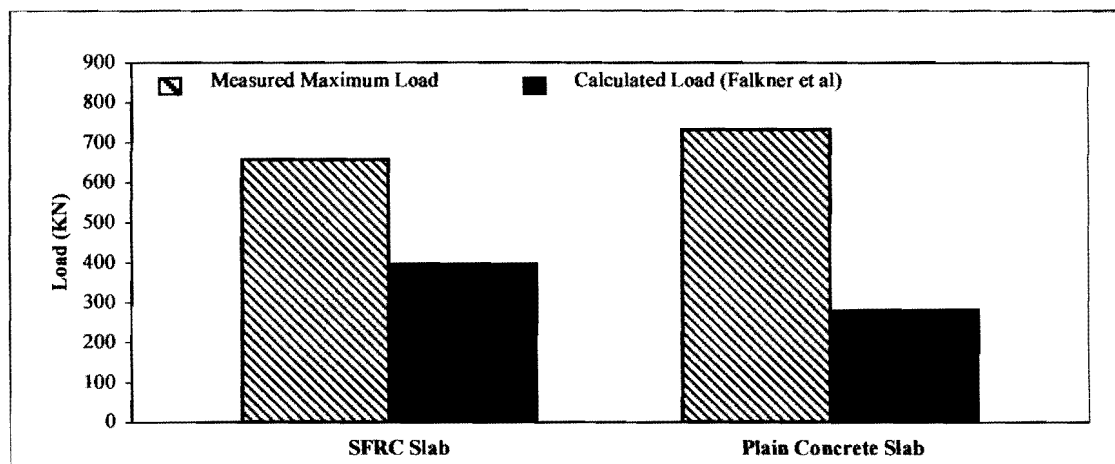


Figure 8-10: Measured Load and Falkner et al Load for SFRC and Plain Concrete Slabs

Although the measured load capacities do not agree with the calculated loads, less difference is found than that obtained from Westergaard and Meyerhof. Falkner model was adjusted using data from (3 x 3m) slabs so the effect of the slab size on calculated loads is eliminated.

Better agreement between the calculated load and measured load for the SFRC slab than the plain concrete slab, imply that Falkner et al model is better in

considering the after cracking behaviour for the SFRC.

The calculated load capacity (using Falkner et al model) increases with the increase of the K-value. As discussed before, the stiffness of the support could have influenced the correlation between measured and calculated values.

Apart from considering the three load case, analytical models used for designing SFRC ground slabs should have the capability to include the after cracking toughness imparted by addition of steel fibers. Although Falkner et al model considers for the after cracking toughness, it does not take edge and corner load into account beside it does not calculate the ultimate deflection.

8.3.3.2 Failure Characteristics

Figure 8-11 shows the failure criterion considered by the model of Falkner et al [73]. The graph shows three stages of failure and the slab sketches on the right hand shows the physical consequences of each stage. This type of failure was observed for the tested slabs and the load-deflection diagrams for the slabs seem to follow a similar sequence to that considered by Falkner et al. The disagreement of the calculated load capacities using Falkner et al and the measured values might basically relate to the difference of mode of failure actually obtained and that considered by the used model.

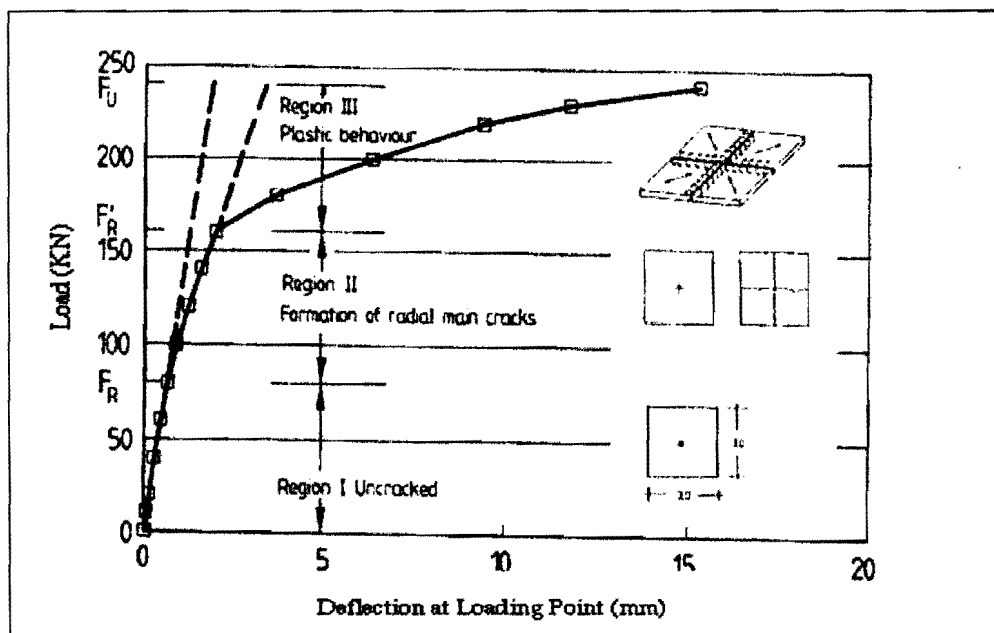


Figure 8-11: Principle Load-Deflection Behaviour and Failure Mechanism (Falkner et al)

8.3.4 Shentu et al

Load capacities calculated using the model of Shentu et al are compared to the *Maximum loads "at failure"* because Shentu et al formulas assume an *elastic-plastic* behaviour. In this comparison, the after crack toughness of SFRC can be taken into account.

Figure 8-12 shows a comparison between actual measured ultimate loads and the calculated load using Shentu et al for the SFRC and plain concrete slabs. It was found that the actual measured load for SFRC slab is greater than calculated load by about 27% while the calculated load for the plain concrete slab is 10% greater than the measured load.

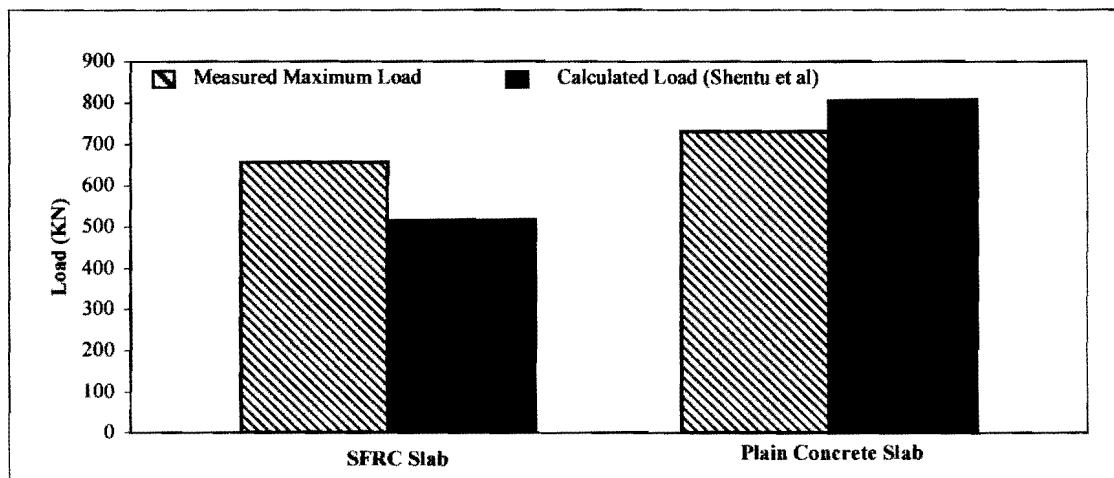


Figure 8-12: Measured Load and Shentu et al Load for SFRC and Plain Concrete Slabs

Reasonably agreed calculated and measured values are obtained. The ultimate load as given by Shentu et al is directly related to sub grade reaction, radius of load, direct tensile strength and the depth of slab and inversely related to modulus of elasticity. The low calculated value for the SFRC is due to the slightly higher modulus of elasticity and the smaller depth while the opposite is true for the plain concrete slab.

Calculated load capacity increases with the increase of the K-value. Figure 8-13 shows that the load-K-value relationship is linear unlike that found for Westergaard Meyerhof and Falkner et al. That might explain the higher loads calculated using Shentu et al compared to loads calculated using the other three models.

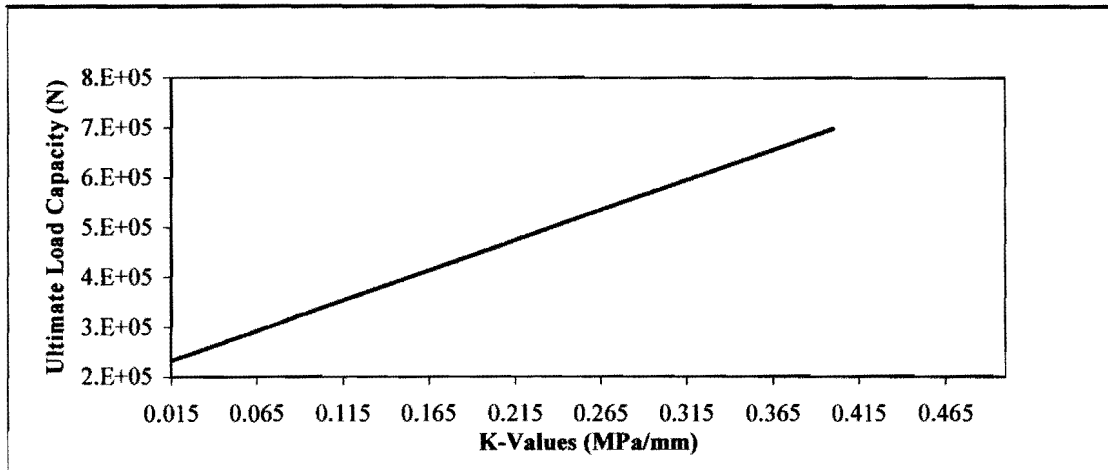


Figure 8-13: Sub grade Reaction-Load Capacity Relationship (Shentu et al)

The model of Shentu et al is found not to be sensitive to the slab width, unlike the other three models. With this model, slabs with different dimensions but having similar other factor will yield the same load capacity. This model uses the uniaxial tensile strength as one of its inputs and the assessment of uniaxial strength is found difficult. The model cannot be used to assess the edge and corner load or any deflections.

8.4 Conclusions

- ❑ The calculated load capacities for the two slabs were found to differ significantly from values calculated using the models of Westergaard and Meyerhof. Some correlation was found with the values calculated using Falkner et al and Shentu et al models.
- ❑ Westergaard model is found not suitable for the SFRC slabs, because it does not consider the after cracking behaviour.
- ❑ Meyerhof model seems to be the most suitable to apply for the SFRC slabs because the after cracking behaviour can be taken into account and the three load cases (interior, edge and corner) can be considered. The shortcoming of this model is that the deflection is not modeled.
- ❑ The model of Falkner et al takes the improved toughness of SFRC into account and it gives better estimation than using Meyerhof. Edge and corner loads and deflection are not modeled. Further research is needed to improve the model to consider the three load cases and deflection.
- ❑ Based on the measured and calculated results, the model of Shentu et al is the most suitable for predicting the load capacity of ground slabs.

Chapter 9

Conclusions and Recommendations

9.1 Background

The general conclusions and recommendations are given in this chapter. The conclusion is divided into four sections viz: conclusions from literature reviewed, effect of steel fiber content on concrete properties, slab tests and the comparison between theoretical and actual behaviour. General recommendations are given for further investigation.

9.2 Conclusions

9.2.1 Literature Reviewed

According to the literature, the following conclusions can be drawn:

- The hook-ended steel fibers are found to yield the best performance compared to the other types of the steel fibers. The addition of the steel fibers should follow a certain procedures to avoid the clumping and to achieve better distribution of these steel fibers. The addition of the steel fibers to concrete requires additional paste to produce a workable mix. Therefore an alteration is required to proportioning mix design procedure to compensate for the additional required paste. The practice of transporting, placing and finishing for the conventional concrete is applicable to the SFRC.
- The steel fiber reinforced concrete is found to improve the mechanical and the physical characteristics of the concrete. The steel fiber imparts an after cracking toughness due to the mechanism of the crack arrest, which hinder the development of cracks unless higher load values are applied. That toughness is responsible for that improvement in the engineering properties of the SFRC. The improvement is ranging between significant in some characteristics and insignificant in others depending on the steel fiber dosage and type.
- The improved engineering properties of the SFRC affect the properties of ground slabs as follows:
 - Improved performance capability due to the reduction or elimination of most of concrete distresses.

- Less thickness can be provided due to the higher flexural strength (compared to the plain concrete). The reduced section depth implies higher deflection values.
- Design methods for conventional concrete ground slabs can be used to design SFRC, the only alteration required is that, deflection should be taken into account in choosing the slab depth.
- Better economy for the SFRC ground slabs due to savings in materials, joint spacing and maintenance cost.

9.2.2 Effect of Steel Fiber Content on Properties of Concrete

The effect of the steel fiber dosage on workability, compressive strength, modulus of rupture, modulus of elasticity and toughness as investigated in this program can be summarized as follows:

- The workability is less sensitive to low steel fiber dosages and the sensitivity increases with the increase of the dosage.
- Steel fibers content up to 30kg/m^3 has the following influence:
 - Negligible influence on the compressive strength at 7 and 28 days.
 - Insignificant influence to the MOR.
 - Slight increase to E-modulus.
 - Increase the first crack strength by about 25%.
 - Significant influence on the toughness.

9.2.3 Slab Test

The investigation on two *full-scale slabs* loaded at interior edge and corners and subjected to static load revealed the following:

- Keeping in mind that the SFRC slab is 16.6% thinner, the plain concrete slab has slightly higher load capacity and slightly less deflection compared to the SFRC slab.
- In comparison to plain concrete slab, a reduction of about 16.6% is possible for ground slabs using hook-ended steel fibers with dosages as low as 15 kg/m^3 .
- The structural advantage for SFRC indicated by steel fiber manufacturer was found to slightly over-estimate that strength of the SFRC.

The investigation conducted on *core specimens* taken from the full-scale slabs and

tested at 90 days is summarized as follows:

- Strength variation among steel fiber cores is less than that for plain concrete. The SFRC seems to have a higher consistency than plain concrete.
- SFRC cores had a gradual or slow failure mechanism compared to plain concrete cores.
- The gain of strength for the SFRC is higher than that for plain concrete.
- The actual and potential compressive strength of the SFRC might be estimated from core specimen using conversion formulas developed for plain concrete.

The investigation performed on *sawn beam specimens* taken from the full-scale slabs and tested at 90 days might be summarized as follows:

- The flexural strength of the SFRC beams was greater than that of plain concrete beams.
- The Japanese method (JSCE-SF4) is found to be more realistic to interpret and calculate the toughness of the SFRC than the American method (ASTM C: 1018).
- Gradual type of failure is obtained for the SFRC beams (unlike plain concrete).
- The modulus of elasticity for SFRC can satisfactorily be calculated using data from third-point loading test.
- The flexural strength of SFRC might be obtained from cube compressive strength using formula similar to that used for plain concrete. The flexural strength of both SFRC and plain concrete is slightly over estimated by the formula.

9.2.4 Comparison Between Theory and Practice

- Huge differences were found between measured load capacity and calculated load using Westergaard and Meyerhof models while less difference was obtained by using the models given by Falkner et al and Shentu et al.
- Westergaard model is found not suitable for the SFRC slabs because it does not take the after cracking strength into account.

- Falkner et al and Shentu et al do consider the after cracking strength but do not calculate edge and corner loads. One of Shentu et al model inputs is the direct tensile strength, which is difficult to assess.
- Based on the result of this investigation, none of the four modes is found suitable to apply for ground slabs.

9.3 Recommendations

- The effects of the fiber dosage on fatigue characteristics, impact strength, shear strength, shrinkage, creep, thermal properties and durability require further investigation.
- Further research to study the influence of fiber contents higher than 30 kg/m³ is required.
- Slabs similar to those investigated in this research can further be tested for cyclic loading. The static or semi-static load can only simulate few cases of the ground slab loadings such as racking or platforms on industrial floors. Cyclic load is seen to be better simulating the other type of ground slabs loading. Behaviour of slabs test with cyclic loading application might differ significantly from those with the semi-static loading. Much improvement might be realized by adding the steel fiber to concrete if the cyclic load is considered.
- Future investigations on slabs should consider the dimension of the slabs and corner and edge conditions. Larger slabs dimensions are recommended.
- The load transfer characteristics and joint efficiency for the SFRC ground slabs can also be evaluated.
- Due to the fact that the SFRC has a higher flexural strength (taking the after crack strength into account) less slab depth can be provided compared to plain concrete. The SFRC slabs therefore yields higher deflection values which might lead to failure of the underlying layers either due to densification or/and the shearing of these layers. Further test are recommended to investigate the deflection characteristics of the steel fiber reinforced concrete and establish a correlation that consider the following aspects:
 - The effect of the slab thickness on deflection.
 - The effect of the steel fiber dosage on the slab thickness (higher

dosage imply higher design flexural strength and thus less slab depth)

- The effect of the modulus of foundation reaction (higher K-value implies less deflection if all other factors remain constant).

The correlation should consider the maximum or allowable deformation that can be withstood by the foundation layers without densification and shearing (for different K-values there should be different deformation characteristics for the specific foundation).

- Although the Japanese method (JSCE-SF4) for interpreting and calculating the toughness of the SFRC has been used in this investigation, it's application on ground slabs should further be investigated. Ground slabs have different deformation characteristics due to the either complete support or/and partial support. Correlation between the allowable ground slabs deflection and the free deflection from beams specimens should be established. The toughness of the SFRC to be used for ground slabs can be calculated at that deflection.
- The gain of strength associated with the SFRC should be investigated. The hydration of the cement in concrete mixes increases the strength of the concrete. With time additional strength develops an additional bond between the steel fibers and the paste, which imply more strength. That strength can be explained by the additional stresses required to pull out or to break the steel fibers. Therefore the assessment of that strength gain might be beneficial for thickness designs of ground slabs and eventually affect the whole economy of that specific pavement, especially for pavements that doesn't require an early opening for the traffic.
- Further investigations are required by using larger slabs to further assess Meyerhof formula.
- Theoretical formula to assess the plastic deflection is required.
- Finite element analysis can be performed and the correlation between theoretical and practical results can then be investigated.

Chapter 10

List of References

- [1] ACI Committee 544, "State-of-the-Art Report on Fiber Reinforced Concrete", (544-IR), American Concrete Institute, Detroit/USA, 1982, 22 PP.
- [2] Edgington, J.; Hannant, D. J.; and Williams, R. I. T., "Steel Fiber Reinforced Concrete", Current Paper No. CP69/74, Building Research Establishment, Garston, Watford, July 1974, 17 PP.
- [3] Hanna, A. N, "Steel Fiber Reinforced Concrete Properties and Resurfacing Applications", Research and Development Bulletin (RD049.01P), Portland Cement Institute Association, Illinois/USA, 1977, 18 PP.
- [4] Schrader, E. K., "Fiber Reinforced Concrete Pavements and Slabs (A State-of-the-Art Report)" Proceedings, Steel Fiber Concrete US-Sweden Joint Seminar (NSF-STU), Swedish Cement and Concrete Research Institute, Stockholm /Sweden, June 1985, PP. 109-131.
- [5] Wallis, S., "Steel Fiber (Development in South Africa)" Concrete Technology, tunnels & tunneling, South Africa, March 1995, PP. 22-24.
- [6] Soroushian, P.; and Bayasi, Z., "Fiber-Type effects on the Performance of Steel Fiber Reinforced Concrete" ACI Material Journal, Vol. 88, No.2, March-April 1991, PP. 129-134.
- [7] Ramakrishnan, V., "Steel Fiber Reinforced Shotcrete (A state-of-the-Art Report)", Proceedings, Steel Fiber Concrete US-Sweden Joint Seminar (NSF-STU), Swedish Cement and Concrete Research Institute, Stockholm/ Sweden, June 1985, PP. 7-22.
- [8] ACI Committee 544, "Guide for Specifying Proportioning Mixing Placing and Finishing Steel Fiber Reinforced Concrete", ACI Material Journal, Vol. 90, No. 1, January-February 1993, PP. 94-101.
- [9] Vandewalle, M., "The Use of the Steel Fiber Reinforced Concrete In Heavy Duty Port Pavements", Proceedings 6th International Symposium on Concrete Roads, Madrid/ Spain, October 1990, PP. 121-128.
- [10] Association of Concrete Industrial Flooring Contractors, "Steel Fiber Reinforced Concrete Industrial Ground Floor: An Introductory Guide" Concrete ACIFC, Vol. 33, No.10, Leamington Spa/ UK, November-December 1999, 12 PP.
- [11] Bekeart N.V., "Steel Fiber Reinforced Industrial Floor (design in Accordance with the Concrete Society TR34)", Dramix manual, 1998, 44 PP.

[12] Packard, R.G.; and Ray, G.K., "Performance of Fiber-Reinforced Concrete Pavements", International Symposium, American Concrete Institute, Detroit/USA, 1984, PP. 325-349.

[13] Vondran, G. L., "Applications of Steel Fiber Reinforced Concrete", Concrete international, American Concrete Institute, Vol. 13, No. 11, November 1991, PP. 44-49.

[14] Nordin, A.; and Skarendahl, A., "Steel Fiber Concrete- development and Use by Ekebro AB", Proceedings, Steel Fiber Concrete US-Sweden Joint Seminar (NSF-STU), Swedish Cement and Concrete Research Institute, Stockholm/ Sweden, June 1985, PP. 143-157.

[15] Annual Book of American Society for Testing Material, "Concrete and Aggregate", Vol. 04.02, ASTM West Conshohocken/ USA, 1998.

[16] Johnston, C. D., "Toughness of Steel Fiber Reinforced Concrete", Proceedings, Steel Fiber Concrete US-Sweden Joint Seminar (NSF-STU), Swedish Cement and Concrete Research Institute, Stockholm/ Sweden, June 1985, PP. 333-360.

[17] Gopalaratnam, V. S.; Shah, S. P.; Batson, G. B.; Criswell, M. E.; Ramakrishnan, V.; and Wecharatana, M., "Fracture Toughness of Fiber Reinforced Concrete", ACI Material Journal, Vol. 88, No. 4, July-August 1991, PP. 339-353.

[18] Chen, L.; Mindess; Morgan, D. R.; Shah, S. P.; Johnston, C. D.; and Pigeon, M., "Comparative Toughness Testing of Fiber Reinforced Concrete", ACI Publications, Detroit/USA, 1995, SP.155-3, PP. 41-75.

[19] Snyder, M. J.; and Lankard, D. R., "Factors Affecting the Flexural Strength of Steel Fibrous Concrete", ACI Journal, Proceedings Vol. 69, No. 2, February 1972, PP. 96-100.

[20] Perrie, B. D., "The Effect of Steel Fiber Reinforcement on the Behaviour and Structural Properties of Concrete" Study Notes: Prepared for the Post Graduate Course in Behaviour of Structural Material at the University of Witwatersrand /South Africa, 1985, 11 PP.

[21] Neville, A. M.; and Brooks, J. J., "Concrete Technology", Longman Group/UK, 1998, PP. 195-200.

[22] Batson, G.; Ball, C.; Bailey, L.; Landers, E.; and Hooks, J., "Flexural Fatigue Strength of Steel Fiber Reinforced Concrete Beams", ACI Journal, Proceedings vol. 69, No. 11, November 1972, PP. 673-677.

[23] Ramakrishnan, V.; Wu, G. Y.; and Hosalli, G., "Flexural Fatigue Strength, Endurance Limit, and Impact Strength of Fiber Reinforced Concretes", Transportation Research Record 1226, 1989, PP. 17-24.

- [24] Johnston, C. D.; and Zemp, W. R., "Flexural Fatigue Performance of Steel Fiber Reinforced Concrete- Influence of Fiber Content, Aspect Ratio, and Type", *ACI Material Journal*, Vol. 88, No. 4, July-August 1991, PP. 374-383.
- [25] Hsu, T. T. C., "Fatigue of Plain Concrete", *ACI Journal*, Vol. 78, No. 4, July-August 1981, PP. 292-305.
- [26] Schrader, E. K., "Design Methods for Pavements", *International Symposium, American Concrete Institute, Detroit/USA, 1984*, PP. 198-212.
- [27] Bernard, E. S.; and Ayton, G., "The Performance of Steel Fiber Reinforced Concrete in Pavements", *18th Biennial Conference (Concrete 97), Concrete Institute of Australia, Adelaide/ Australia, May 1997*, PP. 221-230.
- [28] Morgan, D. R.; and Mowat, D. N., "A Comparative Evaluation of Plain, Mesh and Steel Fiber Reinforced Concrete", *International Symposium, American Concrete Institute, Detroit/USA, 1984*, PP. 305-318.
- [29] Lankard, D. R.; and Newell, J. K., "Preparation of Highly Reinforced Steel Fiber Reinforced Concrete Composites", *International Symposium, American Concrete Institute, Detroit/USA, 1984*, PP. 287-304.
- [30] Fibresteel, "Fibercrete Properties and Pavement Design", *Technical Manual, No. CI/SfB, Australian Wire Industry, Five Dock/ Australia, November 1981*, 46 PP.
- [31] Gopalarantnam, V. S.; and Shah, S. P., "Strength, Deformation and Fracture Toughness of Fiber Cement Composites at Different Rates of Flexural Loading", *Proceedings, Steel Fiber Concrete US-Sweden Joint Seminar (NSF-STU), Swedish Cement and Concrete Research Institute, Stockholm/ Sweden, June 1985*, PP. 299-331.
- [32] Banthia, N.; Chokri, K.; and Trottier, J.F., "Impact Tests on Cement-Based Fiber Reinforced Composites", *ACI Publications, Detroit/USA, 1995*, SP.155-9, PP. 171-188.
- [33] Raju, N. K.; Basavarajaiah, B.S.; and Rao, K. J., "Compressive Strength and Bearing Strength of Steel Fiber Reinforced Concrete", *Indian Concrete Journal*, Vol. 51, No. 6, June 1977, PP. 183-188.
- [34] Burgess, I.C., "Steel Fiber Reinforced Concrete: A Viable Pavement Material", *Proceedings, Symposium on Exploiting the Innovative Potential of Concrete, Concrete Society of Southern Africa, Johannesburg/ South Africa, September 1992*, 15 PP.
- [35] Khaloo, A. R.; and Kim, N., "Influence of Concrete and Fiber Characteristics on Behaviour of Steel Fiber Reinforced Concrete Under Direct Shear", *ACI Materials Journal*, Vol.94, No. 4, November-December 1997, PP. 592-601.

- [36] Ashour, S. A.; Hasanain, G. S.; and Wafa, F. F., "Shear Strength Behaviour of High-Strength Fiber Reinforced Concrete Beams", *ACI Structural Journal*, Vol. 89, No.2, March-April 1992, PP. 176-183.
- [37] Jindal, R. L., " Shear and Moment Capacities of Steel Fiber Reinforced Concrete Beams", *International Symposium, American Concrete Institute, Detroit/USA, 1984, PP. 1-16.*
- [38] Grondziel, M., " Restoration of Concrete Floors with Steel-Fiber Concrete for Aircraft at Frankfurt Airport – West Germany", *International Conference on Recent Developments in Fiber Reinforced Cements and Concrete, London/ UK, September 1989, PP.610-619.*
- [39] The British Concrete Society, " Concrete Industrial Ground Floors: A Guide to Their Design and Construction", *Technical Report No.34 (TR34), 2nd Edition, February 1995.*
- [40] Armelin, H. S.; and Helene, P., " Physical and Mechanical Properties of Steel Fiber Reinforced Dry-Mix Shotcrete", *ACI Materials Journal*, Vol. 92, No. 3, May-June 1995, PP. 258-267.
- [41] Alexander, M. G., "A Simple Bending Test for Elastic and Rupture Moduli for Plain Concrete and Mortar", *Concrete/Beton, South Africa*, Vol. 9, No. 27, 1982, PP.18-24.
- [42] Beckett, D., " Thickness Design of Concrete Industrial Ground Floors", *Concrete Journal*, Vol. 29, No. 4, August 1995, PP. 21-23.
- [43] Kaushik, S. K.; and Vasan, R. M., " Performance Evaluation of SFRC Pavements", *Proceedings of 4th International Symposium Held by RILEM, University of Sheffield/ UK, July 1992, PP. 883-887.*
- [44] Banthia, N.; Azzabi, M.; and Pigeon, M., "Restrained Shrinkage Tests on Fiber Reinforced Cementitious Composites", *ACI Publications, Detroit/USA, 1995, SP.155-7, PP. 136-151.*
- [45] Balguru, P., " Contribution of Fibers to Crack Reduction of Cement Composites During the Initial and Final Setting Period", *ACI Materials Journal*, Vol. 91, No. 3, May-June 1994, PP. 280-288.
- [46] Grzybowski, M.; and Shah, S. P., " Shrinkage Cracking of Fiber Reinforced Concrete" *ACI Materials Journal*, Vol. 87, No. 2, March-April 1990, PP. 138-148.
- [47] Chern, J-C.; and Young, C-H., " Study of Factors Influencing Drying Shrinkage of Steel Fiber Reinforced Concrete", *ACI Materials Journal*, Vol. 87, No. 2, March April 1990, PP. 123-129.

[48] Hassani, A.; and Mohammed, S., "The Study of the Mean Time Drying Shrinkage Behaviour of Steel Fiber Reinforced Concrete Pavements", 8th International Symposium on Concrete Roads, Theme II, Progress in Concrete Road Materials and in the Construction Process, Lisbon/ Portugal, September 1998, PP. 216-224.

[49] Mangat, P. S.; and Azari, M. M., "Shrinkage of Steel Fiber Reinforced Cement Composites", Materials and Structures, 1988, PP. 163-171.

[50] Ong, K. C. G.; and Paramasivam, P., "Crack of Steel Fiber Reinforced Mortar Due to Restrained Shrinkage", International Symposium, American Concrete Institute, Detroit/USA, 1984, PP. 179-187.

[51] Mangat, P. S.; and Azari, M. M., "Compression Creep Behaviour of Steel Fiber Reinforced Cement Composites", Materials and Structure, Vol. 19, No. 113, 1986, PP. 361-369.

[52] Kosa, K.; and Naaman, A. E., "Corrosion of Steel Fiber Reinforced Concrete", ACI Materials Journal, Vol. 87, No. 1, January-February 1990, PP. 27-37.

[53] Sanjuan, M. A.; Moragues, A.; Bacle, B.; and Andrade, C., "Durability of Steel Fiber Reinforced Concrete When Held in Sewage Water", 5th International Conference 'Durability of Building Materials and Components', Brighton/UK, November 1990, PP.681-689.

[54] Schupack, M., "Durability of SFRC Exposed to Severe Environments", Proceedings, Steel Fiber Concrete US-Sweden Joint Seminar (NSF-STU), Swedish Cement and Concrete Research Institute, Stockholm/ Sweden, June 1985, PP. 479-496.

[55] Cook, D. J.; and Uher, C., "The Thermal Conductivity of Fiber-Reinforced Concrete", Cement and Concrete Research, Vol. 4, No. 4, July 1974, PP.497-509.

[56] Frazier Parker, Jr.; and Rice, J. L., "Steel Fibrous Concrete For Airport Pavements", International Conference on Concrete Pavement Design, Purdue University, Indiana/USA, February 1977, PP. 541-555.

[57] Raghavendra, N.; Kulshrestha, H. K.; and Lal, R., "Fiber Reinforced Concrete for Airfield Pavements", Indian Concrete Journal, Vol.59, No. 3, March 1985, PP.64-67.

[58] Spires, J. W.; Romualdi, J. P.; and Pichumani, R., "Analysis of Steel-Fiber Reinforced Concrete Warehouse Floor Slabs", ACI Journal, December 1977, PP. 616-622.

[59] Rolling, R. S., "Corps of Engineers Design Procedure for Rigid Airfield Pavements", 2nd International Conference on Concrete Pavement Design, Purdue University, Indiana/ USA, April 1981, PP. 185-198.

- [60] Huang, Y. H., "Pavement Analysis and Design", Prentice-Hall, New Jersey/USA, 1993.
- [61] Schrader, E. K.; and Lankard, D. R., "Inspection and Analysis of Curl in Steel Fiber Reinforced Concrete Airfield Pavements", Bekaert Steel Wire Publications, Pennsylvania/USA, April 1983, 9 PP.
- [62] South African Department of Transport, "Concrete Pavement Design and Construction", Manual M10, 2nd Draft, Pretoria/ South Africa, 1997.
- [63] Verhoeven, K., "Thin Overlays of Steel Fiber Reinforced Concrete and Continuously Reinforced Concrete: State of the Art in Belgium", 4th International Conference on Concrete Pavement Design and Rehabilitation, Purdue University, Indiana/USA, April 1989, PP. 205-219.
- [64] Hoff, G. C., "Use of Steel Fiber Reinforced Concrete in Bridge Decks and Pavements", Proceedings, Steel Fiber Concrete US-Sweden Joint Seminar (NSF-STU), Swedish Cement and Concrete Research Institute, Stockholm/ Sweden, June 1985, PP. 67-108.
- [65] Johnston, C. D., "Steel Fiber Reinforced Concrete Pavement Trial", Concrete International, December 1984, PP. 39-43.
- [66] Addis, B. J., "Fulton's Concrete Technology" Portland Cement Institute, Midrand/ South Africa, 6th Edition, 1986.
- [67] Stock, A. F., "Concrete Pavements", Elsevier Science Publishing, New York/USA, 1988.
- [68] Gehring, D., "Steel Fiber Concrete Saves A \$ 1m" International Construction, March 1982, PP. 19.
- [69] Kukreja, C. B.; Kaushik, S. K.; Kanchi, M. B.; and Jain, O. P., "Economics and Applications of Steel Fiber Reinforced Concrete", Indian Concrete Journal, Vol.58, No.3, August 1984, PP. 202-206.
- [70] Dramix Publications, "Why Dramix Steel Fiber Reinforced Concrete for Floors" N.V. Bekaert, South Africa.
- [71] Westergaard, H. M., 'Stresses in Concrete Pavements Computed by Theoretical Analysis' Public Roads, Vol. 7, No. 2, April 1926, PP. 25-35.
- [72] Meyerhof, G. G., "Load Carrying Capacity of Concrete Pavements", Journal of the Soil Mechanics and Foundations Division, Proceedings of the American Society of Civil Engineers, June 1962, PP. 89-116.
- [73] Falkner, H.; Huang, Z.; and Teutsch, M., "Comparative Study of Plain and Steel Fiber Reinforced Concrete Ground Slabs", Concrete International, January 1995, PP. 45-51.

[74] Shentu, L.; Jiang, D.; and Hsu, C-T. T., "Load Carrying Capacity for Concrete Slabs on Grade", *Journal of Structural Engineering*, Vol. 123, No. 1, January 1997, PP. 95-103.

[75] Kaushik, S. K.; Vasan; and Godbole, P. N., "Analysis of Steel Fiber Reinforced Concrete Pavements Based on Infinite Element Analysis", *International Conference on Recent Developments in Fiber reinforced Cements and Concrete*, London/UK, September 1989, PP. 620-629.

[76] Beckett, D., "Comparative Tests on Plain, Fabric Reinforced and Steel Fiber Reinforced Concrete Ground Slabs", *Concrete*, Vol. 24, No. 3, March 1990, PP. 43-45.

[77] Beckett, D., "Corner and Edge Loading on Concrete Industrial Ground Floors Reinforced with Steel Fibers", *Concrete*, Vol. 33, No. 3, September 1999, PP. 22-24

[78] South African Standard: Concrete Tests, "Consistencies of Freshly Mixed Concrete: Slump Test", SABS Method 862-1: 1994.

[79] South African Standard: Concrete Tests, "Compressive Strength of Hardened Concrete", SABS Method 863: 1994.

[80] South African Standard: Concrete Tests, "Flexural Strength of Hardened Concrete", SABS Method 864: 1994.

[81] American Standard, "Test for Static Modulus of Elasticity and Poisson's Ratio of Concrete in Compression", ASTM C469-87a: 1992.

[82] South African Standard: Concrete Tests, "The Drilling, Preparation, and Testing of Concrete Cores", SABS Method 865: 1982.

[83] Beckett, D., "Thickness Design of Concrete Industrial Ground Floors", *Concrete*, Vol. 29, No. 4, July/August 1995, PP. 21-23.

[84] Ioannides, A. M.; Thompson, M. R.; and Barenberg, E. J., "Westergaard Solutions Reconsidered" *Transportation Research Records* 1043, Transportation Research Board (TRB), Washington, D. C./USA, 1985, PP. 13-23.

[85] Rao, K.S. S. and Singh S. "Concentrated Load-Carrying Capacity of Concrete Slabs on Ground", *ASCE Journal of Structural Engineering*, 112(12), PP. 2628-1645.

[86] Chen, W. F. "Plasticity in Reinforced Concrete" McGraw-Hill, New York/USA, 1st Edition, 1982, PP. 333-334.

[87] Scanfibre pamphlets, "Flooring Fiber Specification" Scancem Materials, Natal/South Africa.

Chapter 11

Appendices

Appendix A

Systematic Approach for SFRC Mixes Proportioning

The method was developed by Hanna ^[1] in 1977. It basically suggests a mechanistic approach to adjust SFRC mixes made of pre-designed plain concrete mixes and steel fibers. It takes into account the fact that both mix parameters and fibers parameters are affecting the final product of the SFRC

The amount of paste required to coat the fibers was determined experimentally. Cement mixes prepared with different water-cement ratios were added to pre-weighed amounts of fibers and vibrated to produce a uniform mix. The fiber -paste mix was then placed on a No.4 sieve, shaken by hand to drain the excess paste, and weighed. The amount of the paste coating the fibers was determined by subtracting the weigh of the sieve and the uncoated steel fibers from the total weigh. Test results showed that the relationship between the weight of steel fibers and the required paste could be expressed as given in equation A-1.

After adjusting the plain concrete mix for specific compressive strength using plain concrete systematic mix proportioning methods, the adjustment of water and cement for the SFRC could possibly be calculated by using equations A-2 to A-4.

For straight steel fibers (0.25x0.56x0.254 mm), the values of A and B were obtained experimentally as described before. Test results provided values of $A = 3.0$ and $B = -1.4$. Although the straight steel fibers are no longer in use, the values of A and B above can give an indication of their expected values when applying the same approach to the hook-ended steel fibers.

This method does however not go further in determining the flexural strength after the addition of the steel fiber (which is normally the aim of the addition of the steel fiber). Moreover, the extra cement for the steel fiber coating is expected to increase the compressive strength of the final product, which is not considered by the method. The author's view is that, the method can be used successfully to optimize the aggregate blend and minimize the cement content while assuring adequate paste content, which is typically higher for SFRC. Flexural strength could be predicted for

the specific type of steel fibers by doing trial mixes. The steel fiber suppliers formulas and tables in appendix B could be used successfully to give an indication prior preparing trial mixes.

$$\text{Log} \left(\frac{w_f}{w_p} \right) = A \frac{w}{c} + B \quad \Rightarrow \text{Eq. A - 1}$$

$$w_{cf} = w_{co} \left[1 - 0.01p - \frac{pC \left(0.318 + \frac{w}{c} \right)}{10^{\left(\frac{A w}{c} \right)} \left(1 + \frac{w}{c} \right)} \right] + \frac{\lambda_w p c}{10^{\left(\frac{A w}{c} \right)} \left(1 + \frac{w}{c} \right)} \quad \Rightarrow \text{Eq. A - 2}$$

$$w_{af} = w_{ao} \left[1 - 0.01p - \frac{pC \left(0.318 + \frac{w}{c} \right)}{10^{\left(\frac{A w}{c} \right)} \left(1 + \frac{w}{c} \right)} \right] \quad \Rightarrow \text{Eq. A - 3}$$

$$C = \frac{\gamma_f}{\gamma_w 10^B}$$

$$w_{wf} = \frac{w}{c} w_{cf} \quad \Rightarrow \text{Eq. A - 4}$$

Where :

w_f = weight of steel fibers

w_p = weight of paste (water and cement)

$\frac{w}{c}$ = water - cement ratio by weight

A, B and C = parameters dependent on the characteristics of the fiber material. A and B are obtained from the slope and intercept of the line defined in Eq. A - 1 can be calculated as in Eq. A - 4.

w_{cf} = cement content in SFRC mix

w_{co} = cement content in plain concrete mix

w_{af} = aggregate content in SFRC mix

w_{ao} = aggregate content in plain concrete mix

p = fiber content in volume percentage.

c = parameter dependent on fiber characteristics

γ_f = density of fibers

γ_w = density of water

w_{wf} = water content for SFRC mix

Appendix B

Flexural Strength Ratios:

Steel fibers manufacturer provides formulas and table to estimate the equivalent flexural strength ratios for different fibers parameter and dosage. The following equations were provided for the hook-ended steel fibers of two different manufacturers.

$R_{e,3}$ values in table B-1 are for hook-ended steel fibers generated from third-point loading test according to the JSCE-SF4 method ^[11].

Table B-1: Equivalent Strength Ratios for Various Steel Fiber Dosages

Dosage (kg/m ³)	RC-8/60-BN	*RC-65/60-BN	*RL-45/50-BN
15	42	38	-
20	52	47	38
25	60	56	45
30	68	63	52
35	75	69	58
40	80	75	63
45	86	80	68
50	90	85	72
55	95	89	77
60	99	93	80
65	102	97	84

*RL for Round section and loose fibers

*RC for Round section Collated fibers

Another estimation for the equivalent flexural strength ratio is given by equation B-1. The equivalent flexural strength ratio and equivalent flexural strength for a mixture with a compressive strength of 32 MPa is given in table B-2. ^[87].



$$R_{e,3} = \frac{180WLD^{1/4}}{(180C) + (WLD^{1/4})} \Rightarrow \text{Eq. B-1}$$

Where :

D = fiber diameter (mm)

W = fiber dosage (kg/m³)

L = fiber aspect ratio

C = constant ≈ 16

Table B-2: Equivalent Flexural Strength Characteristics

Steel fiber dosage (kg/m ³)	$f_{e,3}$	$R_{e,3}$
15	2.4	50
20	2.9	61
25	3.3	71
30	3.7	79
35	4.0	85
40	4.3	92



Appendix C

First Crack Determination Technique:

There is no unique definition for the first crack. It may be defined as follows:

- The point at which the load reaches its first maximum point.
- The point from which a series of 20 consecutive data points (over total deformation of 0.01 mm or more) have a slope at least 5% less than the average slope of the load-deflection curve between 45% and 70% of the peak load.
- The point at which the load-deflection curve first become non-linear (ASTM C: 1018).

For the purpose of this research, the last definition is adopted. Differentiation techniques were used to estimate the point of the first crack. Ideal elastic behaviour was not found for all tests conducted and some engineering judgment was used. The following steps were followed:

- Spot readings at 10 KN intervals are considered and used to plot the load-deflection diagram.
- The first portion of the curve (curved portion) is omitted by deducting the deflections due to seating at the start of loading.
- The zone of the load-deflection curve at which the first crack point could lie is initially estimated (the most straight portion).
- The first two readings of the straight portion are used to draw the load-deflection curve. Similar curves are generated by adding one reading each time, and the correlation factor (R^2) was computed.
- The relation between the load and the R^2 is established. The load at which the Load- R^2 relation has its first deviation is deemed to be the first crack point.

As an example, the above steps were followed to determine the first crack point for the corner (at the Plain Concrete slab).

Step 1:

The data as recorded from the closed-loop servo system is plotted as in figure C-1. As it can be seen the data is noisy because of the foam concrete sub base used in the experiment (compressible) and the high recording rate used. Also it is obvious that the very first portion of the curve is not linear (due to seating).

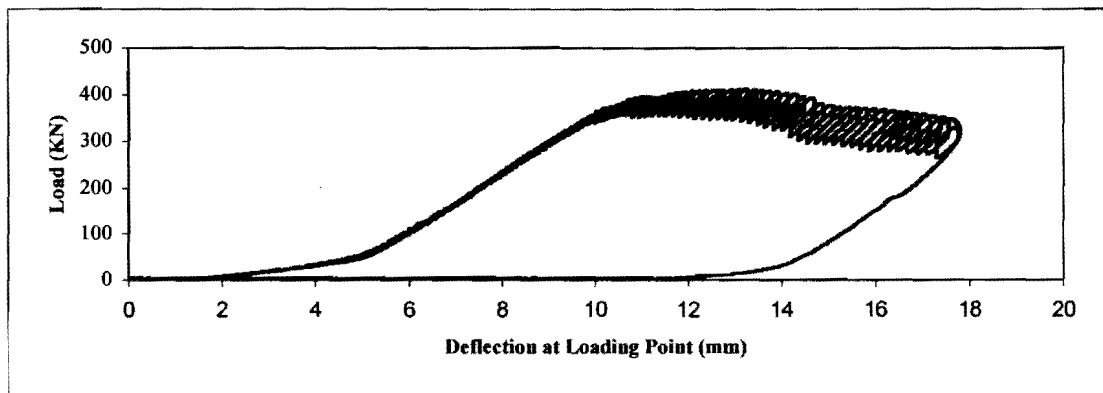


Figure C-1: Load-Deflection Diagram for the Plain Concrete Slab Corner

Step 2: The data is normalized by taking a spot reading at 10 kN intervals and the first portion of the curve is cut off by deducting the seating deflections. Figure C-2 shows the plot of the normalized data.

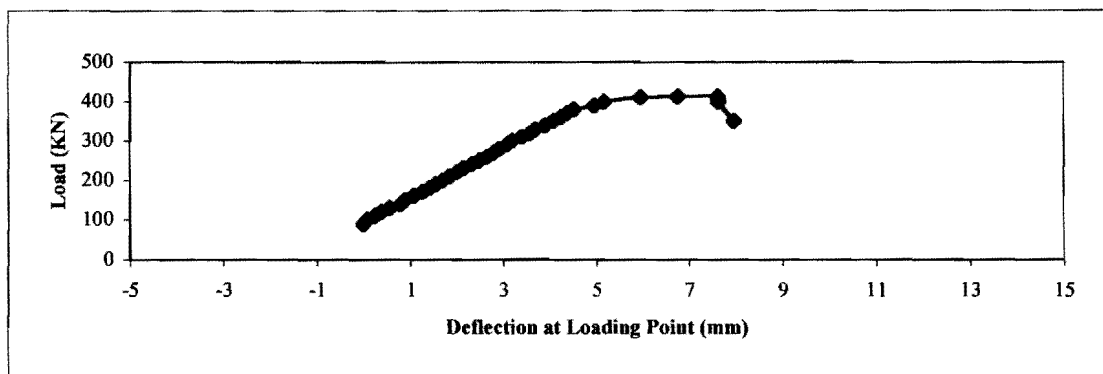


Figure C-2: shows the Load-Deflection Diagram for the Normalized Data

Step 3: The region of the load-deflection curve at which the crack point may occur was estimated as between 170 kN and 230 kN. The readings beyond 170 kN were investigated by adding a portion of these readings and draw the best-fit line. Several trials were conducted by adding readings each trial till the last line is drawn from the full range of readings of which the first crack estimated to fall in. The correlation factor (R^2) is found from each trial in step and a plot of load- R^2 is developed as in

figure C-3. The point at which the curve has the first deviation is deemed to be the first crack point. From figure C-3, it is obvious that the first crack strength is approximately 200 KN.

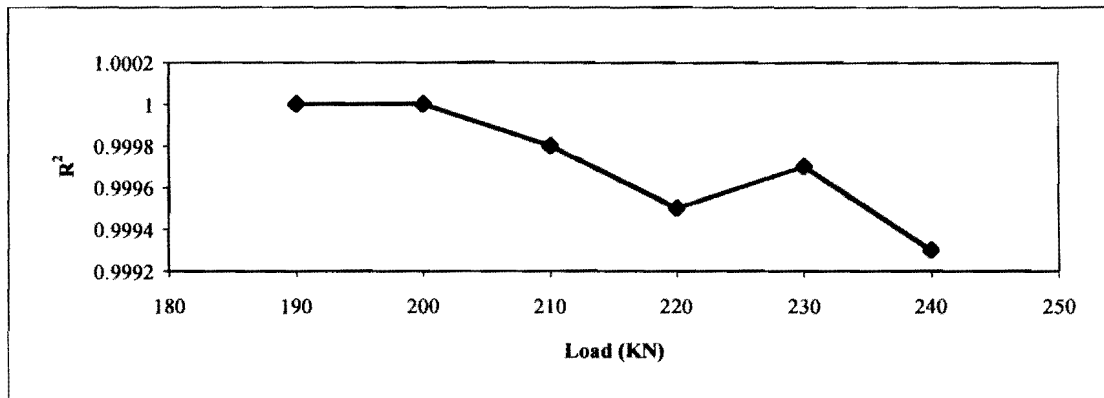


Figure C-3: Load-R² Diagram

Step 4: Further investigation on the data between 200 and 210 KN revealed that the first crack point is better estimated at load equal to 202 KN.

Appendix D

Example of Modulus of Elasticity Calculation

The sawn SFRC beam (IS) is considered as an example of the calculations of the modulus of elasticity. The followings are the characters of the beam:

Supported length = 450 mm Section depth (d) = 131 mm

Section width (b) = 122 mm Poisson's ratio (μ) = 0.15

Second moment of inertia (I) = $[122 \times (131)^3] / 12 = 22.85 \times 10^6 \text{ mm}^4$

Equation D-1 is used to calculate the modulus of elasticity using data from a third-point loading test:

$$E(\text{M.Pa}) = \frac{23}{1296} * \frac{F}{\delta} * \frac{l^3}{I} \left[1 + \frac{216}{115} * \left(\frac{d}{l} \right)^2 (1 + \mu) \right] * 10^3 \Rightarrow EqD-1$$

Where:

$\frac{F}{\delta}$ = the slope of the best - fit straight line drawn through the plotted points of the initial portion of the load - deflection curve (N/mm^2).

l = support span, (mm).

I = second moment of area of the section $\left(\frac{bd^3}{12} \right)$.

b, d = width and depth of the prism section respectively (mm).

μ = poisson's Ratio

Equation D-1 further requires the slope of the straight portion (elasticity zone) of the load-deflection curve. Figure D-1 shows the load-deflection curve for the sawn SFRC beam and figure D-2 shows the best-fit line on the data with in the straight portion to compute the required slope.

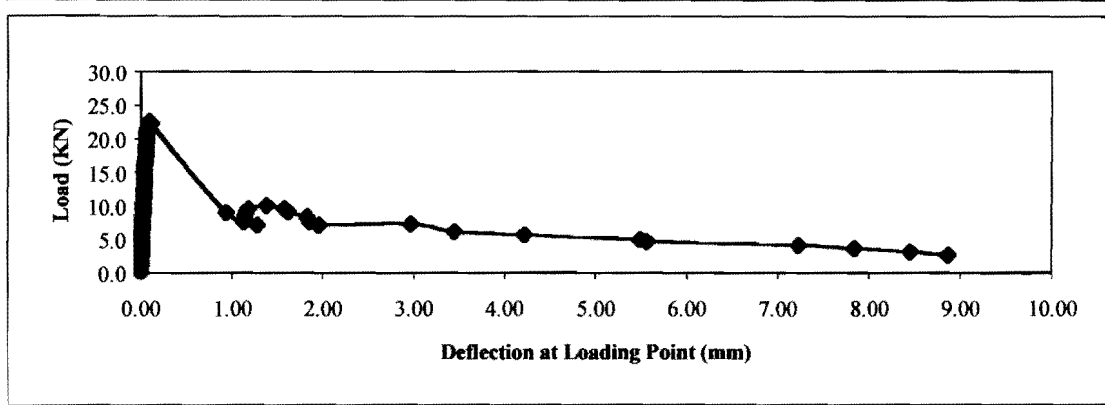


Figure D-1: Load-Deflection Diagram for the Sawn SFRC Beam (IS)

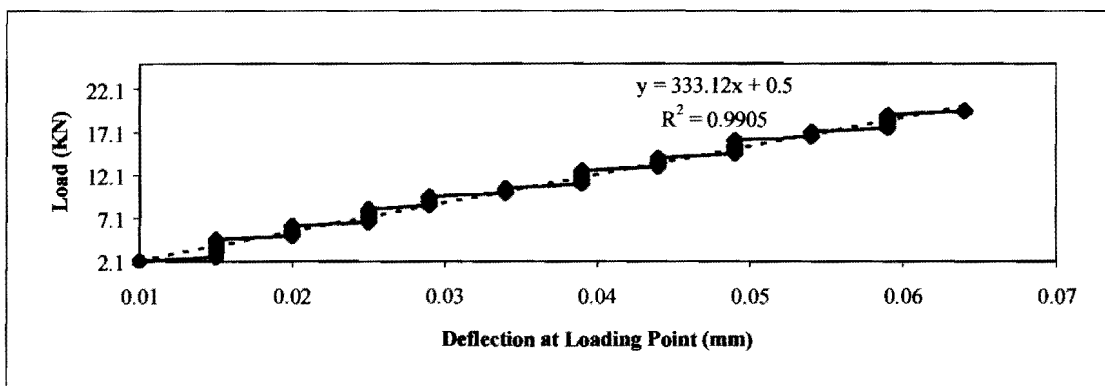


Figure D-2: Slope Determination for the Elastic Zone of Sawn SFRC Beam (IS)

Hence, the value of $(F/\delta) = 333 \times 10^3 \text{ N/mm}$.

Substituting in equation 2-5:

$E = 27.8 \times 10^3 \text{ MPa}$

Appendix E

Example of Theoretical Analysis Calculation

Interior Load

SFRC Slab :

$$\text{Radius of relative stiffness } l = \left[\frac{27.5 * 10^3 * (125)^3}{12(1 - (0.15)^2) * 0.3} \right]^{0.25} = 351.5 \text{ mm} \rightarrow K = 0.3$$
$$= 367.9 \text{ mm} \rightarrow K = 0.25$$

$$\text{Equivalent Radius of contact area } a = \left(\frac{100 * 100}{\pi} \right)^{0.5} = 56.41 \text{ mm}$$

$$b = \left[1.6 * (56.41)^2 + (125)^2 \right]^{0.5} - 0.675 * 125 = 59.56 \text{ mm}$$

Westergaard :

$$P_{\text{FirstCrack}} = \frac{4.8 * (125)^2}{0.275(1 + 0.15) * \log_{10} \left(\frac{0.36 * 27500 * (125)^3}{0.25 * (59.56)^4} \right)} = 62.4 \text{ KN}$$

Meyerhof :

$$M_0 = \frac{6.8 * 1000 * (125)^2}{6} * 10^{-6} = 17.71 \text{ KN.m/m width}$$

$$P_{\text{Ultimate}} = 6 * 17.7 * \left(1 + \frac{2 * 56.41}{367.9} \right) = 138.8 \text{ KN}$$

Falkner :

$$P_{\text{Ultimate}} = 62.4 * \left[1 + \left(\frac{0.25}{27500 * (125)^3} \right)^{0.25} * 3000 * \frac{100}{125} \right] \left[1 + \frac{1.9}{4.8} \right] = 395.4 \text{ KN}$$

Shentu :

$$P_{\text{Ultimate}} = 1.72 * 2.2 * (125)^2 \left[\left(\frac{0.25 * 56.41}{27500} \right) * 10^4 + 3.6 \right] = 516.1 \text{ KN}$$

Plain Concrete Slab :

$$\text{Radius of Relative stiffness } l = \left[\frac{24 * 10^3 * (150)^3}{12(1 - (0.15)^2) * 0.3} \right]^{0.25} = 389.5 \text{ mm} \rightarrow K = 0.3$$
$$= 407.4 \text{ mm} \rightarrow K = 0.25$$

$$b = \left[1.6 * (56.41)^2 + (150)^2 \right]^{0.5} - 0.675 * 150 = 64.9 \text{ mm}$$

Westergaard :

$$P_{\text{FirstCrack}} = \frac{4.1 * (150)^2}{0.275 * (1 + 0.15) * \log_{10} \left(\frac{0.36 * 27500 * (150)^3}{0.25 * (64.9)^4} \right)} = 76.4 \text{ KN}$$

Meyerhof :

$$M_0 = \frac{4.1 * 1000 * (150)^2}{6} 10^{-6} = 15.4 \text{ KN.m/m width}$$

$$P_{\text{Ultimate}} = 6 * 15.4 * \left(1 + \frac{2 * 56.41}{407.7} \right) = 117.8 \text{ KN}$$

Falkner :

$$P_{\text{Ultimate}} = 76.4 * \left[1 + \left(\frac{0.25}{24000 * (150)^3} \right)^{0.25} * 3000 * \frac{100}{150} \right] = 278.9 \text{ KN}$$

Shentu :

$$P_{\text{Ultimate}} = 1.72 * 2.2 * (150)^2 \left[\left(\frac{0.25 * 56.41}{24000} \right) * 10^4 + 3.6 \right] = 806.8 \text{ KN}$$

Edge and Corner Load

FRC Slab :

Westergaard :

Edge :

$$P_{FirstCrack} = \frac{4.8 * (125)^2}{0.529 * (1 + 0.54 * 0.15) * \log_{10} \left(\frac{0.2 * 27500 * (125)^3}{0.3 * (59.56)^4} \right)} = 38 \text{ KN}$$

Corner :

$$P_{FirstCrack} = \frac{4.8 * (125)^2}{3 * \left[1 - 1.41 \left(12 \left(1 - (0.15)^2 * \frac{0.3 * (59.56)^4}{27500 * (125)^3} \right) \right)^{0.25} \right]} = 32.4 \text{ KN}$$

Meyerhof :

Edge :

$$M_0 = 17.7 \text{ KN.m/m width}$$

$$P_{Ultimate} = 3.5 * 17.7 * \left[1 + \frac{3 * 56.41}{351.5} \right] = 91.8 \text{ KN}$$

Corner :

$$M_0 = 17.7 \text{ KN.m/m}$$

$$P_{Ultimate} = 2 * 17.7 * \left[1 + \frac{4 * 56.41}{351.5} \right] = 58.1 \text{ KN}$$

Plain Concrete Slab :

Westergaard :

Edge :

$$P_{FirstCrack} = \frac{4.1 * (150)^2}{0.529 * (1 + 0.54 * 0.15) * \log_{10} \left(\frac{0.2 * 24000 * (150)^3}{0.3 * (64.9)^4} \right)} = 46.3 \text{ KN}$$

Corner :

$$P_{FirstCrack} = \frac{4.1 * (150)^2}{3 * \left[1 - 1.41 \left(12 \left(1 - (0.15)^2 * \frac{0.3 * (64.9)^4}{24000 * (150)^3} \right) \right)^{0.25} \right]} = 40.2 \text{ KN}$$

Meyerhof :

Edge :

$$P_{Ultimate} = 3.5 * 15.4 * \left[1 + \frac{3 * 56.41}{389.5} \right] = 77.2 \text{ KN}$$

Corner :

$$P_{Ultimate} = 2 * 15.4 * \left[1 + \frac{4 * 56.41}{389.5} \right] = 48.6$$

Elastic Deflection

SFRC Slab :

Westergaard formula was used to calculate slab settlement beneath the loading point :

Interior load :

$$Z = \frac{62.6 * 10^3}{8 * 0.25 * (367.9)^2} = 0.22 \text{ mm.}$$

Edge :

$$Z = \frac{1}{\sqrt{6}} (1 + 0.4 * 0.15) \frac{38 * 10^3}{0.3 * (351.5)^2} = 0.44 \text{ mm}$$

Corner :

$$Z = \left(1.1 - 0.88 \frac{212}{351.5} \right) * \frac{32.8 * 10^3}{0.3 * (351.5)^2} = 0.5 \text{ mm}$$

Plain Concrete Slab :

Interior :

$$Z = \frac{76.4 * 10^3}{8 * 0.25 * (407.7)^2} = 0.23 \text{ mm}$$

Edge :

$$Z = 0.433 * \frac{46.3 * 10^3}{0.3 * (407.7)^2} = 0.44 \text{ mm}$$

Corner :

Distance between loading point and corner $a_1 = 212 \text{ mm}$

$$Z = \left(1.1 - 0.88 \frac{212}{407.7} \right) * \frac{40.2 * 10^3}{0.3 * (407.7)^2} = 0.55 \text{ mm}$$

Appendix F

Properties of Concrete Used for the Slabs

Cube and beams specimens were taken from the mix used to cast the SFRC slab and the plain concrete slab. Compressive strength test, third-point loading test were conducted to assess the cube strength, Flexural strength.

Compressive Strength

Table F-1: Cube Compressive Strength for SFRC and Plain Concrete

Property \ Age	7 days			28 days		
	C1	C2	C3	C4	C5	C6
Specimen No.						
SFRC Cubes Strength (MPa)	17.7	18.3	18.2	33.4	35	32.5
P.C. Cubes Strength (MPa)	18.1	16.8	17.3	34.8	31.9	34

7 days strength for SFRC = 18.1 MPa.

28 days strength for SFRC = 33.6 MPa.

7 days strength for plain concrete = 17.4 MPa.

28 days strength for plain concrete = 33.6 MPa.

Flexural Strength

SFRC Beams

Table F-2: Results from Third-point Loading Test (SFRC Beams)

Property		Beams	SF. 1	SF.2	SF.3	SF.4	SF.5	SF.6
At First Crack	Load (KN)		36.6	36.0	31.3	33.7	37.1	31.9
	Strength (MPa)		4.9	4.8	4.2	4.5	4.9	4.3
	Deflection (mm)		0.006	0.005	0.004	0.005	0.006	0.001
At Maximum Load	Load (KN)		41.7	41.3	36.4	38.9	42.8	37.8
	Strength (MPa)		5.6	5.5	4.85	5.2	5.7	5.05
	Deflection (mm)		0.009	0.009	0.006	0.006	0.009	0.004
Japanese Standard JSCE-SF4 Properties	Equivalent Load	Pe,3	14.71	16.5	9.9	15.1	14.0	13.5
	Equivalent Strength	f e,3	1.96	2.2	1.32	2.0	1.9	1.8
	Equivalent Strength	Re,3	35	40	27.2	38.5	33.3	35.6

The average first crack strength = 4.6 MPa.

The average MOR = 5.3 MPa.

The average equivalent strength = 1.86 MPa.

The average equivalent strength ratio = 34.9

Figure F-1 to figure F-6 show the load deflection diagrams for the SFRC beam specimens.

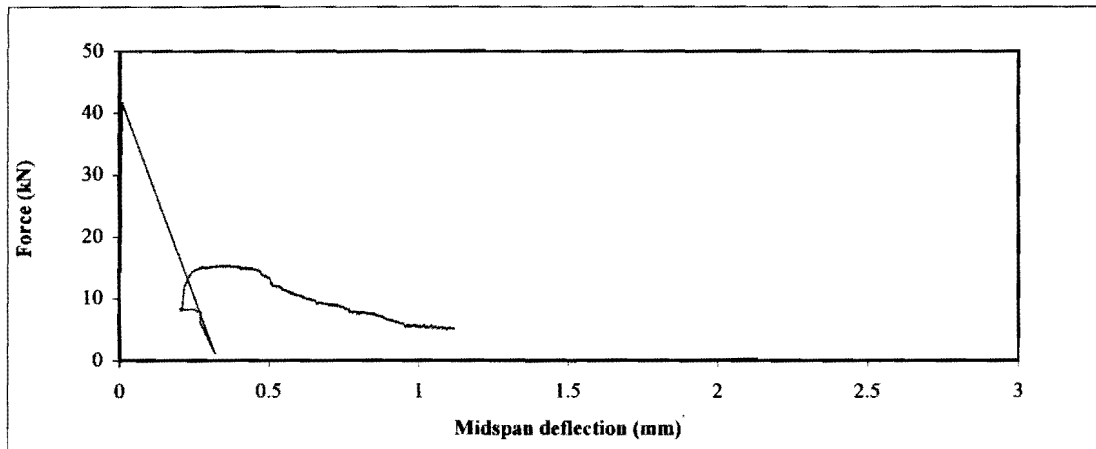


Figure F-1: Third-Point Loading Test: Load-Deflection Diagram (SF.1)

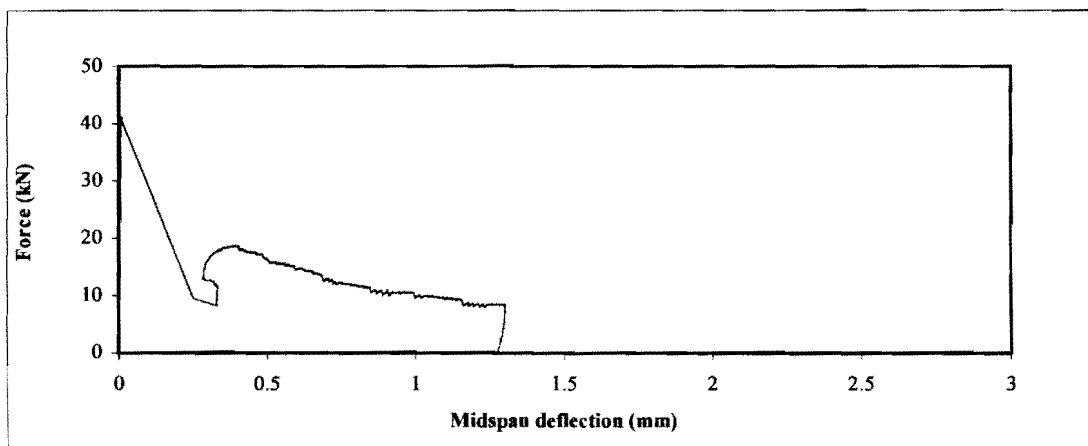


Figure F-2: Third-Point Loading Test: Load-Deflection Diagram (SF.2)

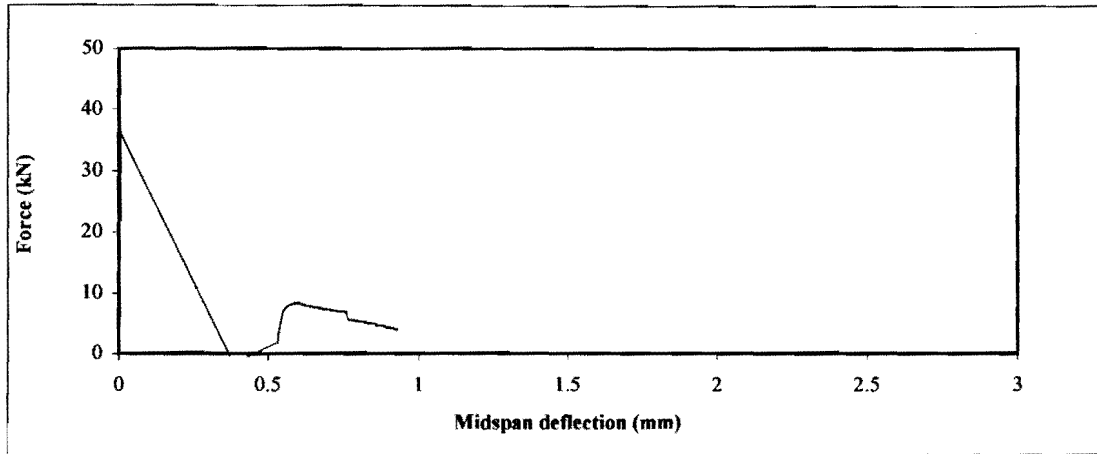


Figure F-3: Third-Point Loading Test: Load-Deflection Diagram (SF.3)

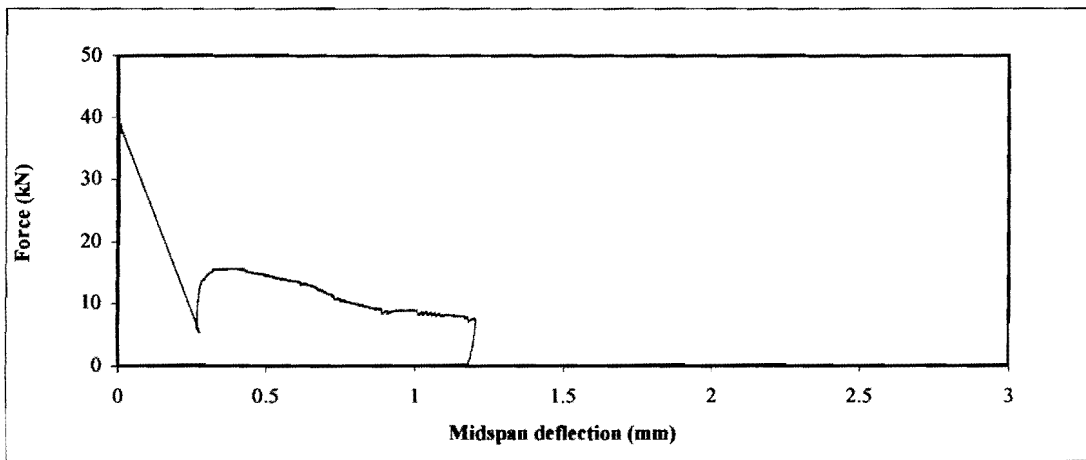


Figure F-4: Third-Point Loading Test: Load-Deflection Diagram (SF.4)

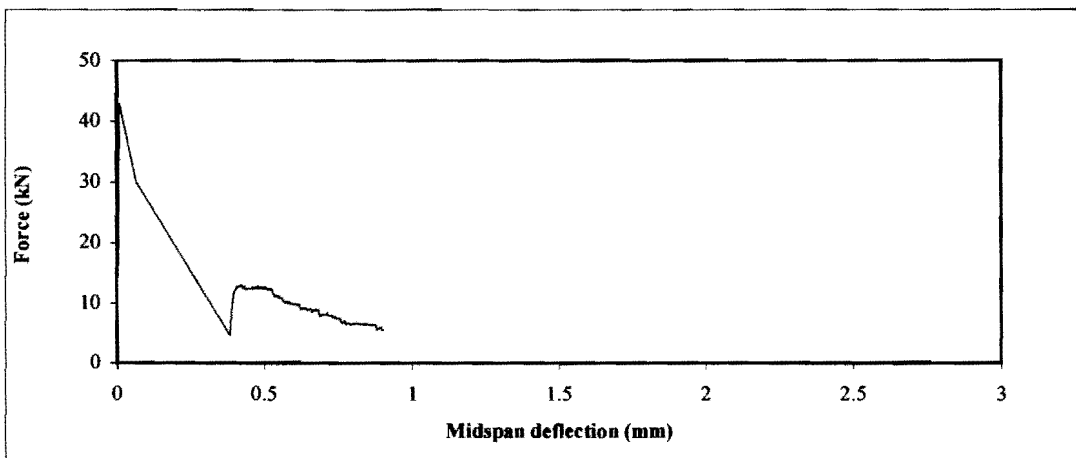


Figure F-5: Third-Point Loading Test: Load-Deflection Diagram (SF.5)

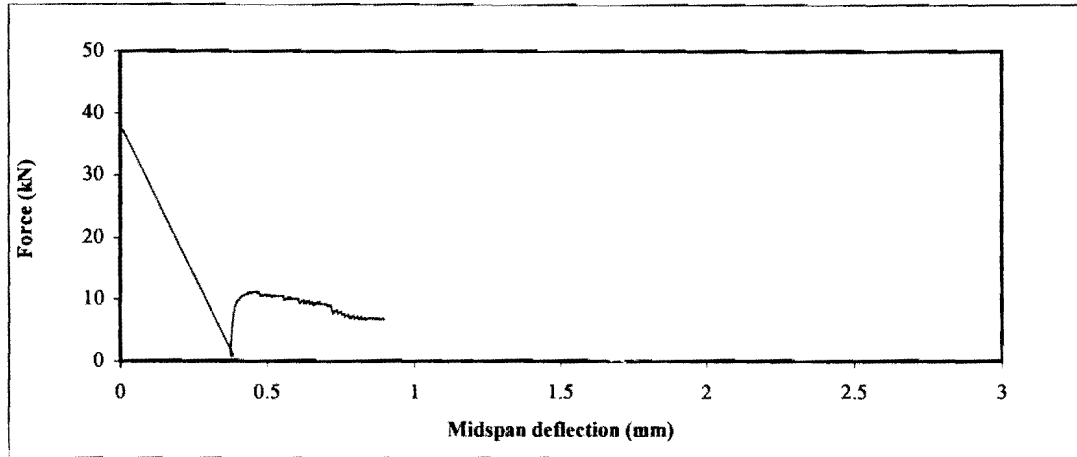


Figure F-6: Third-Point Loading Test: Load- Deflection Diagram (SF.6)

Plain Concrete Beams

Table F-3: Results from Third-Point Loading Test (Plain Concrete Beams)

Property		Beams	P.C. 1	P.C.2	P.C.3	P.C.4	P.C.5	P.C.6
At First Crack	Load (kN)		29.3	33.0	30.8	34.5	30.0	31.5
	Strength (MPa)		3.9	4.4	4.1	4.6	4.0	4.2
	Deflection (mm)		0.004	0.005	0.004	0.005	0.004	0.004
At Maximum Load	Load (kN)		33.2	42.6	41.6	42.6	37.4	45.0
	Strength (MPa)		4.43	5.68	5.5	5.7	5.0	5.6
	Deflection (mm)		0.006	0.007	0.007	0.007	0.007	0.007

The average first crack strength = 4.2 MPa.

The average MOR = 5.3 MPa.

Figure F-7 to figure F-12 show the load deflection diagrams for the plain concrete specimens.

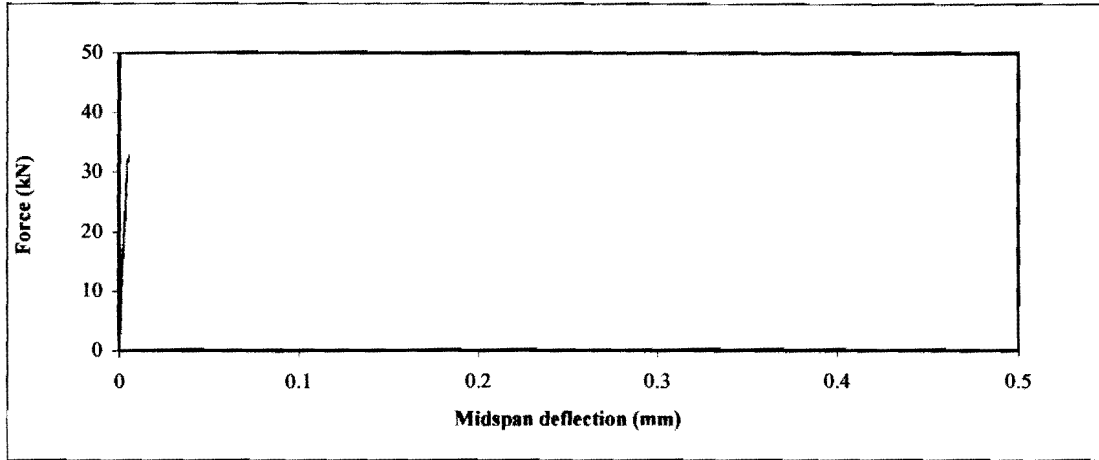


Figure F-7: Third-Point Loading Test: Load-Deflection Diagram (P.C.1)

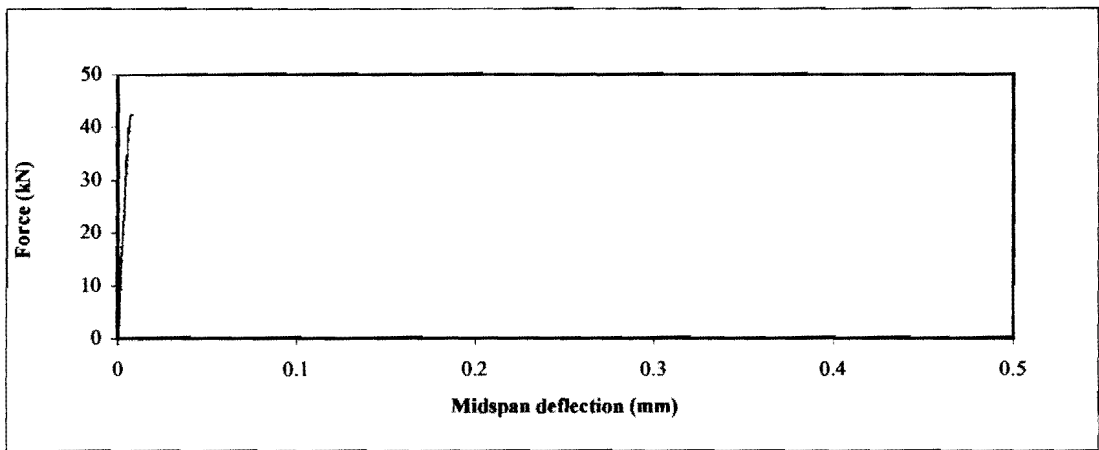


Figure F-8: Third-Point Loading Test: Load-Deflection Diagram (P.C.2)

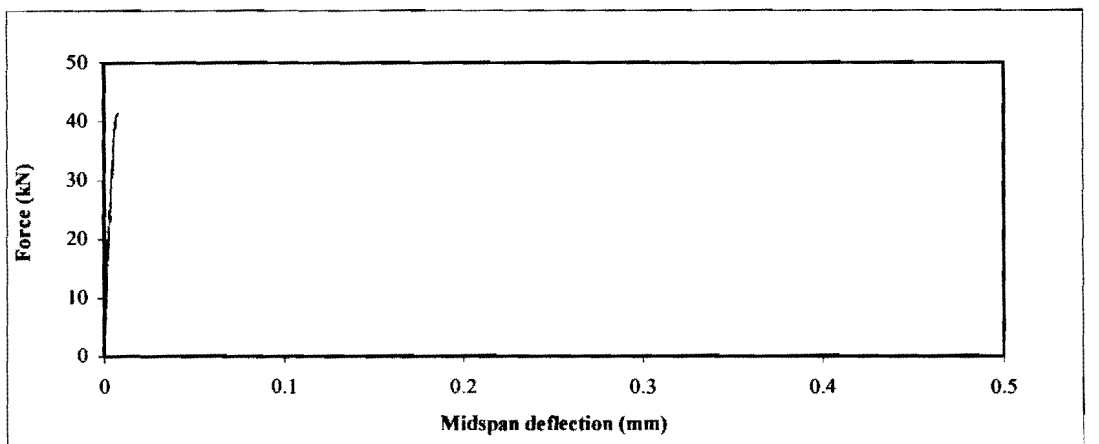


Figure F-9: Third-Point Loading Test: Load-Deflection Diagram (P.C.3)

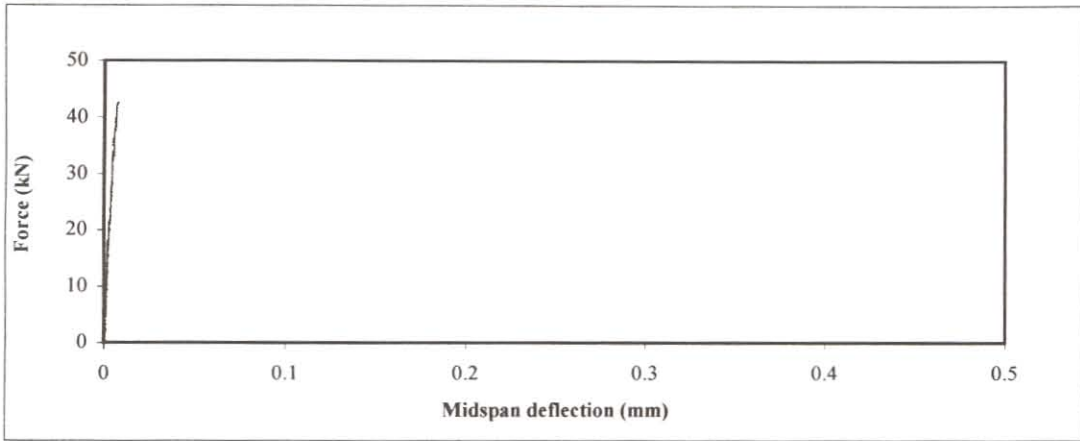


Figure F-10: Third-Point Loading Test: Load-Deflection Diagram (P.C.4)

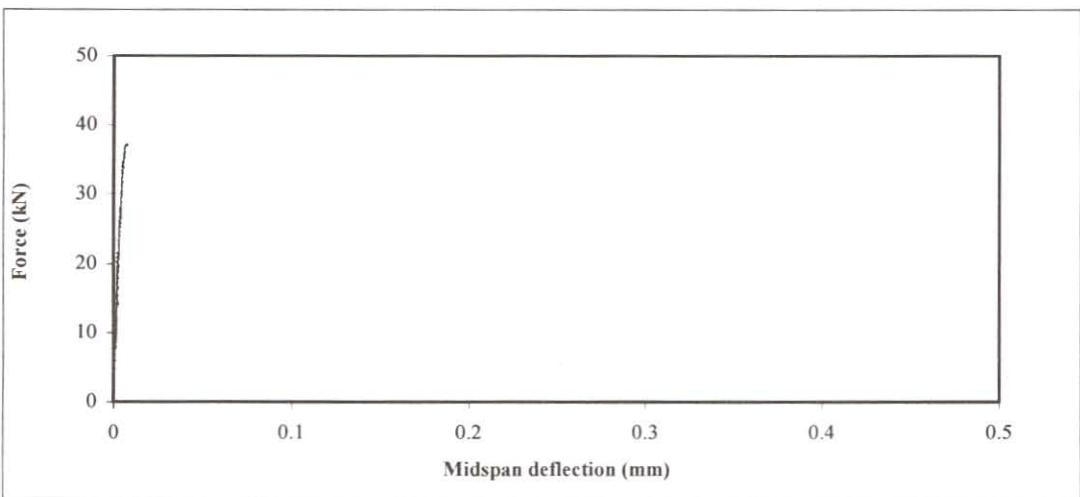


Figure F-11: Third-Point Loading Test: Load-Deflection Diagram (P.C.5)

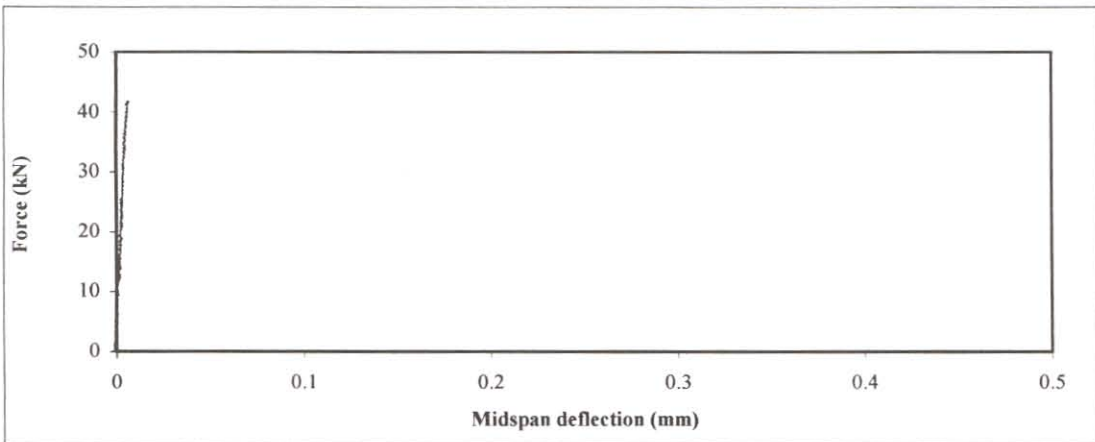


Figure F-12: Third-Point Loading Test: Load-Deflection Diagram (P.C.6)